Study of Solid-solid crystal structure phase transformations

Benzene undergoes a phase transition from monoclinic to orthorhombic structure

Most solids undergo a phase transformation from one structure to another.

Ice, for example, has many forms or solid phases, one of the most complex phase diagrams.

How does one study these solid-solid phase transformations?

In general, the volume of the crystallographic unit cell also changes when there is a phase transformation.

Click to edit Master text styles
Second level
- Third level
- Fourth level
- Fifth level

Constant Pressure Calculations

In microcanonical ensemble (NVE) or canonical ensemble (NVT), volume is fixed or constant. Pressure fluctuates. So, these are not suitable for study of crystal-structure transformations.

We need constant pressure ensembles, permitting changes in volume. This was first proposed by Anderson in 1980, for MD.

Click to edit Master text styles

- Second level
  - Third level
    - Fourth level
      - Fifth level

In NVT ensemble,

$$\langle a \rangle_{NVT} = \frac{\int d\bar{r}_1 \int d\bar{r}_2 \cdots \int d\bar{r}_N \; a(\bar{r}_1, \bar{r}_2, \cdots \bar{r}_N) \; e^{-U(\bar{r}_1, \cdots \bar{r}_N)/k_B T}}{\int d\bar{r}_1 \int d\bar{r}_2 \cdots \int d\bar{r}_N \; e^{-U(\bar{r}_1, \cdots \bar{r}_N)/k_B T}}$$

Transition probability is given by

$$W(i \to i+1) = \min \left\{ 1, \; e^{-(U_{i+1} - U_i)/k_B T} \right\}$$

In NPT ensemble,

$$\langle a \rangle_{NPT} = \frac{\int dV \int d\bar{r}_1 \cdots d\bar{r}_N \; a(\bar{r}_1, \cdots \bar{r}_N, V) \; e^{-U/k_B T} \; e^{+PV/k_B T}}{\int dV \int d\bar{r}_1^N \; e^{-U/k_B T} \; e^{+PV/k_B T}}$$

V is a variable of integration in NPT

Click to edit Master text styles
Second level
- Third level
- Fourth level
- Fifth level

This approach has a problem. Imagine the following situation: where volume contracts $L' < L$. What happens to particles near the boundary? Suddenly there are particles outside

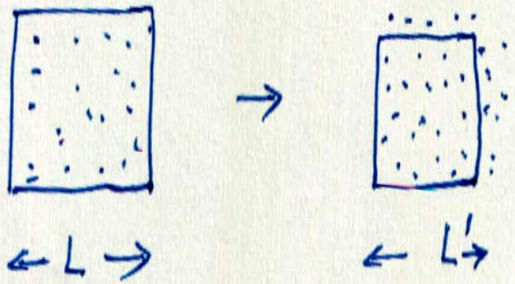

$(L^3 = V)$

the simulation cell. If volume expends then there are void regions:

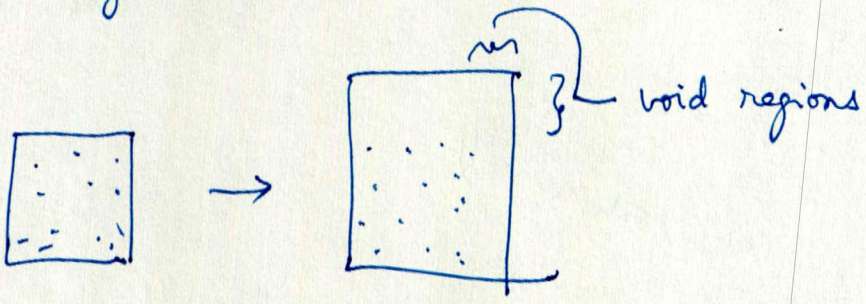

To overcome this problem we define $\bar{s}_i = \bar{r}_i / L$

$$\langle a \rangle = \frac{\int dV \int d\bar{s}_1 \ldots d\bar{s}_N \; \bar{a}(\bar{s}_1 \ldots \bar{s}_N, V) \; e^{-U(\bar{s}^N, V)/k_B T} \; V^N}{\int d\bar{s}_1 \ldots d\bar{s}_N \; e^{-U(\bar{s}^N, V)/k_B T} \; V^N}$$

$$V^N = \ln e^{V^N} = e^{\ln V^N} = e^{N \ln V}$$

$$W = (U_{i+1} - U_i) + P(V' - V) + N \ln(V'/V)(k_B T)$$

Scaled variables $\bar{s}_i$ are within a unit cube.

Simulation cell is now like a balloon.

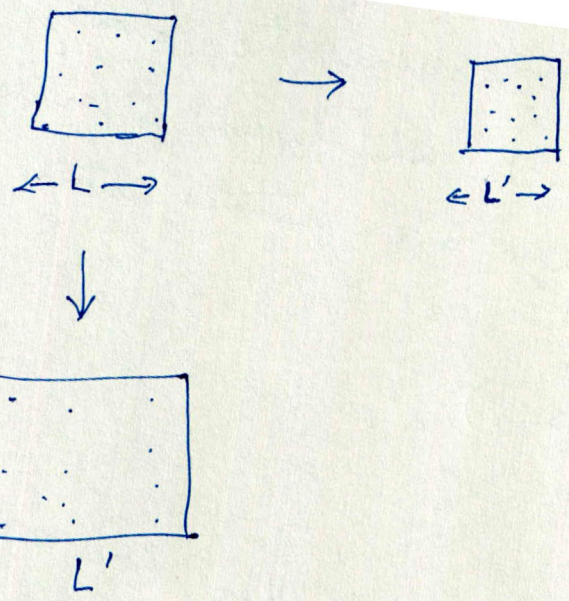

Difficulty in using NPT simulations for crystal structure transformations:

Crystal Structure

Crystal structure of a material can be specified by the unit cell and atomic positions within the unit cell. This repeats to fill the whole space.

The unit cell is described by lattice parameters, the length of the edges of the cell and the angle between them.

There are seven seven unique crystal systems – cubic, hexagonal, tetragonal, rhombohedral, orthorhombic, monoclinic, triclinic.

(1) Cubic

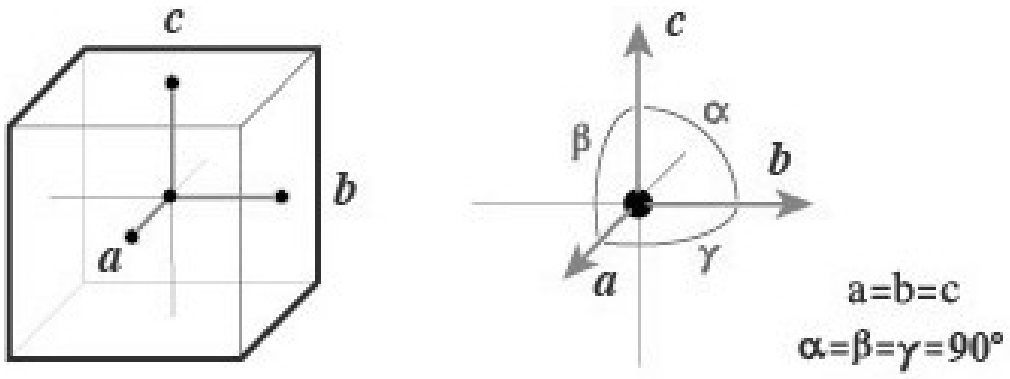

(2) Hexagonal

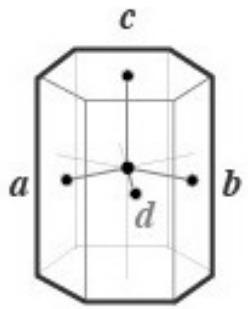

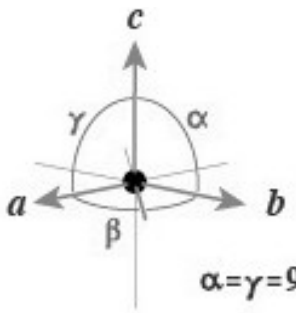

a≠c
α=γ=90° β=120

(5) Monoclinic

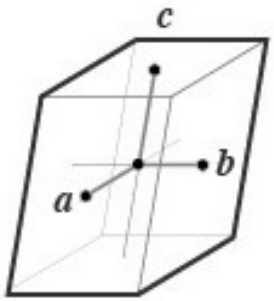

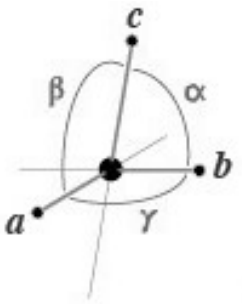

a≠b≠c
α=γ=90°≠β

(3) Tetragonal

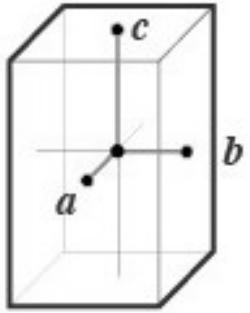

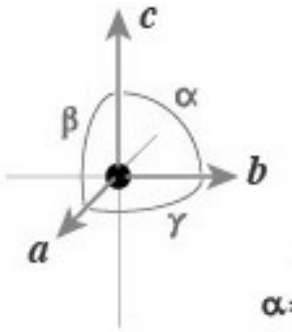

a=b≠c
α=β=γ=90°

(6) Rhombohedral

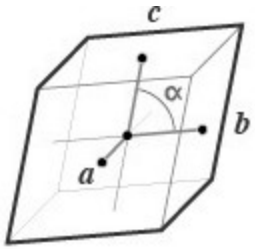

a = b = c
α = β = γ ≠ 900

(4) Orthorhombic

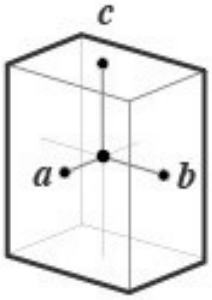

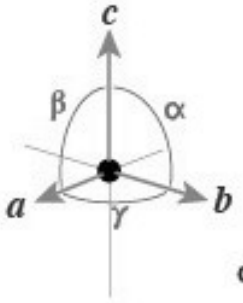

a≠b≠c
α=β=γ=90°

(7) Triclinic

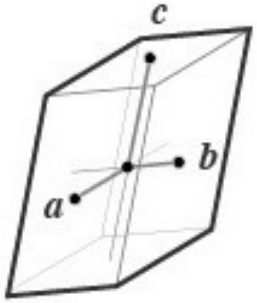

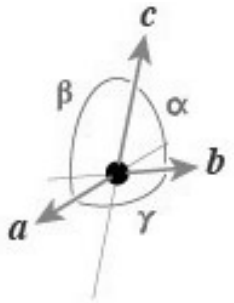

a≠b≠c
α≠β≠γ≠90°

Difficulty in packing crystallographic unit cells

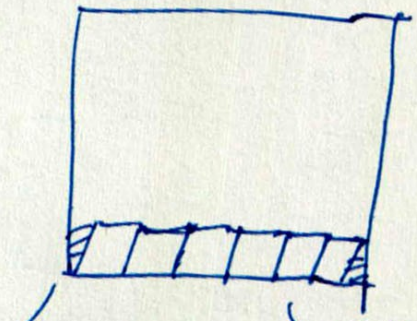

cubic/square cell

void space

monoclinic crystallographic unit cell.

Since it is not possible to fill all cubic space with non-cubic unit cells of a crystal, some void space is inevitable. This means no PBC!

NO PBC means no bulk simulations!

The formulation of Parrinello Rahman method

Let us consider a , b and c are the three vectors forming the edges of the MD cell.

$\underline{h}$ is a matrix formed by { a , b , c }

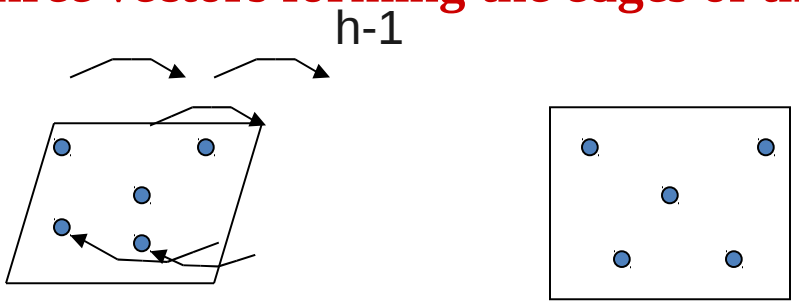

The volume of the MD cell containing *N* particles is given by $\Omega = a.(b \times c)$

Now the position of a particle *i* defined by $r_i = \xi_i a + \eta_i b + \zeta_i c = \underline{h} s_i$

Where s_i has components (ξi, ηi, ζi) each going from 0 to 1.

The Lagrangian of the system can be written in the following way

$$L = \frac{1}{2}\sum m_i \dot{s}_i' \underline{G} \dot{s}_i - \sum_{i \neq j} \varphi(r_{ij}) + \frac{1}{2} W \, Tr(\dot{\underline{h}}' \dot{\underline{h}}) - p_{ext}\Omega$$

G = h'h, pext is the externally applied hydrostatic pressure.

The prime denotes the transpose of the matrix and dot denotes the time derivative

Various terms in the Lagrangian

- The first term of the Lagrangian is the kinetic energy of the particles.

$$\dot{\vec{s}}_i' G \dot{\vec{s}}_i = (h^{-1}\dot{\vec{r}}_i)' h' h (h^{-1}\dot{\vec{r}}_i)$$
$$= \dot{\vec{r}}_i' (h^{-1})' h' h h^{-1} \dot{\vec{r}}_i$$
$$= \dot{\vec{r}}_i' (h')^{-1} h' \dot{\vec{r}}_i$$
$$= \dot{\vec{r}}_i' \dot{\vec{r}}_i$$
$$= \dot{r}^2$$

- The second term is the interaction potential energy of the particles in the system.

- The third term is the kinetic energy associated with the MD cell deformation and W has the dimension of mass.

- The remaining term arises from the external pressure pext.

The equations of motion

There are two generalized coordinates in the system **s** and **h.** Thus we will have two equations of motion.

The Lagrange's equation of motion is defined as

$$\frac{d}{dt}\left(\frac{\partial L}{\partial \dot{q}_i}\right)-\frac{\partial L}{\partial q_i}=0$$

where qi's are the generalized coordinates

Equation of motion with respect to the generalized coordinate **s**

$$\frac{d}{dt}\left(\frac{\partial L}{\partial \dot{s}_i}\right)=\frac{d}{dt}\left(m_i G\dot{s}_i\right)=m_i\dot{G}\dot{s}_i+m_i G\ddot{s}_i$$

$$\frac{\partial L}{\partial s_i} = -\sum_{i \neq j} \frac{\partial \varphi(r_{ij})}{\partial s_i} = -h' \sum_{i \neq j} \frac{\partial \varphi(r_{ij})}{\partial r_i}$$

$$= -h' \sum_{i \neq j} \frac{\partial \varphi(r_{ij})}{\partial r_i} \frac{r_{ij}}{r_{ij}}$$

$$= h' \sum_{i \neq j} \chi(r_{ij}) h(s_i - s_j), \chi(r_{ij}) = -\frac{\partial \varphi(r_{ij})}{r_{ij} \partial r_i}$$

$$= G \sum_{i \neq j} \chi(r_{ij})(s_i - s_j)$$

Now equating the two terms

$$m_i G \ddot{s}_i + m_i \dot{G} \dot{s}_i = G \sum_{i \neq j} \chi(r_{ij})(s_i - s_j)$$

$$\Rightarrow m_i G \ddot{s}_i = G \sum_{i \neq j} \chi(r_{ij})(s_i - s_j) - m_i \dot{G} \dot{s}_i$$

$$\Rightarrow \ddot{s}_i = m_i^{-1} \sum_{i \neq j} \chi(r_{ij})(s_i - s_j) - G^{-1} \dot{G} \dot{s}_i$$

Equation of motion with respect to **h**

$$\frac{d}{dt}\left(\frac{\partial L}{\dot{\partial h_{ij}}}\right) = W\ddot{h}_{ij}$$

$$\frac{\partial L}{\partial h_{ij}} = \sum m_i (h\dot{s}_i)'\dot{s}_i - \sum_{i\neq j} \frac{\partial \varphi(r_{ij})}{\partial r_{ij}} s_{ij} - p_{ext}\frac{\partial \Omega}{\partial h_{ij}}$$

$$= \sum m_i v_i h^{-1} v_i - \sum \frac{\partial \varphi(r_{ij})}{\partial r_{ij}} \frac{r_{ij}}{r_{ij}} s_{ij} - p_{ext}\frac{\partial \Omega}{\partial h_{ij}}$$

$$= \sum m_i v_i \frac{\sigma}{\Omega} v_i + \sum \chi(r_{ij})(r_i - r_j)\frac{\sigma}{\Omega}(r_i - r_j) - p_{ext}\frac{\partial \Omega}{\partial h_{ij}}$$

$$W\ddot{h} = (\pi - p_{ext})\sigma$$

$$\Rightarrow \ddot{h} = W^{-1}(\pi - p_{ext})\sigma$$

where

$$\Omega\underline{\pi} = \sum m_i v_i v_i + \sum_{i\neq j} \chi(r_{ij})(r_i - r_j)(r_i - r_j) \quad \text{and} \quad \sigma = \Omega h^{-1}$$

Example of Parrinello-Rahamn method

f.c.c to b.c.c transition

Lennard-Jones potential and a pair potential suitable for rubidium metal is used to investigate the f.c.c. to b.c.c. transition.

Initially a system consisting of 500 particles forming an f.c.c. structure of cubic length l^* is taken. The equivalent number density is $\rho^* = 0.96$.

MD simulation is performed with a time step $\Delta t^* = 0.005$.

In this calculation the values of various parameters are as follows:

$W^* = 20$, pext = 4.0

Temperature $T^* = 0.15$

Monitoring radial distribution function

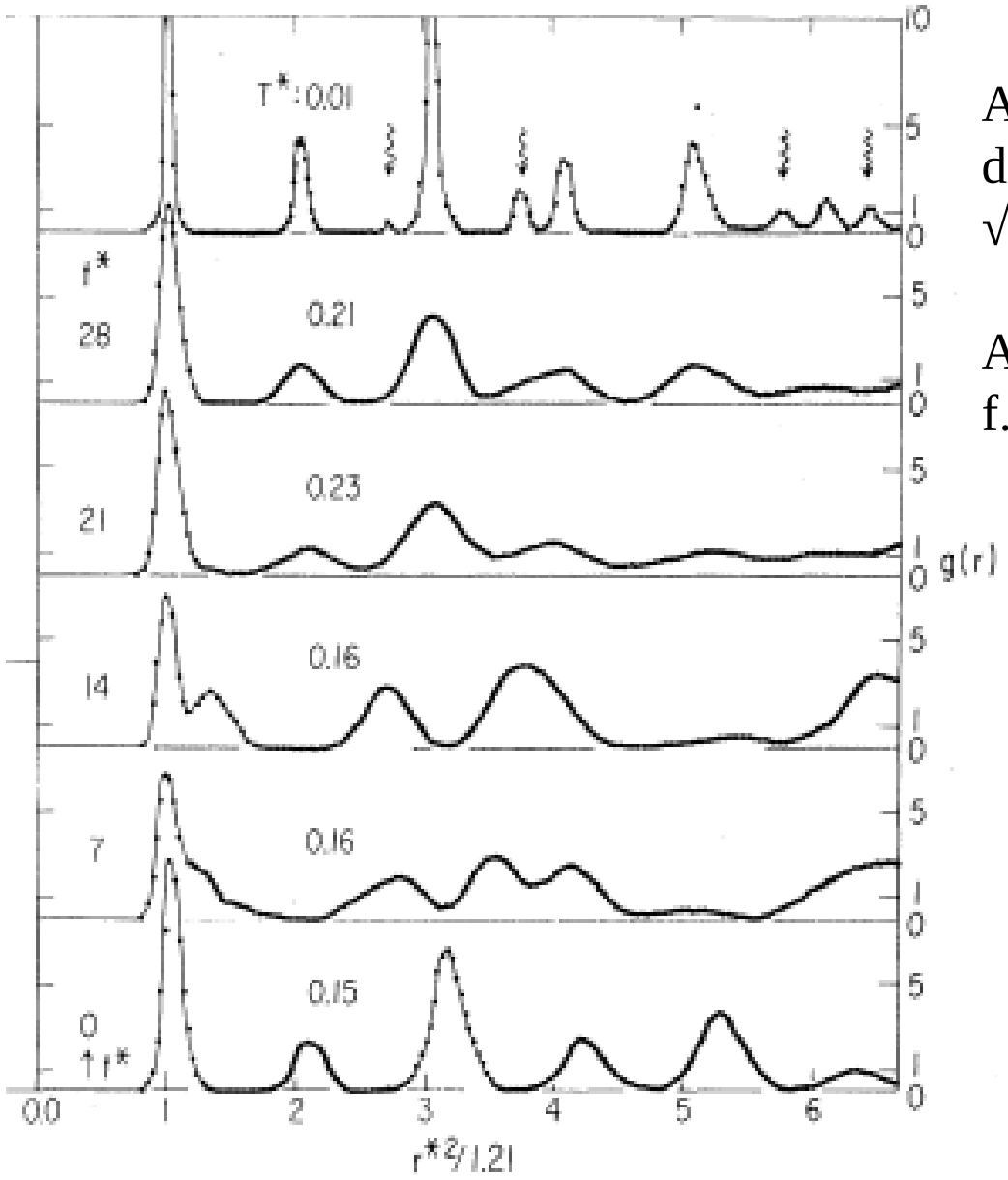

At t* = 0, f.c.c. structure with sharply defined shells at distances 1, √2, √3, √4 etc.

At t* = 14, structure had changed from f.c.c. to b.c.c.

Polyatomic systems

Similar problem in MC simulation

In the simulation of the ordered phase III of carbon tetrachloride, it was observed that the matrix elements of matrix h were continuously changing even after several thousand MC moves.

MC move	Components of **a** in Å	Components of **b** in Å	Components of **c** in Å
20	(18.3, 0, 0.2)	(0, 11.5, 0)	(-4.7, 0.1, 17.9)
600	(18.1, -0.4, 0.6)	(0.3, 11.7, -0.1)	(-4.2, 0.3, 17.8)
1200	(18.3, -0.2, -0.5)	(0.1, 12, 0.3)	(-3.9, -0.2, 17.9)
1950	(18.1, -0.8, -1.1)	(0.7, 11.9, 0.9)	(-2.9, -1.2, 17.8)

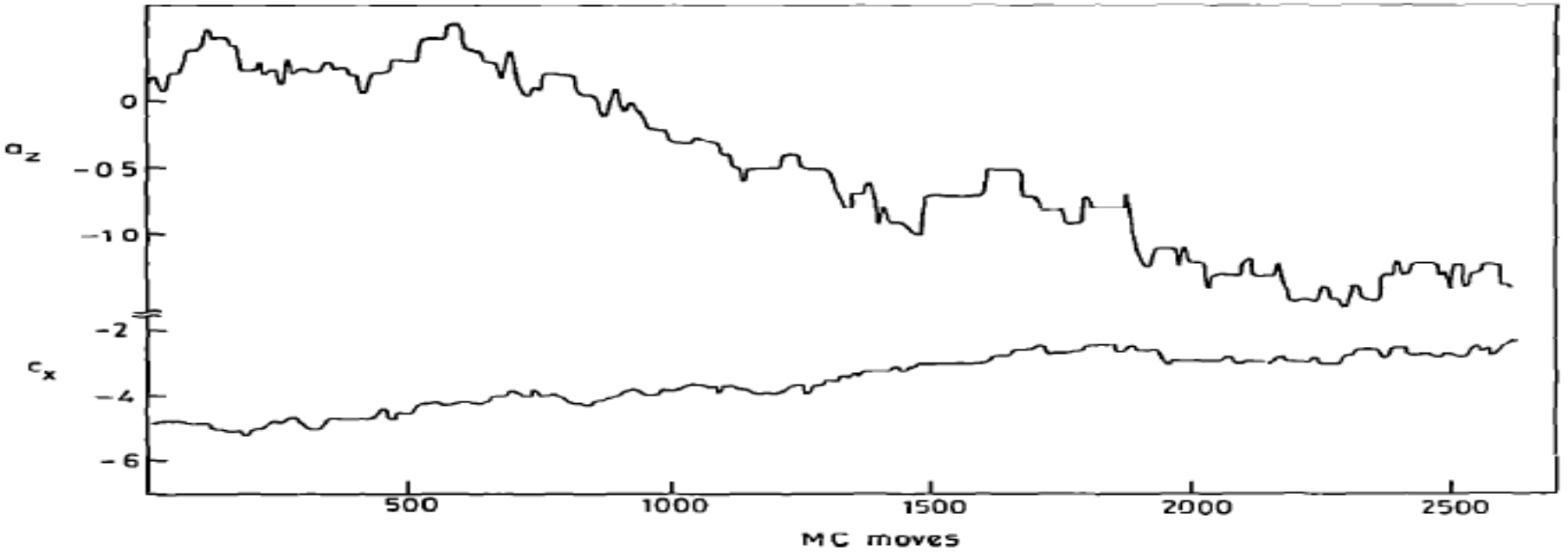

The magnitude of the cell vectors and the angles between them fluctuate around the mean values.

On the other hand the components cx and az are continuously drifting during the course of the simulation.

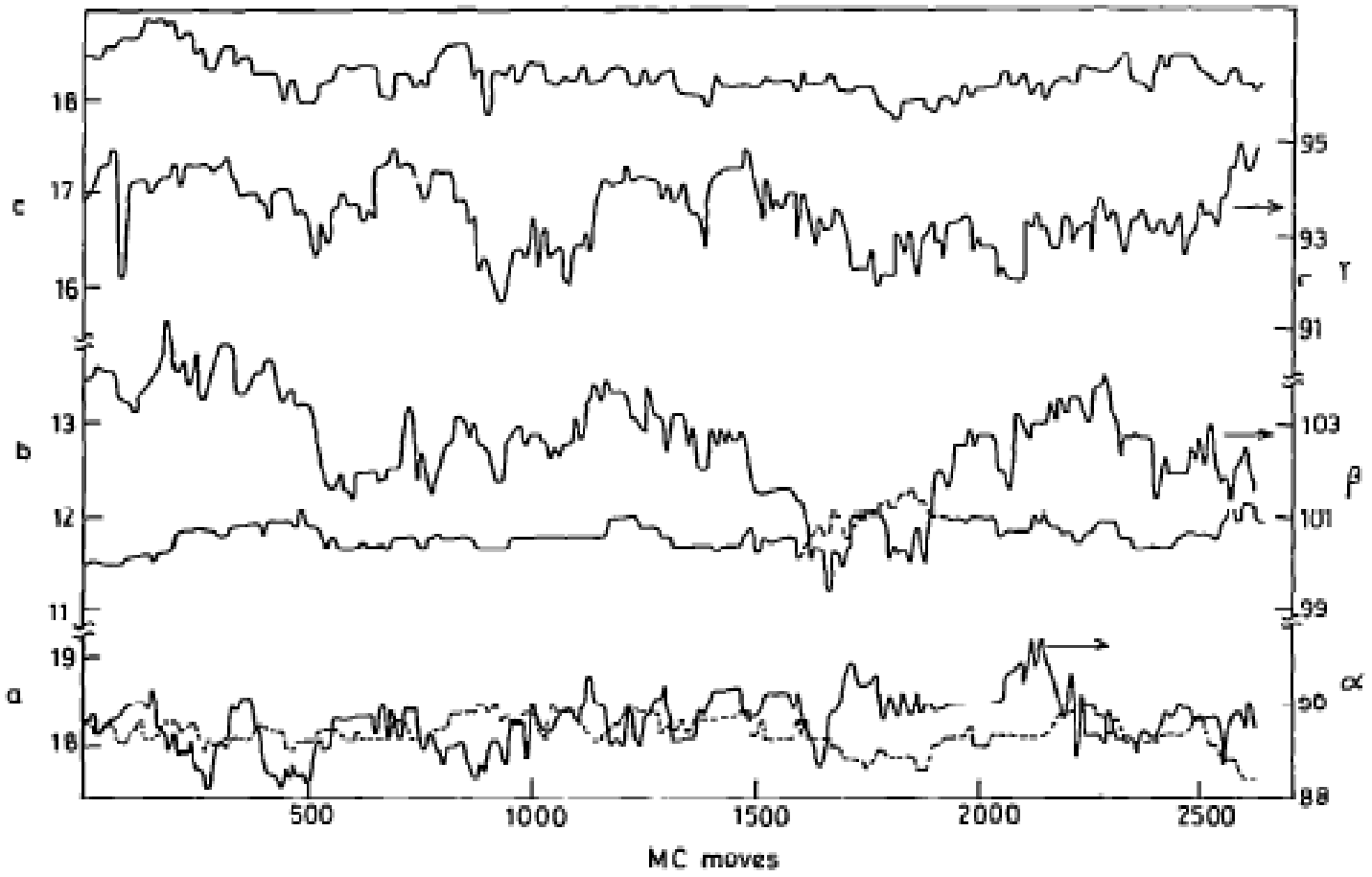

A problem in variable shape MD simulation

In the simulation of solid nitrogen in its high pressure cubic phase, the MD cell vectors are found to be changing continuously for long time.

In the figure below, the MD cell vectors have been projected on the surface of a sphere and the sphere is viewed from the X, Y and Z directions respectively.

The upper portion of the figure shows the trajectories of the MD cell basis vectors indicating the continuous drift in the components of the cell vectors.

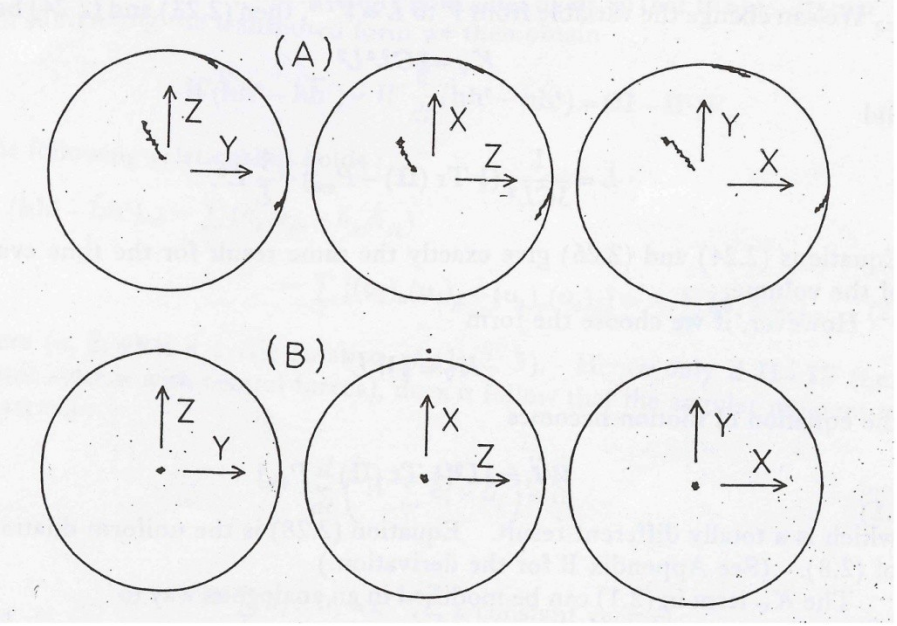

Rotation of the simulation cell

The observations from the previous slides indicates that the simulation cell And the molecules are constantly rotating as a whole in space.

The reason for the rotation of the cell is due to the following reason.

The matrix $\underline{h}$ has nine components.

Only 6 parameters are necessary to define the shape of the simulation cell. These are a, b, c, α, β, γ.

The remaining three parameters describe the rotation of the cell.

Stopping the rotation of the MD cell

- Matrix h can be separated into a symmetric part S and an antisymmetric part A.

$$\underline{h} = S + A$$

- If we initially select the h matrix in a symmetric form, the growth of the antisymmetric component A is closely related to the rotation of the MD cell.

- The imposition of the constraint A ≡ 0 reduces the number of independent parameters to six and can stop the rotation of the MD cell.

- The imposition of the symmetry for h in the simulation has the same effect as the addition of a rotation(R) that transforms h in to a symmetric form at each time step.

- The procedure to use the equation of motion for S is as follows:

(1) Choose an initial configuration with an appropriate h matrix.

(2) Transform all the vectors in the real frame by the matrix R and give symmetrical initial values for $h, \dot{h}, \ddot{h}, \ldots\ldots$

(3) Then carry out the simulation using the equation of motion for S.

MC and variable shape simulation

MC approach to variable shape simulation

General isothermal isobaric ensemble

The simulation cell is defined by three vectors $\vec{a}$, $\vec{b}$ and $\vec{c}$

The representation of the cell by these three vectors permits the cell to have any desired crystal symmetry.

The shape of the cell can be varied by appropriate changes in $\vec{a}$, $\vec{b}$ and $\vec{c}$.

The $\underline{h}$ matrix is made in such a way that the lower triangle elements are zero. This will prevent the rotation of the simulation cell by allowing only six out of nine degrees of freedom to vary.

$$\underline{h} = \begin{pmatrix} a_x & b_x & c_x \\ 0 & b_y & c_y \\ 0 & 0 & c_z \end{pmatrix}$$

The scaled coordinates are used to perform the simulation

$$\vec{s}_i = \underline{h}^{-1}\vec{r}_i$$

The advantage of using the scaled coordinates is that it is easier to employ periodic boundary conditions in the scaled coordinates frame than in the real space coordinate frame.

Here coordinates $\vec{r}_i$ are the real coordinates and $\vec{s}_i$ are the scaled coordinates lying in the range from 0 to 1.

The partition function is given by the following expression.

$$\Xi = \frac{\Lambda(2\pi m\beta/h^2)^{3N/2}}{N!}\int_0^{\infty}\int_0^{\infty}\int_0^{\infty} d\bar{a}\, d\bar{b}\, d\bar{c}\exp(-\beta P \det\underline{h}) \int_{\det\underline{h}} \exp\left[-\beta\Phi(r^N)\right] dr^N$$

The Monte Carlo scheme

Take an initial configuration of all the particles in the system.

Give a trial move to the particle coordinates followed by a trial move to the $\underline{h}$ matrix elements.

$$s_i' = s_i + \xi ds_i$$
$$h_{ij}' = h_{ij} + \eta dh$$

Here s_i' and h_{ij}' are the new scaled coordinates and new $\underline{h}$ matrix elements respectively. ξ and η are two random numbers ranging from -1 to 1.

Now calculate the energy of the new configuration Φ'. If Φ is the energy of the old configuration before displacement of the particle then calculate the following quantity.

$$W = (\Phi' - \Phi) + P(\det \underline{h}' - dte\ \underline{h}) + N\beta\text{-}1 \ln(\det \underline{h}'/\det \underline{h})$$

MC scheme

Acceptance of the trial move: the criteria

The probability of acceptance p follows the following rule

(1) if $W \leq 0$ then $p = 1$

(2) If $W > 0$ then $p = \exp(-\beta W)$

The trial configuration is accepted with probability p and rejected with probability (1-p)

Prevention of rotation of the MC cell

- The rotation may occur because of the particular initial configuration of the molecules or due to a particular configuration of the molecules during the course of the simulation.

- Although the rotation of the cell does not cause problem in obtaining the average of the thermodynamic properties, it gives rise to the difficulties in calculating the mean positions of the atoms in elucidating the crystal structure of the phase being simulated.

MC cell

- **The rotation of the cell can be prevented by permitting only six out of nine degrees of freedom to vary during the simulation.**

- **This is done by restricting the lower diagonal elements of the cell matrix to zero. This corresponds to the vector** a **being aligned along x-axis, vector** b **lying in the yz plane.**

Effect of temperature (Disorganized energy) :

(i) Melting of rotational degrees of freedom

(Crystal ⟶ Plastic crystals) Ex: Globular molecules

(ii) Melting of translational degrees of freedom

(Crystal ⟶ Liquid crystal)

(iii) Melting of rotational and translational degrees of freedom

(Crystal ⟶ Liquid)

(iv) Melting of torsional degrees of freedom

(Biphenyl, Stilbene, Azobenzene)

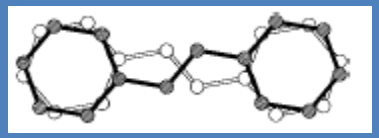

(v) Melting of vibrational degrees of freedom

(as in cyclohexanone crystal)

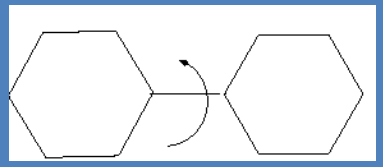

(vi) Structural transformations to other polymorphs

Effect of Pressure (Organized energy):

1. Structural transformations to other polymorphs

2. Partial or complete orientational /conformational ordering

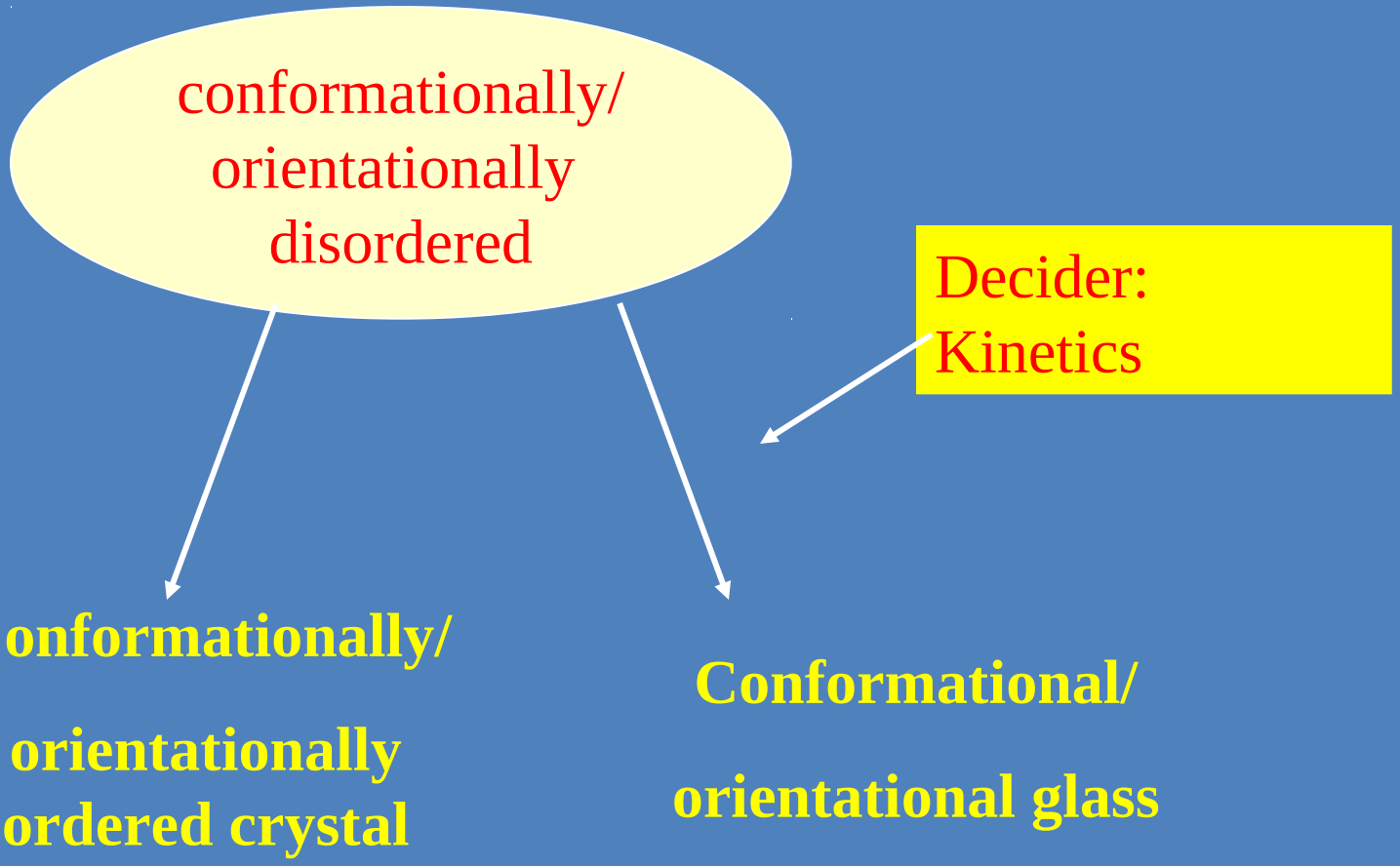

Contents:

1. Pressure induced ordering in biphenyl

2. Pressure induced ordering in p-terphenyl

3. Temperature induced conformational disorder in stilbene

4. Pressure induced ordering in stilbene

5. Adamantane

6. High pressure adamantane up to 26 GPa
   (Rigid body and flexible body assumptions for molecules)

Computer Experimental Techniques:

Structural transformations – associated with volume change
Structural investigations are carried out at constant T and P

Isothermal-isobaric variable shape simulations – ultimate tool to model these structural transformations as it allows the **unit cell** variation as well as the changes in the **molecular level**.

NPT-MC

- Gives only **structural** quantities.

In this ensemble, any average quantity (structural quantity)
Is given as

$$< a >= \frac{\int da \int db \int dc \int d\Omega^N \int d\phi_1^N \int d\phi_2^N \int dr^N a(r^N, \Omega^N, \phi_1^N, \phi_2^N) p(r^N, \Omega^N, \phi^N)}{\int da \int db \int dc \int d\Omega^N \int d\phi_1^N \int d\phi_2^N \int dr^N p(r^N, \Omega^N, \phi_1^N, \phi_2^N)}$$

The integration is only over the configurational phase space.

Flexibility of molecules incorporated by including One or more low frequency modes.

biphenyl and *p*-terphenyl – Torsional mode (associated with flipping motion of phenyl rings)

Stilbene – Torsional mode (associated with the pedal-like motion along ethylene bond)

Adamantane – 6 low frequency modes (from ab initio electronic structure calculations)

Chapter 2

Pressure induced ordering in Biphenyl and structural characterization of high pressure phase.

1. High pressure IR/Raman study shows a possible transition of molecules from a twisted form to planar

2. The transition from twisted to planar conformation involves the transformation of U(Φ) from a W-shaped to U-shaped

3. Disappearance of peaks associated with the out-of-plane bending modes of hydrogens has been observed at high pressures.

Guha et. al., Phys. Rev. Lett., 82, 3625(1999).
Guha et. al., J. Phys. Chem., A105, 6203(2001).

Objectives of our calculations:

1. Structural characterization of high pressure phase at both molecular and unit cell level.

2. What is the nature of the transition?

3. Calculating the IR/Raman spectra as a function of pressure and looking at the intensity variation of out-of-plane bending modes of hydrogen as a function of pressure.

Structure (of the unit cell) as a function of pressure

Cell parameter variation doesn't show any discontinuity.

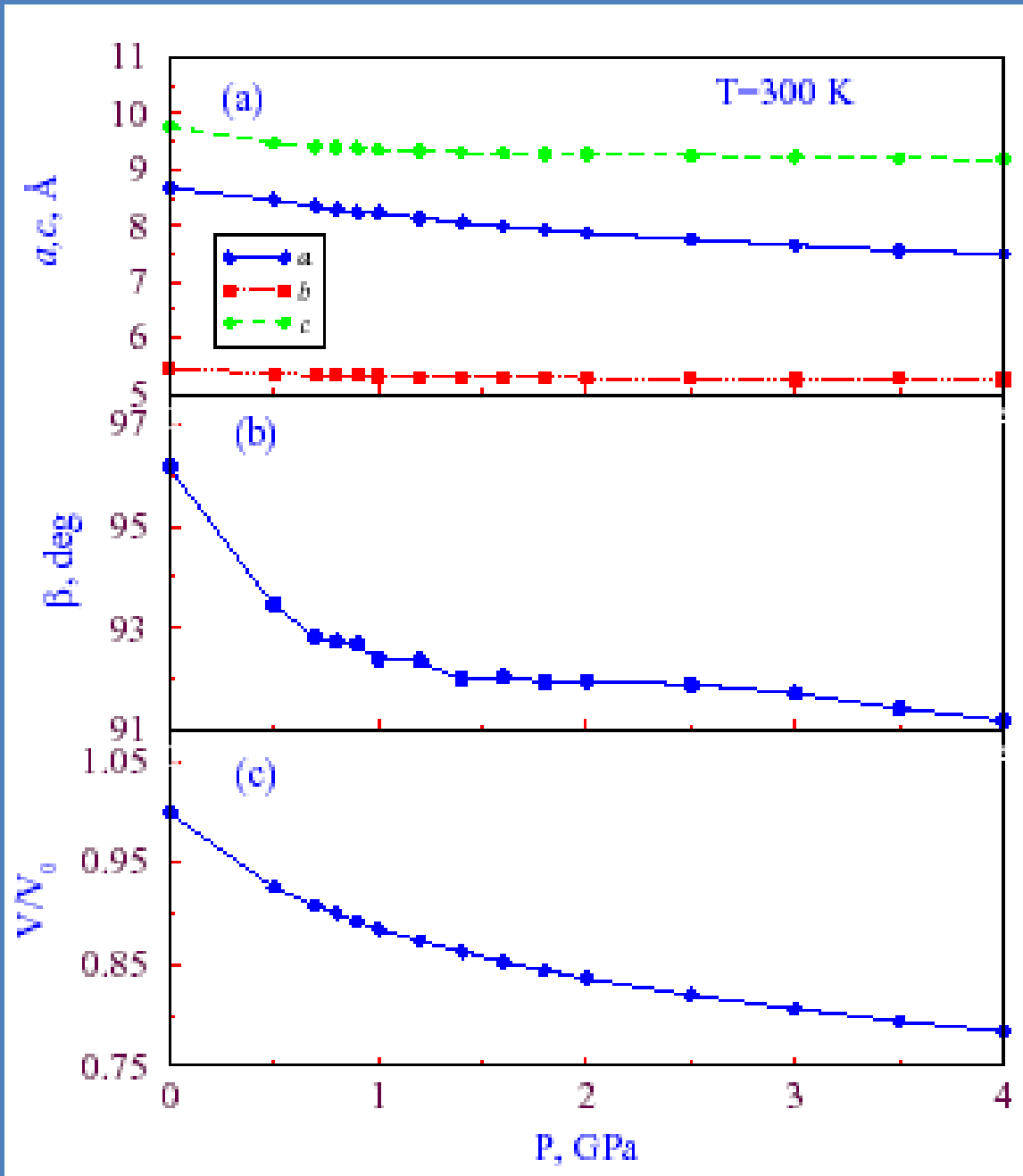

Variation of r.d.f as a function of pressure

Liquid-like behavior in the atom-atom r.d.fs and solid-like behavior (with well defined peaks) in c.o.m-c.o.m. r.d.f is the indication for orientational disorder (at P=1atm, T=300K).

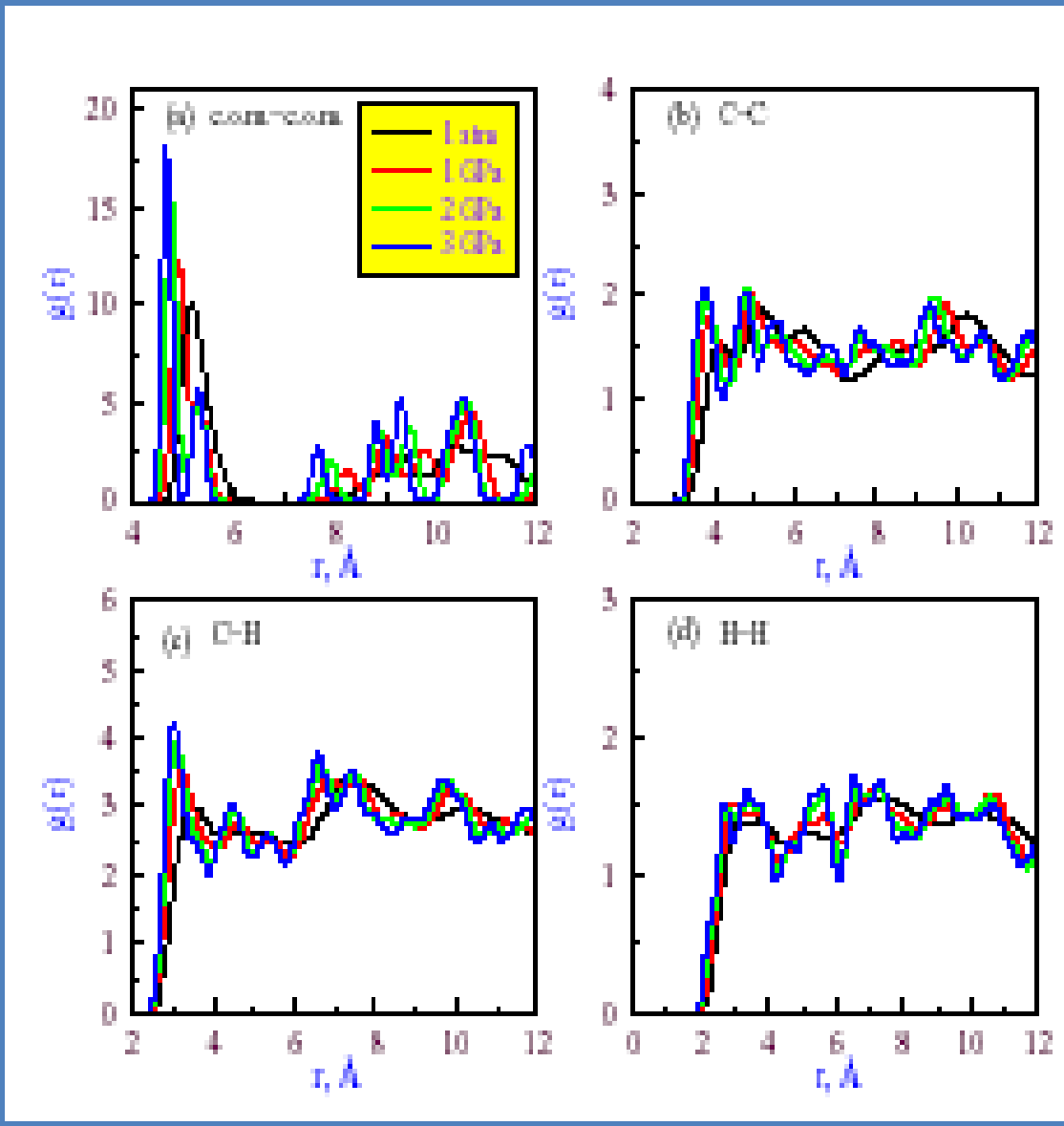

Orientationally ordered at and above 1 GPa and 300 K.

Energetics

U_{inter} shows a minimum. After, a certain pressure value, the atoms try to occupy the same spacial coordinate resulting in increasing the repulsion energy.

U_{intra} increases as the repulsion energy in the BHS potential starts increasing.

(U_{inter} minimum - it corresponds to the transition Pressure.

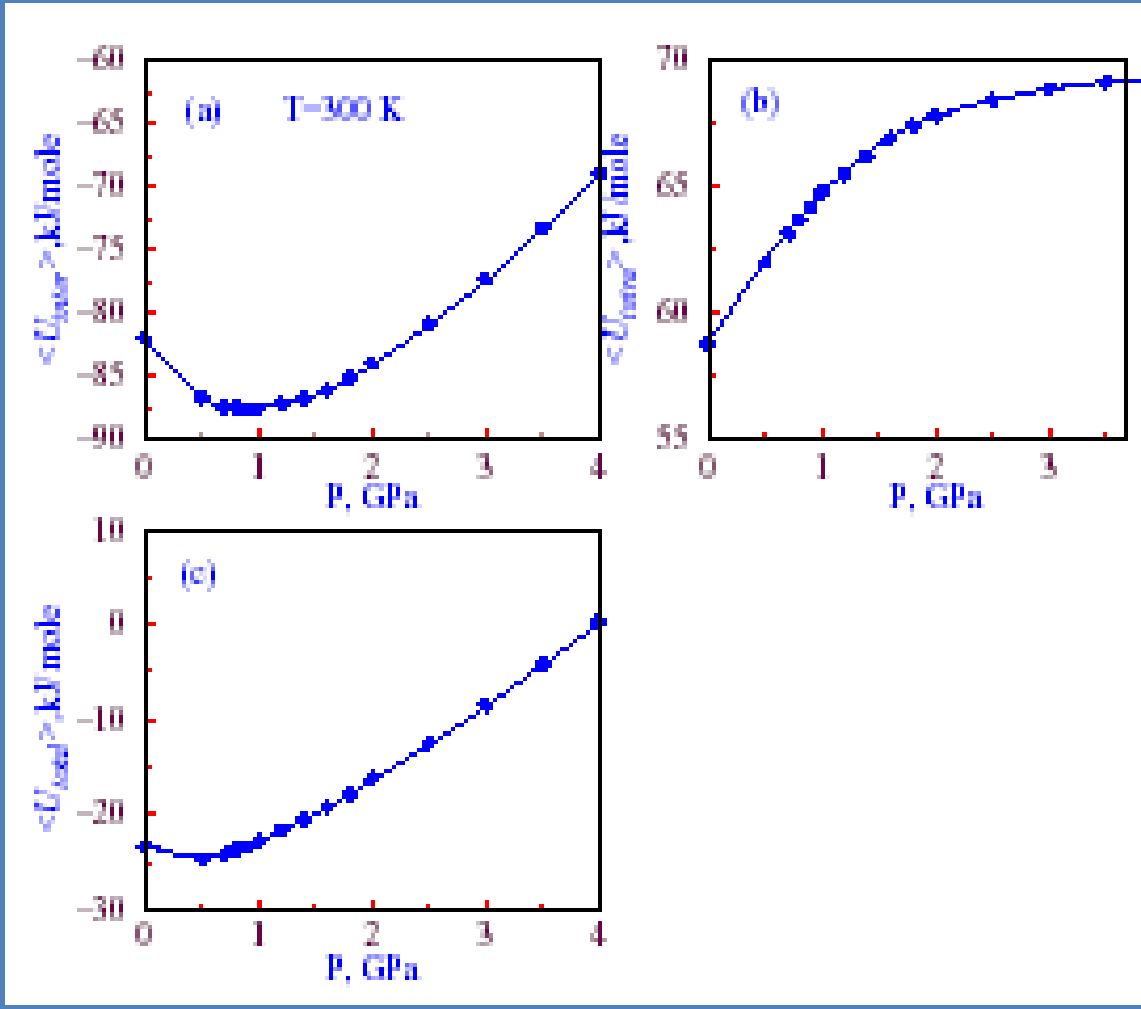

Is this universal behavior?

Twisted to planar conformational change in molecules

Bimodal ⟶ **Unimodal**

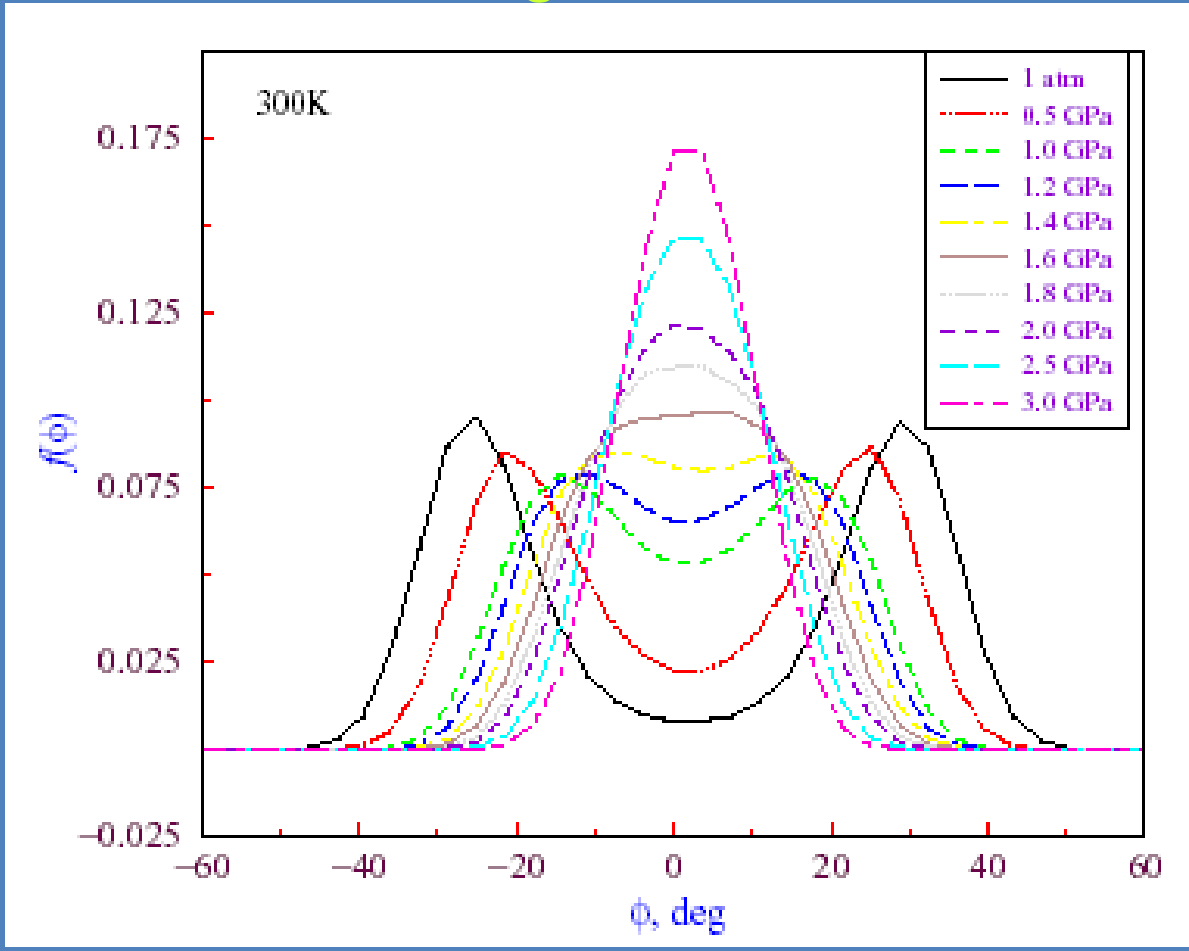

At low pressures the phenyl rings of molecules undergo flipping between the twist angles ±Φ.

As the pressure increases the molecules becoming planar which is evident from the population of molecules with Φ=0º.

Average dihedral angle and average absolute dihedral angle

<Φ> variation

↓

molecules are planar independent of pressure

<|Φ|> quantifies the twisted nature of the molecules at room temperature and the planarisation as a function of pressure.

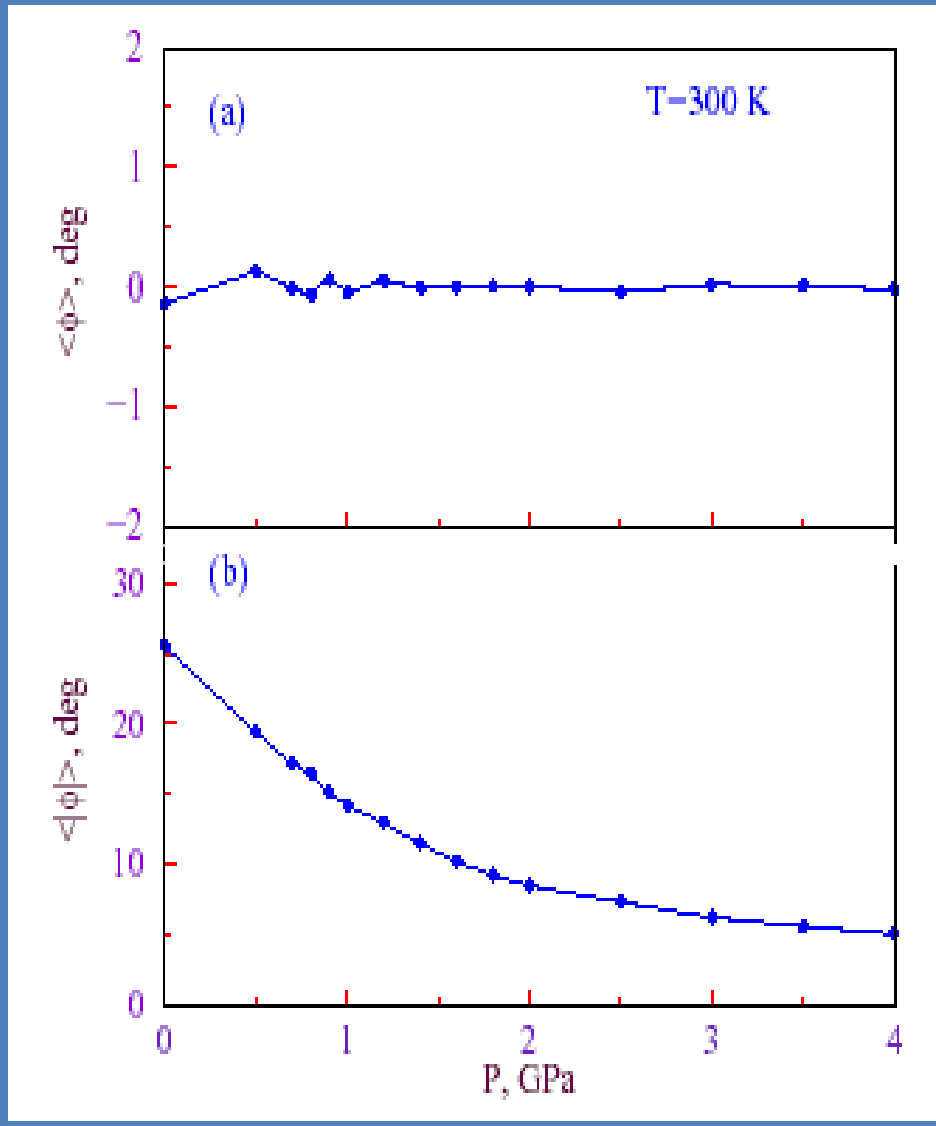

W-shaped to U-shaped transformation of U(Φ)

Effect of pressure is to Transform the shape of U(f) from W-shaped to U-shaped.

Earlier calculated energy difference between $U_{non\text{-}planar}$ U_{twist} is 8.59 kJ/mol.

From the present calculation the value is 8.00 kJ/mol

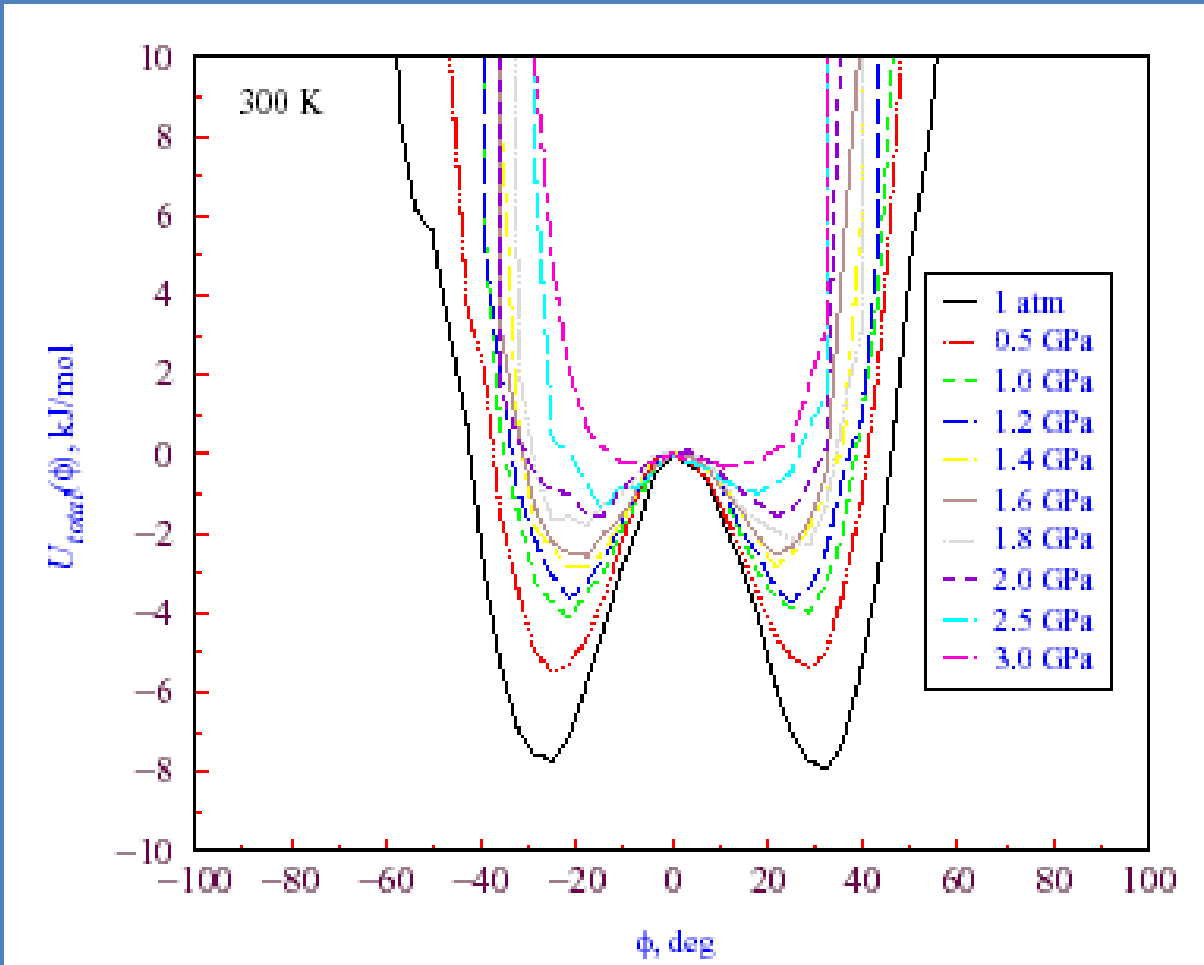

In contrast, temperature variation alters the population of Molecules In different states and doesn't alter the functional form

Nature of transition?

1. **Compressibility** calculated from the **volume fluctuation**.

$$\kappa = \frac{\langle V^2 \rangle - \langle V \rangle^2}{\langle V \rangle k_B T}$$

2. Derivative of volume with respect to pressure.

Compressibility as a function of pressure shows the **discontinuity** between 0.7-0.9 GPa suggesting the transition to be **second order**.

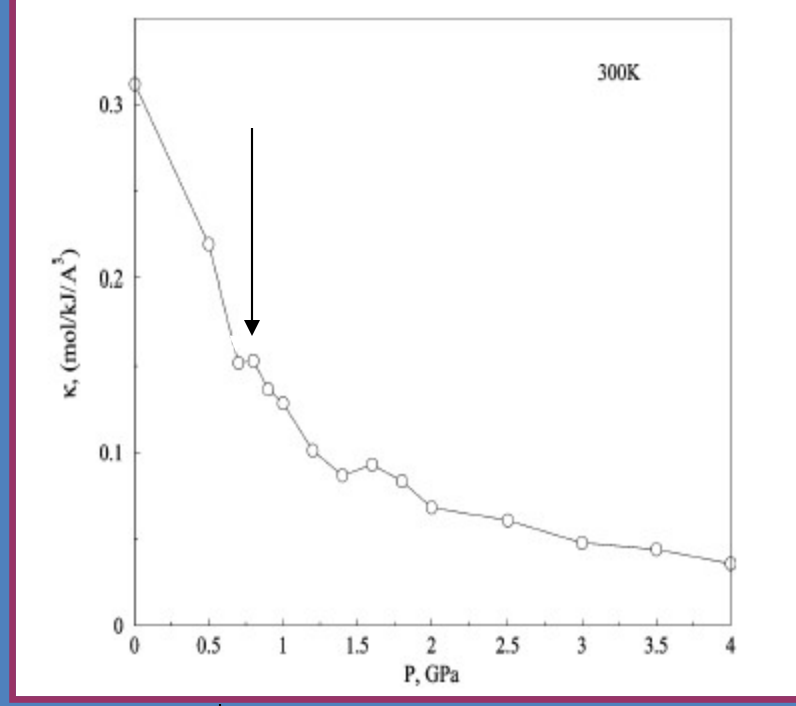

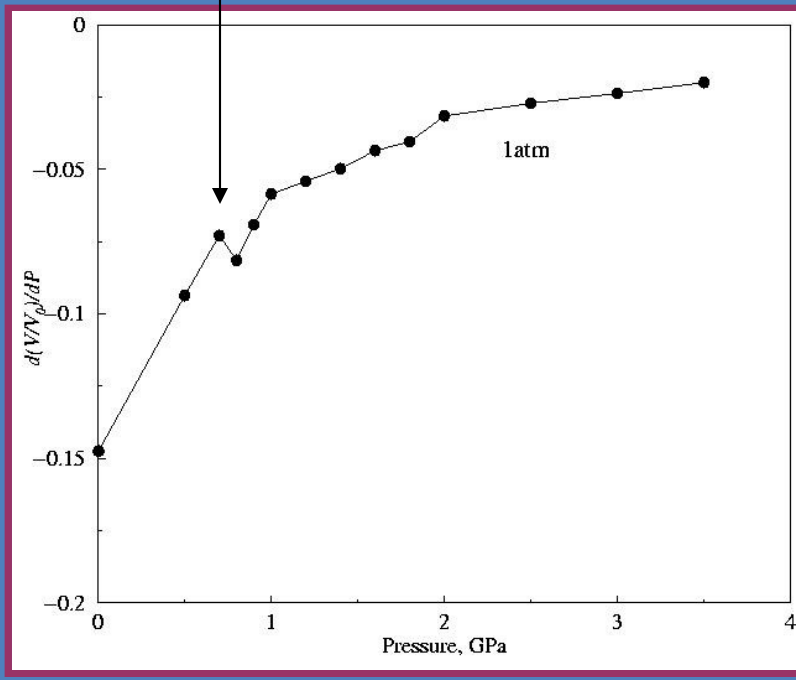

Snapshots during the simulations

A view along *c*-axis of the unit cell

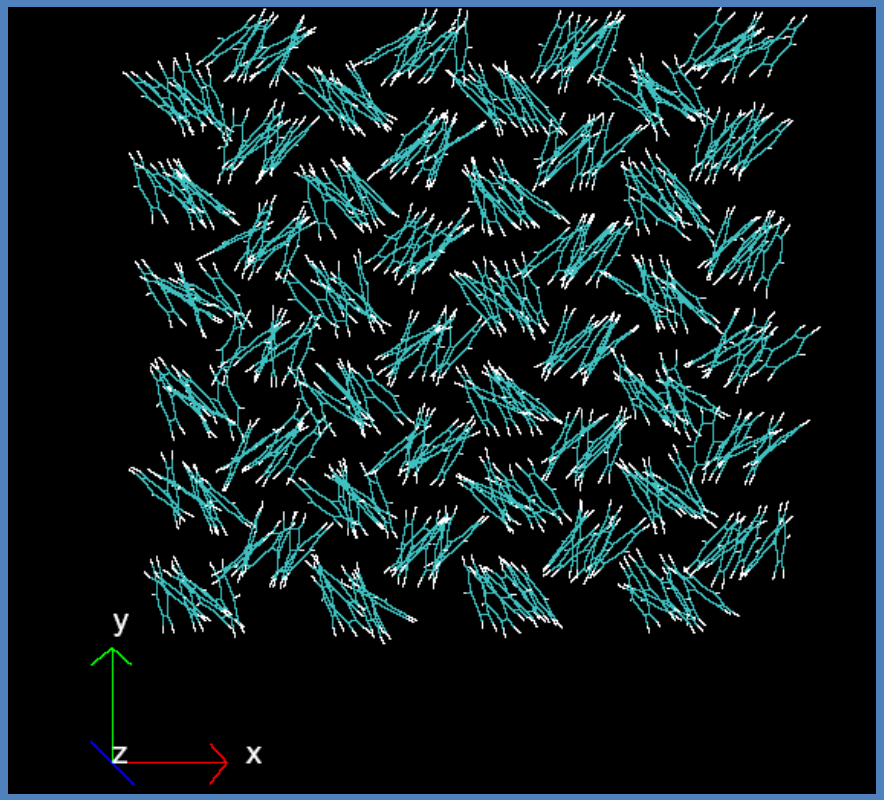

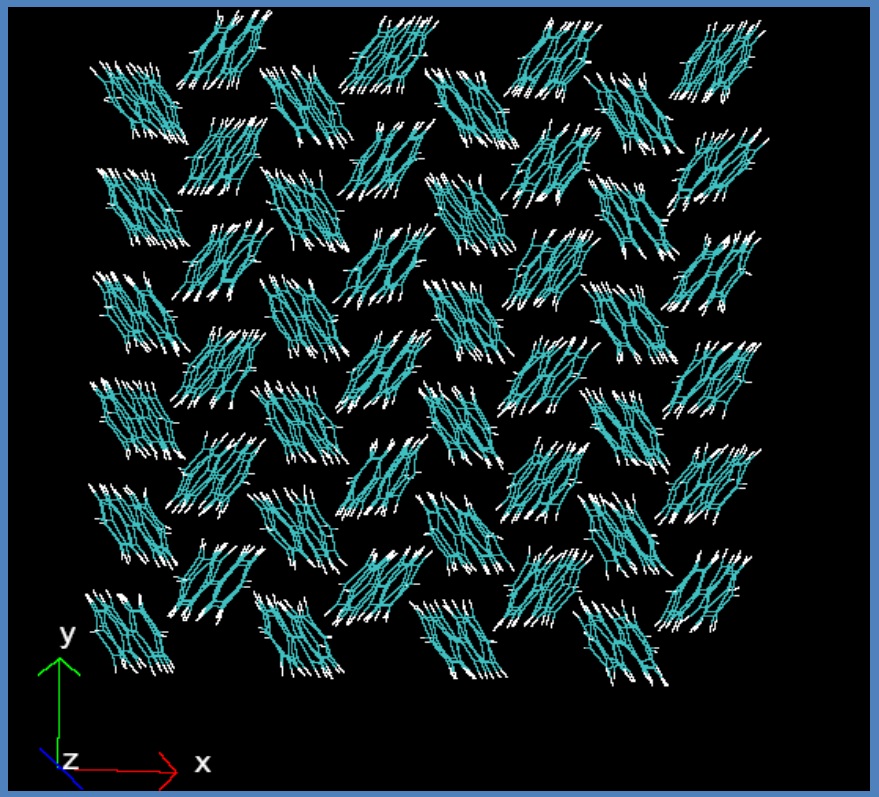

At P=1atm T=300K

At P= 4GPa T=300K

Snapshots during the simulations

A view along long molecular axis of the unit cell

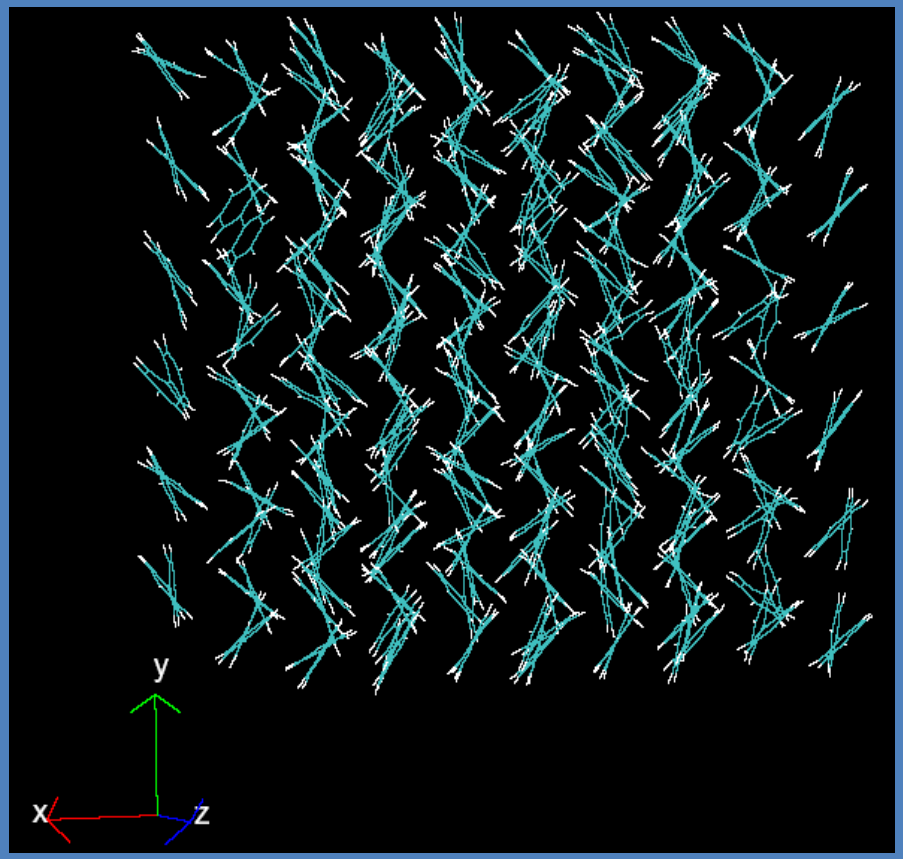

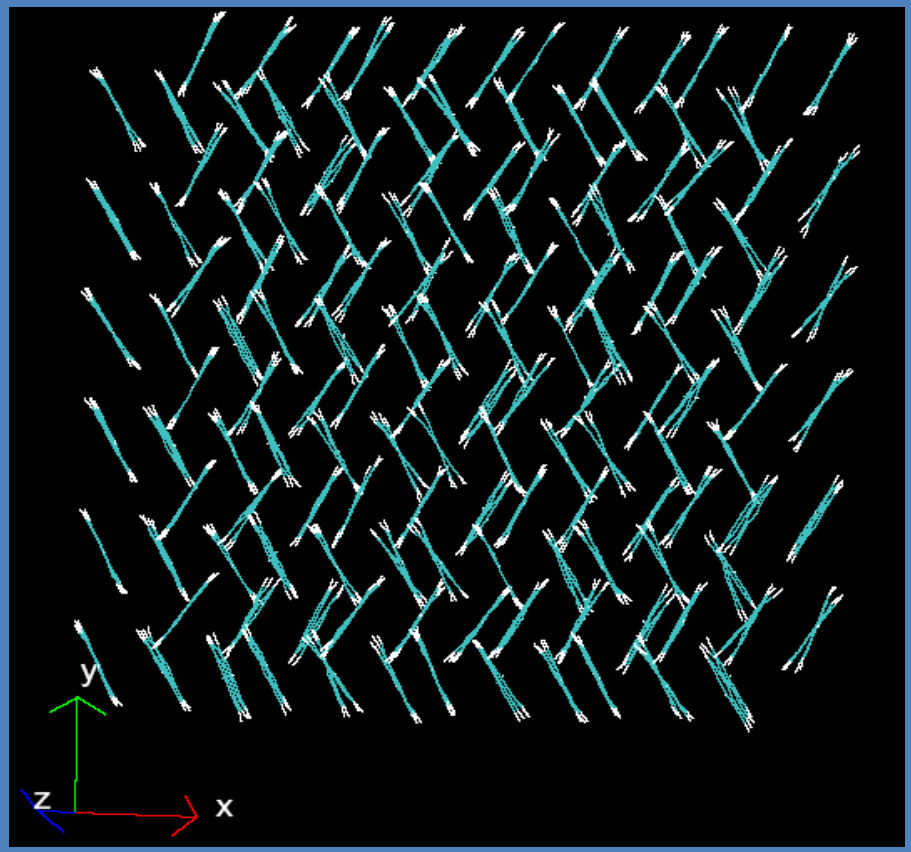

At P=1atm T=300K

At P= 4GPa T=300K

Evolution of IR spectra as a function of pressure

Average structure from simulations

↓

Ab initio electronic structure calculations (with structural constraints)
(Electronic, optical properties)

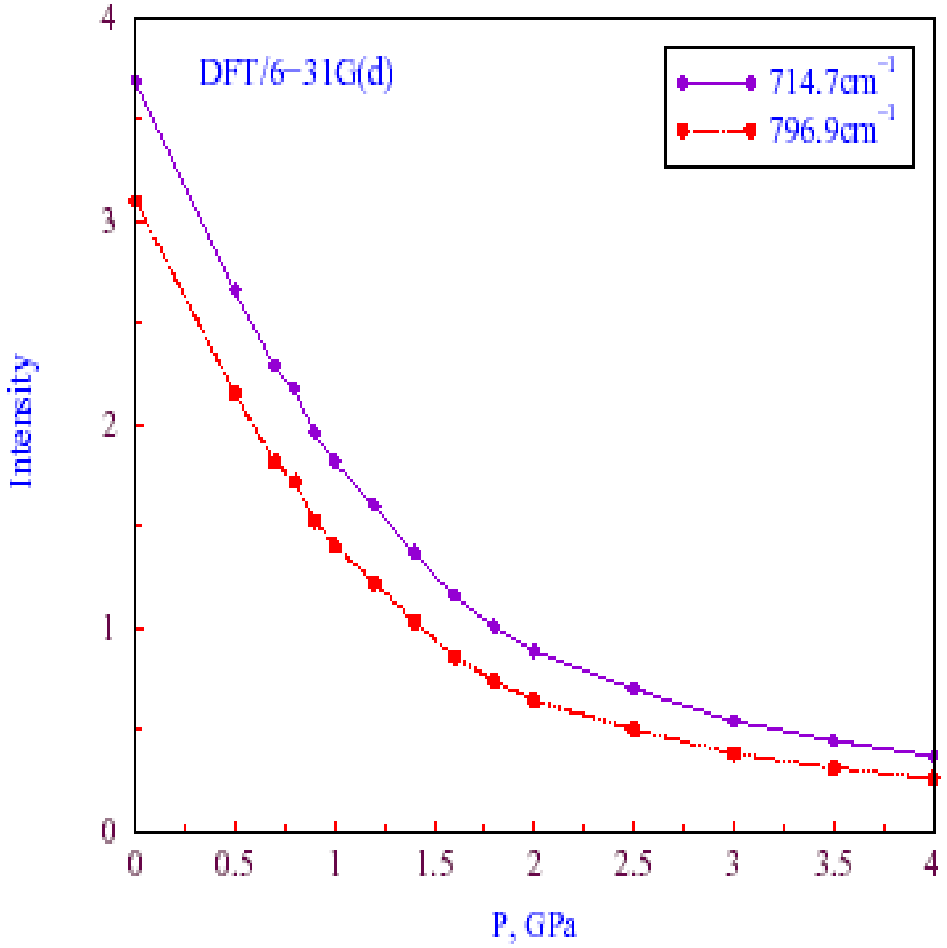

Disappearance of a few peaks (of out-of-plane bending modes
of hydrogen atoms)
indicates the **conformational changes from twisted to planar conformation.**

Out-of-plane bending modes of hydrogen

Conclusions:

1. Transition of the molecular conformation from twisted to planar form has been modeled successfully.

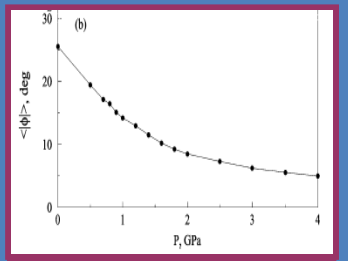

2. The transition may be a second order.

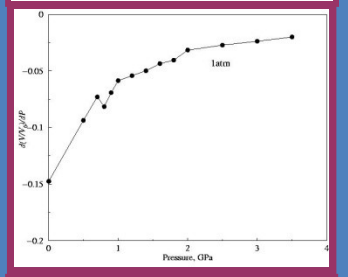

3. Transformation of the functional form of U(ϕ) from W-shaped to U-shaped has been observed

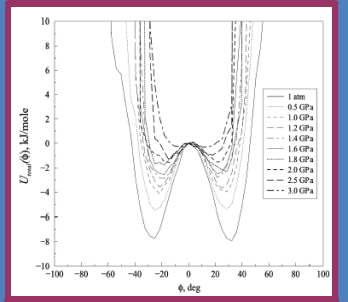

4. Transformation of bimodal distribution of dihedral angles to an unimodal distribution has been observed.

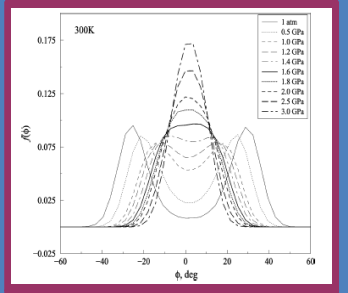

5. IR spectra as a function of pressure has been calculated and disappearance of out-of-plane bending modes of hydrogens has been observed

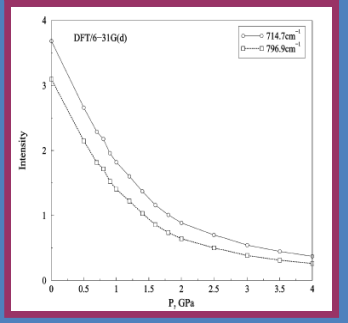

CHAPTER 3

Pressure induced ordering transition in *p*-terphenyl

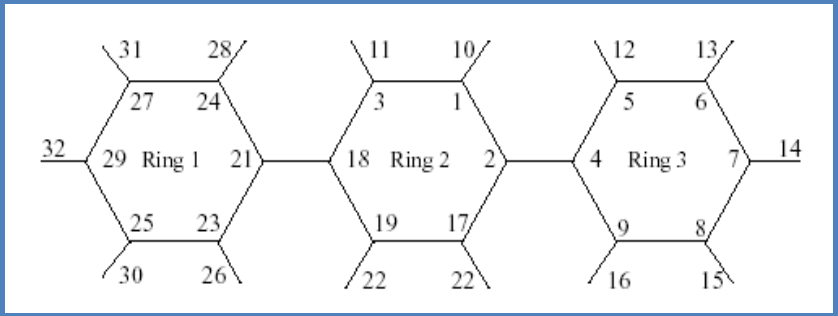

1. Modeling the room temperature phase of p-terphenyl with different potential models including the improved potential model

2. Pressure variation calculation up to 5 GPa and comparing the simulated structure with the X-ray diffraction results

3. Understanding the flipping motion associated with the phenyl rings

Modeling the room temperature phase of p-terphenyl

Model I - Williams intermolecular interactions
- BHS for intramolecular interaction

Model II - Filippini and Gavezzotti intermolecular interactions
- BHS for intramolecular interaction

Model III - Modified Williams intermolecular interactions
- intramolecular interaction from *ab initio* calculations

Model IV - Modified Filippini intermolecular interactions
- BHS for intramolecular interaction

Table 5 Average cell parameters (with the percentage deviation) at 300K for models I-IV compared with the experimental cell parameters.

	a, Å	b, Å	c, Å	α, deg	β, deg	γ, deg
XRD	8.02	5.58	13.58	90.00	92.10	90.00
Model I	8.52 (6.2)	5.47 (-2.0)	16.49 (21.4)	86.67 (-3.7)	91.04 (-1.2)	89.91 (-0.1)
Model II	8.30 (3.5)	5.40 (-3.2)	15.68 (15.5)	91.14 (1.3)	88.85 (-3.5)	89.97(-0.0)
Model III	7.83 (-2.4)	5.77 (3.4)	12.15 (-10.5)	91.25 (1.4)	97.26 (5.6)	89.38 (-0.7)
Model IV	8.11 (1.1)	5.21 (-6.6)	12.73 (-6.3)	88.94 (-1.2)	90.42 (-1.8)	89.87 (-0.1)

Overall, all the potential models fail to reproduce the cell parameter *c*.

Model IV reproduces structure reasonably well within the allowed threshold value for the deviations.

These potential models are derived with the rigid body assumption of molecules.

Structure: (Compared with X-ray diffraction results by Pushnig *et. al*):

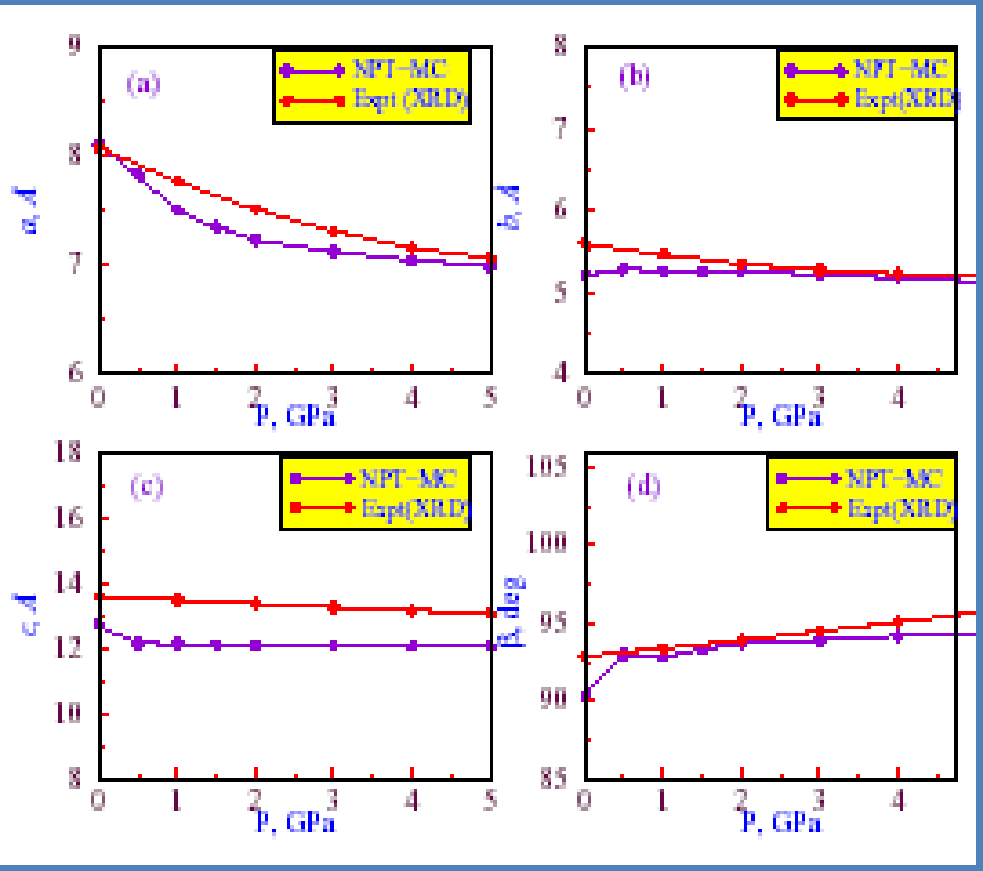

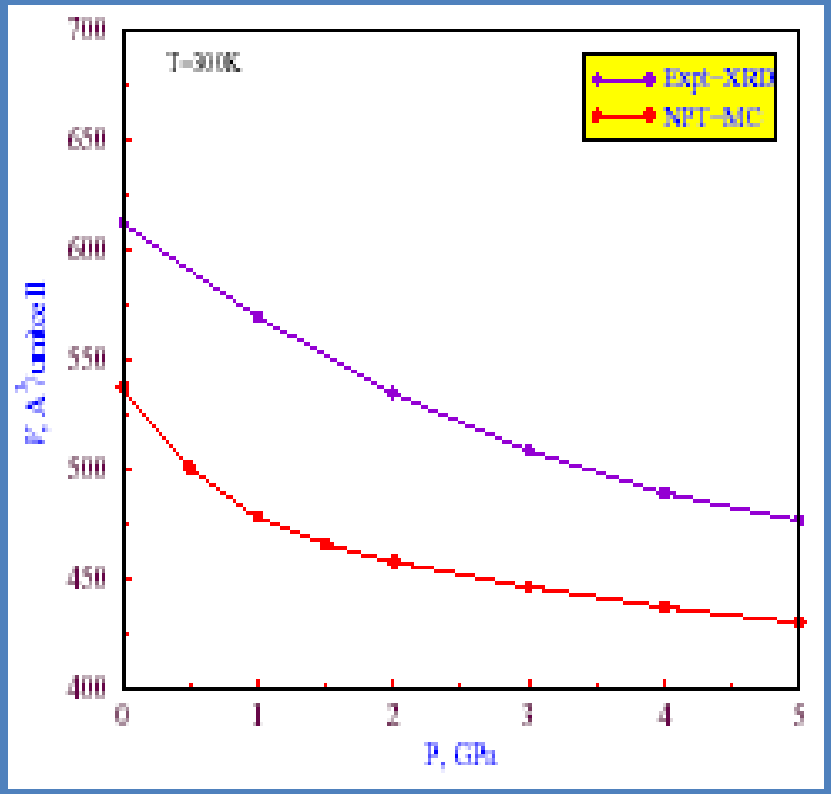

1.Except *c* all cell parameters are reproduced with in the threshold limit all over the pressures at 300K

2. Simulated cell volume is 8-10 % lesser than that of experimental structure.

Puschnig et al., *High Pressure Res.*, **22**, 105(2002)

R.d.fs as a function of P

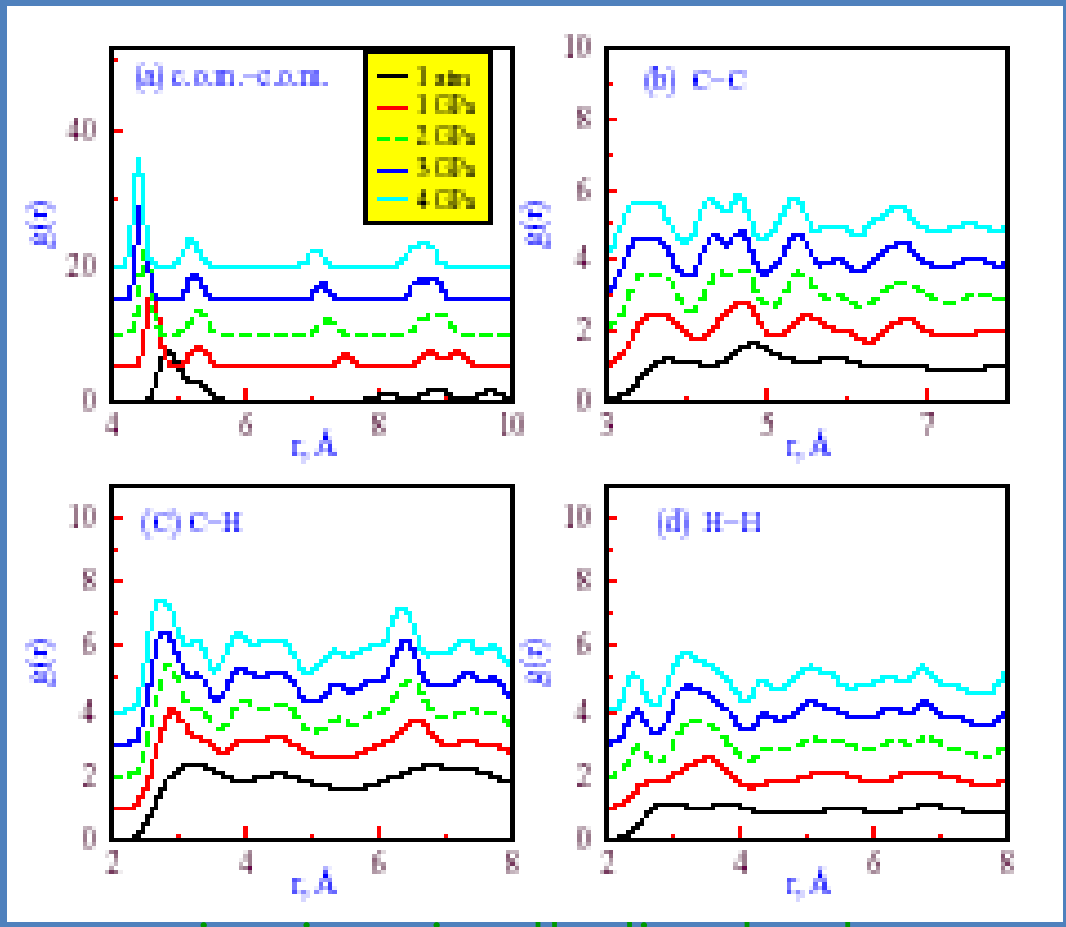

At P=1atm and T=300K the structure is orientationally disordered

At and above P=1 GPa the structure is orientationally ordered

Appearance of a new peak in c.o.m.-c.o.m. r.d.f and shifting of the second peak towards lower *r* suggests that

Orientational order affects the translational order to a greater extent in this case.

Energetics:

U_{inter} shows a minimum

U_{intra} increases and reaches a constant value at 2 GPa suggesting no further changes in the molecular level.

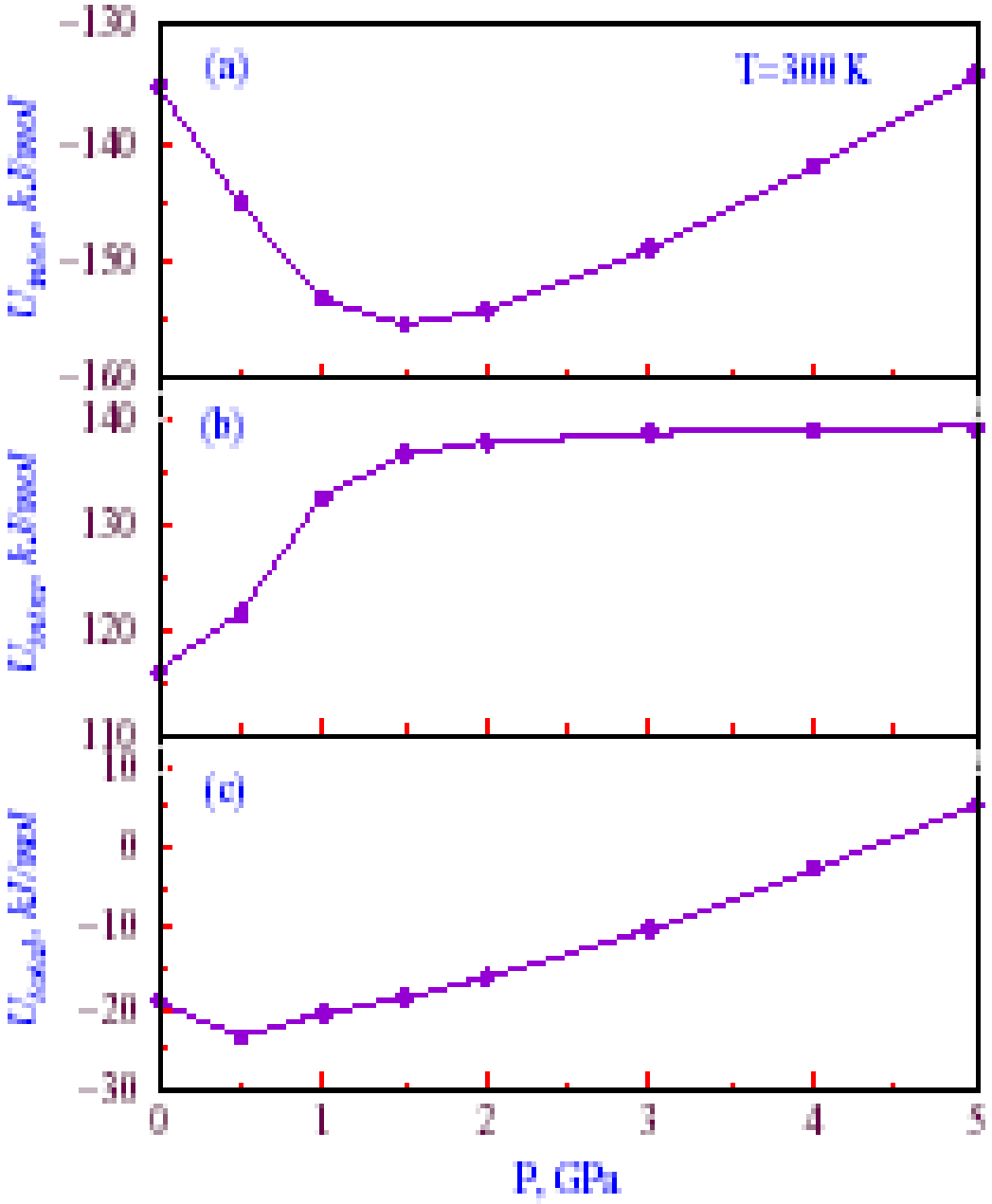

Dihedral angle distributions as a function of pressure:

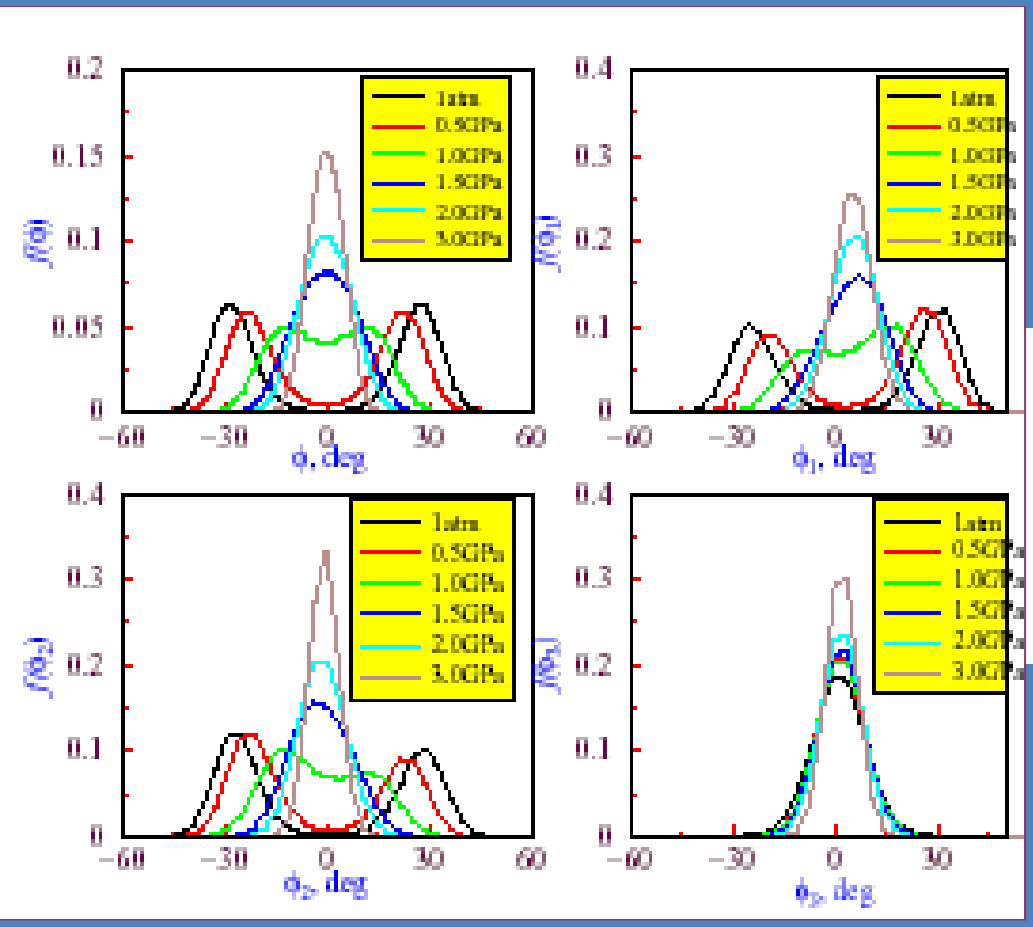

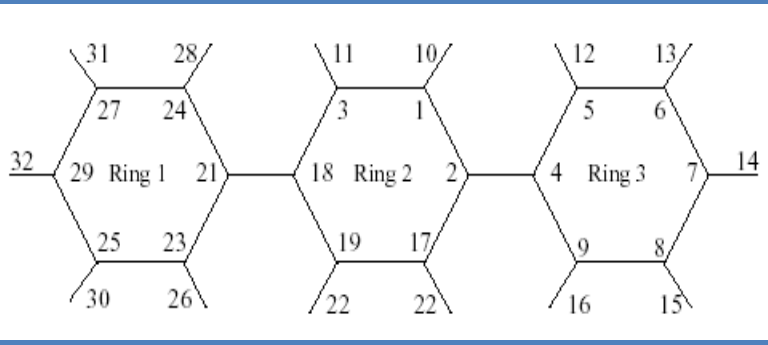

Between the pressures 1 GPa – 1.5 GPa the transition from bimodal to unimodal distribution of dihedral angles occur.

Transformation in functional form of potential energy profile

Probability density function of ϕ is given by

$$f(\phi) = C_1 exp(-u(\phi)/kT$$

$$u(\phi) = C_2 - kT\ ln\ f(\phi)$$

where C_2 is $kTlnC_1$.

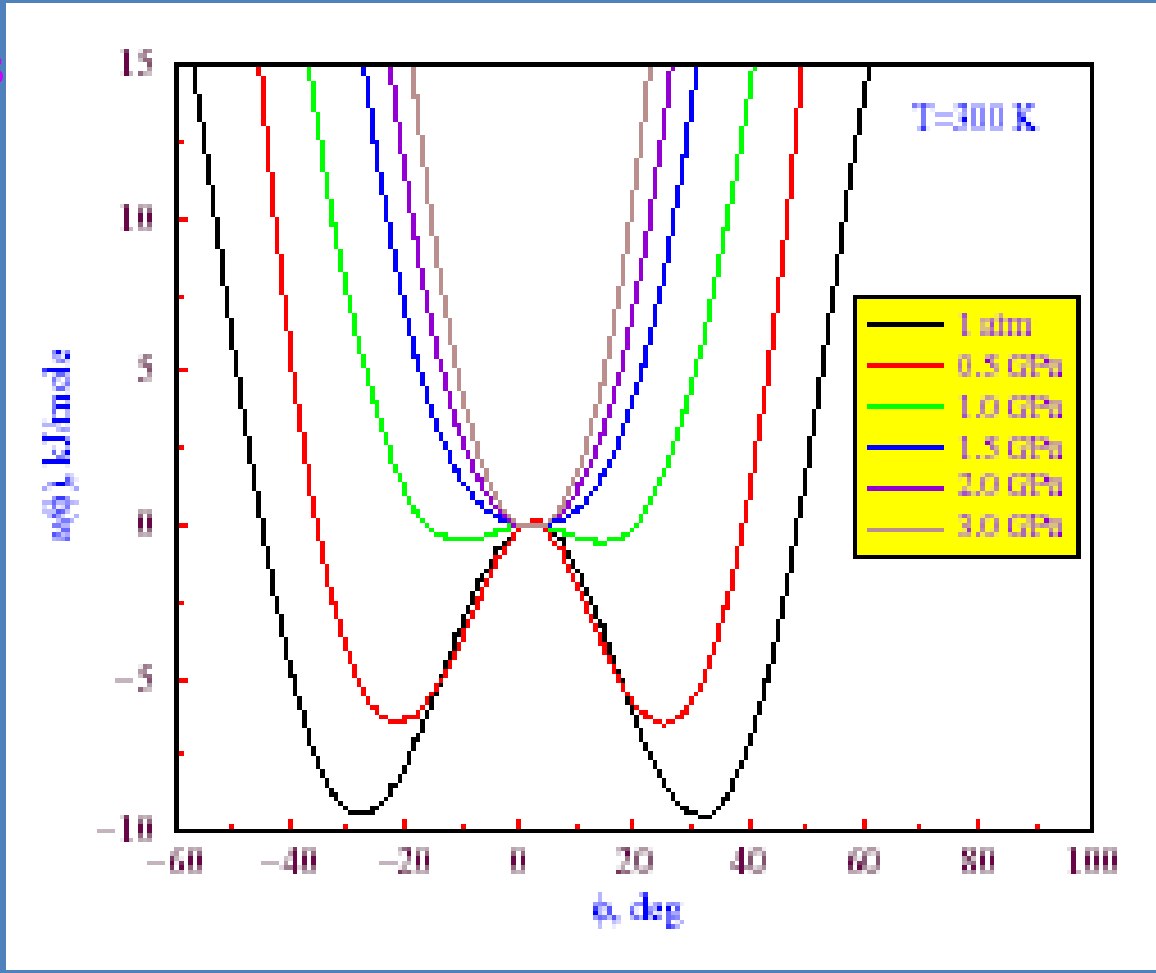

W-Shaped → **U-shaped (at 1.5 GPa)**

Snapshot of simulation

A view along long molecular axis

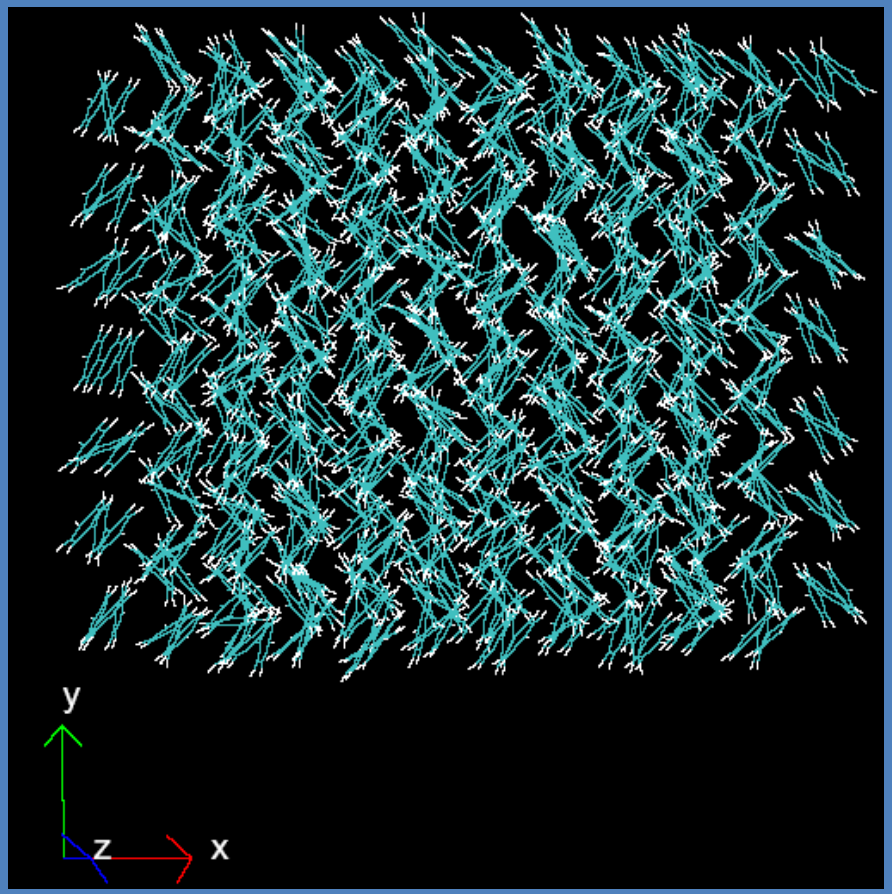

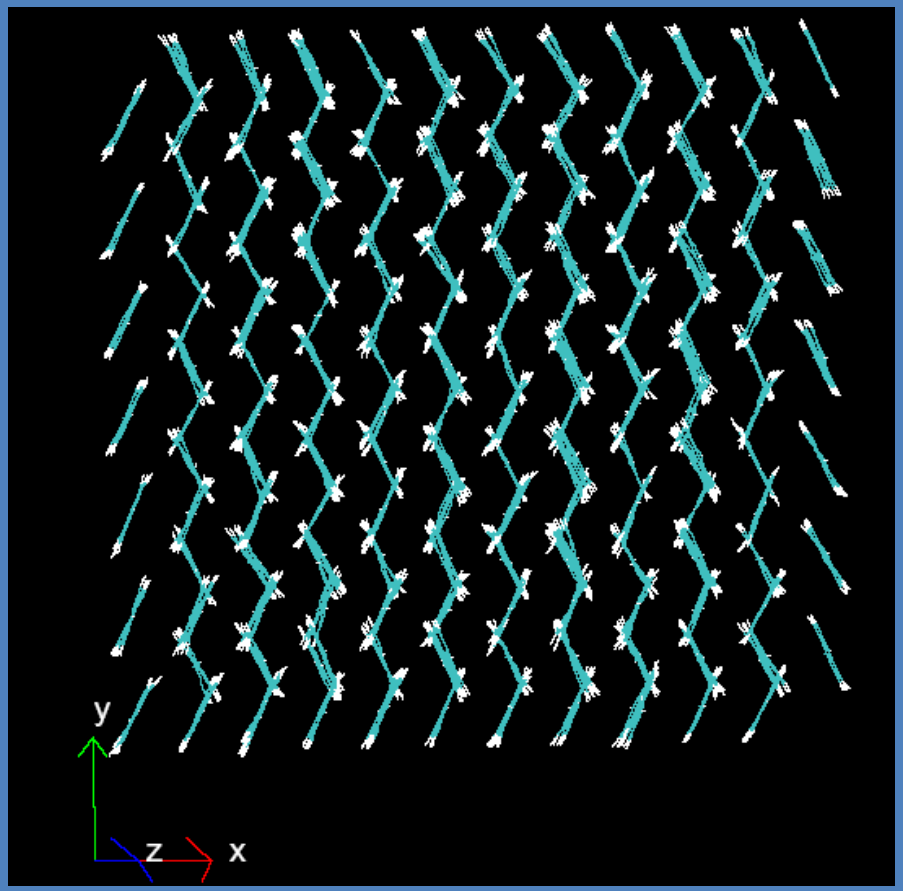

P = 1 atm / T = 300K

P = 4 GPa / T = 300K

Snapshot of simulation

A view along c axis

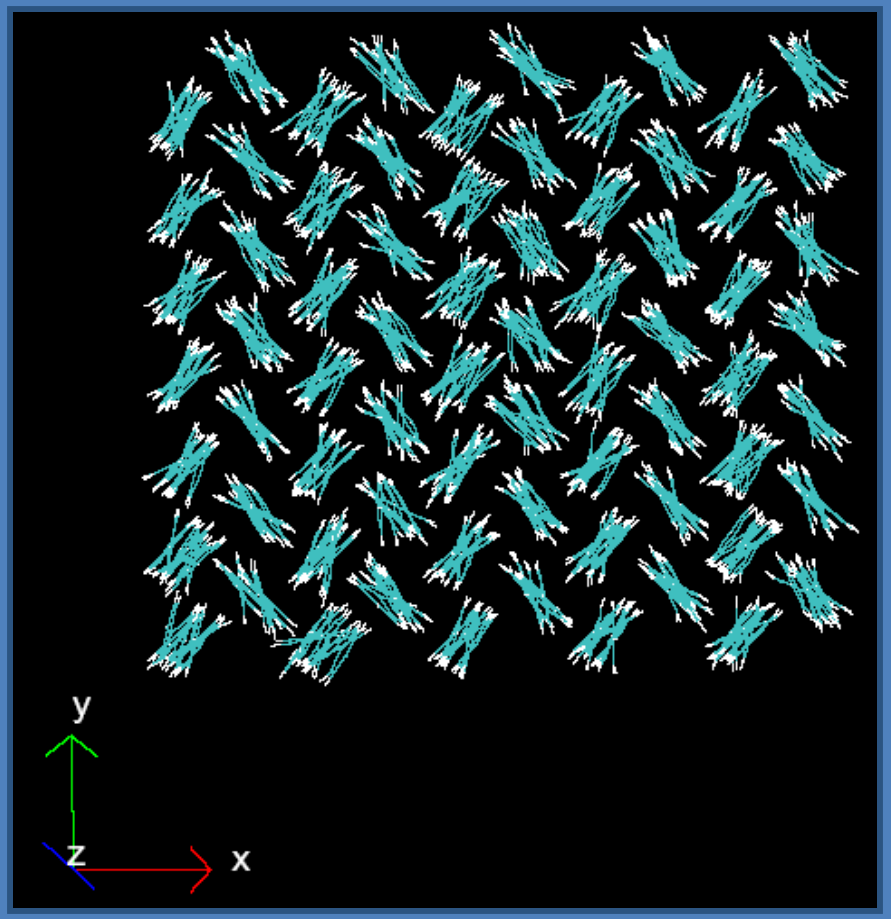

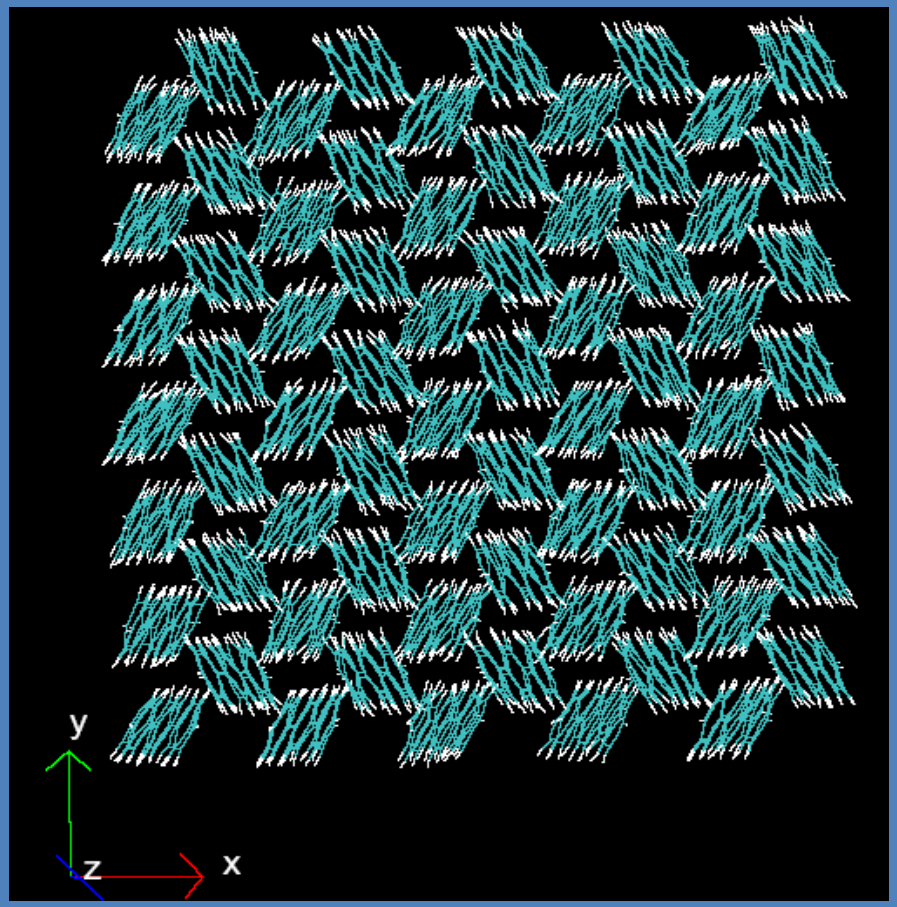

P = 1 atm / T = 300K

P = 4 GPa / T = 300K

Conclusions:

1.Structure of room temperature *p*-terphenyl has been reproduced reasonably well with intermolecular potential refined by us and BHS intramolecular potential

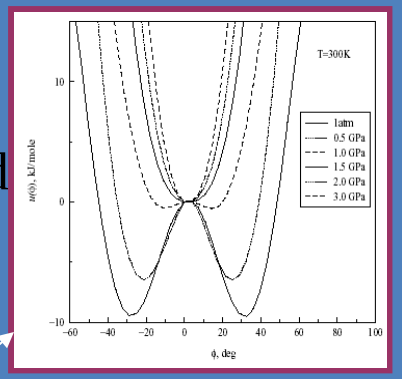

2. Transformation of the functional form of $U(\phi)$ from W-shaped to U-shaped has been observed

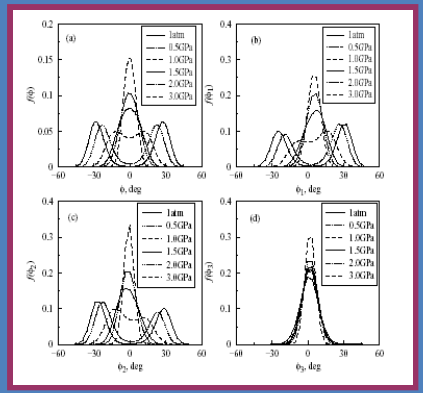

3. Transformation of bimodal distribution of dihedral angles to an unimodal distribution has been observed.

4. Complete planarisation occur at the pressure 1.5 GPa.

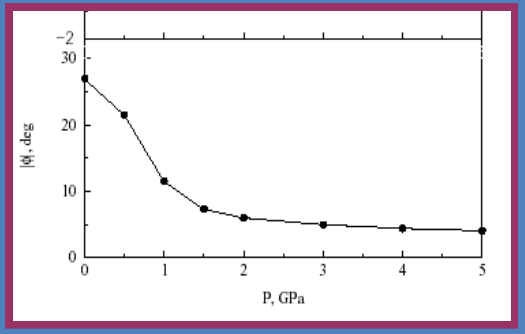

Chapter 4

Temperature induced conformational disorder in stilbene (Molecular pedals)

Experimental results

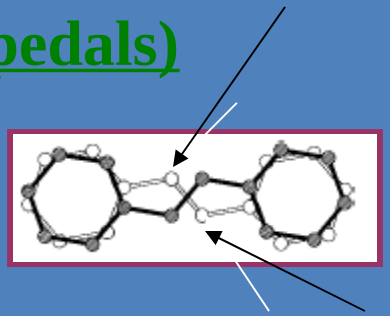

Temperature dependence of the difference Fourier map indicated **two residual peaks** which disappeared at low temperature and **increased in intensity at higher temperatures**.

! INDICATION OF DYNAMICAL DISORDER

The disorder has been attributed to the inter-conversion between the conformers through **pedal-like motion**.

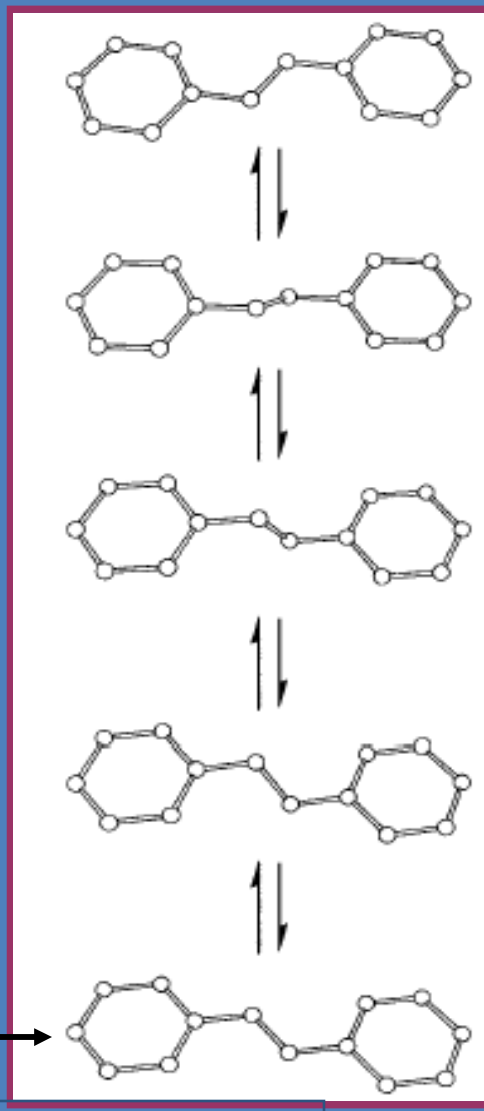

Harada, J.; Ogawa. K.; *J. Am. Chem. Soc.*, **123**, 10884(2001)

Disorder is there even at Site 1

Earlier structural studies report the disorder only at site 2.

Recent studies by Ogawa and Harada Report the disorder at site 1.

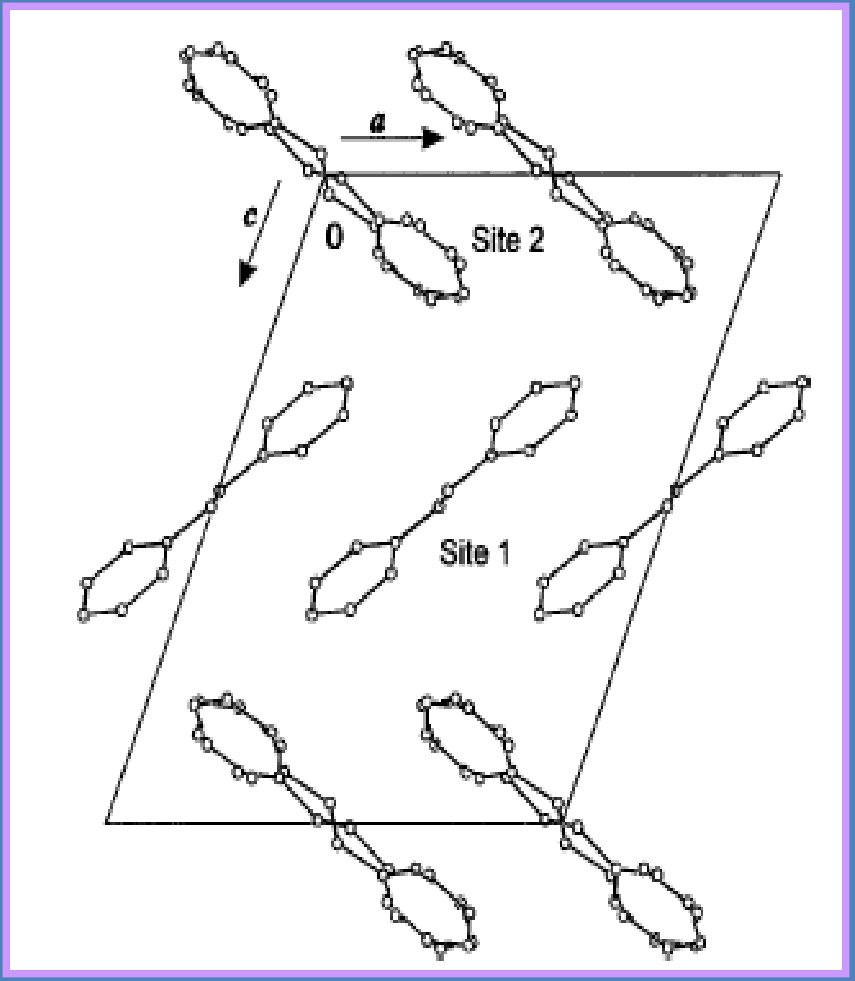

Harada, J.; Ogawa. K.; *J. Am. Chem. Soc.*, **123**, 10884(2001)

Objectives of our calculations

Are site 1 molecules too disordered?

What are the two transitions observed from Raman spectroscopic measurements in the T range 115-375 K

Does the anomalous ethylene bond length variation exist or is it an artifact of fitting procedure used in the disorder model for solving structure?

Structure

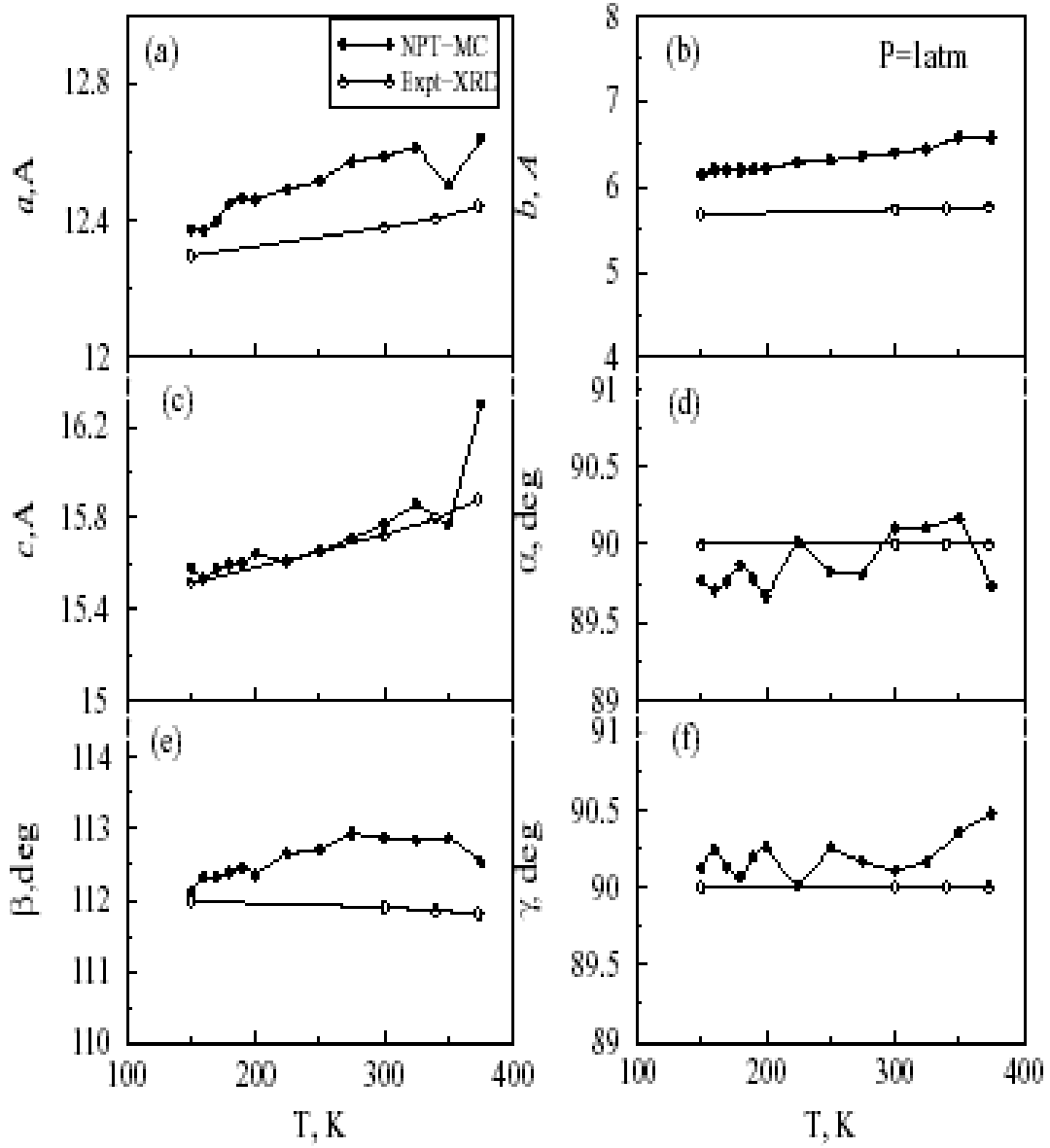

Validity of the potential model

This potential model is able to predict the structural quantities with in the threshold limit except for the cell parameter b Where the deviation is 6-10%.

Dynamical disorder?

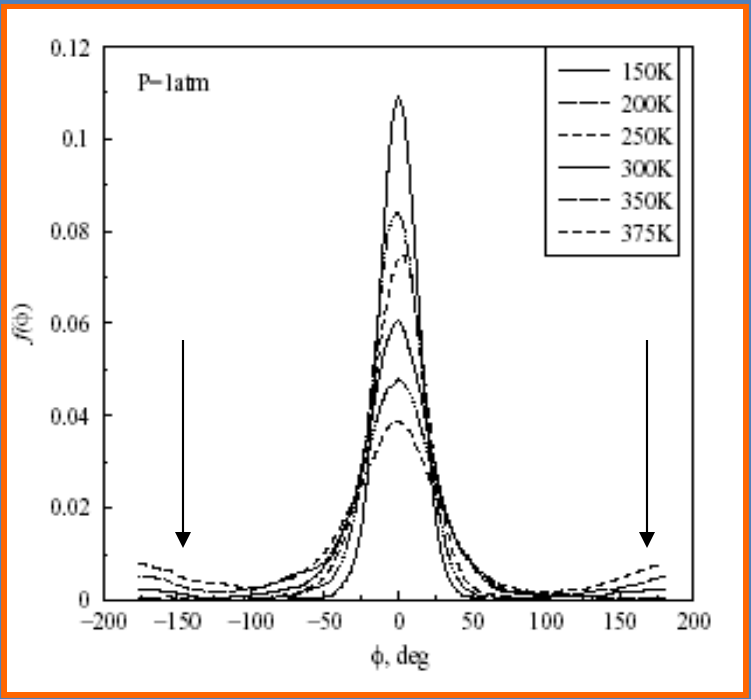

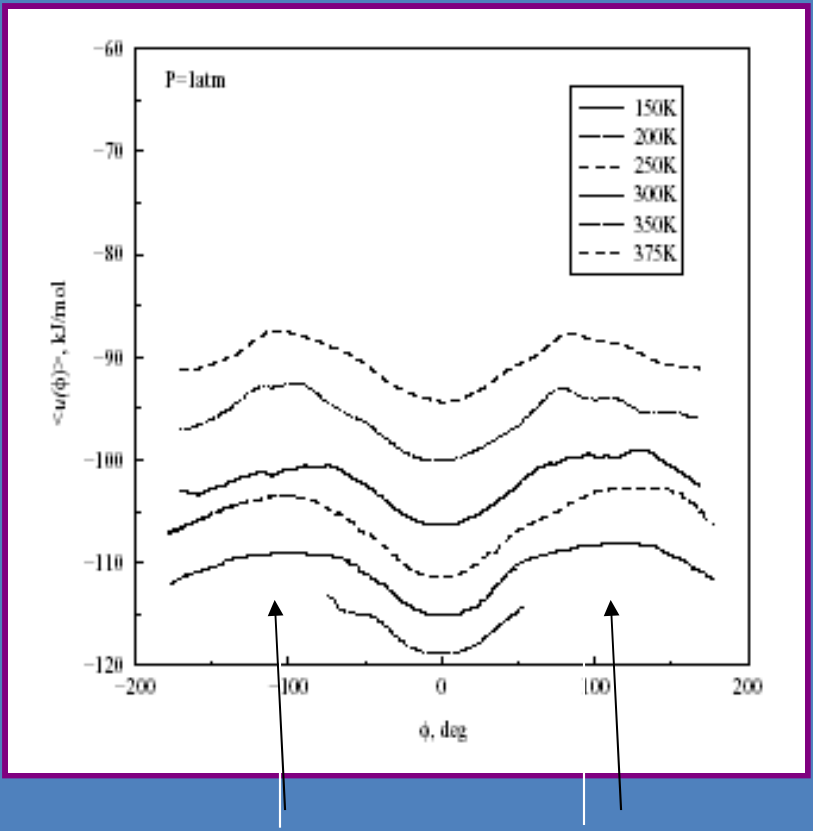

Pedal-like motion seems to **occur** at temperatures higher than **200K (actually at 180K).**

The energies of the minor conformer is **not equal to** the major conformer (with 0° dihedral angle) which is not the case in the **gaseous phase**.

Disorder at Site 1 and site 2

conformational disorder starts at 180K at site 2 and at 250K at site 1.
At 300K the barriers at -90 deg is 7.362 and 6.860kJ/mol (Site 2 and site1)

This corresponds to 59.70 K(0.5093/R)

$$T_1^{onset} = T_2^{onset} + 59.70K$$

With the error bar ±8K.

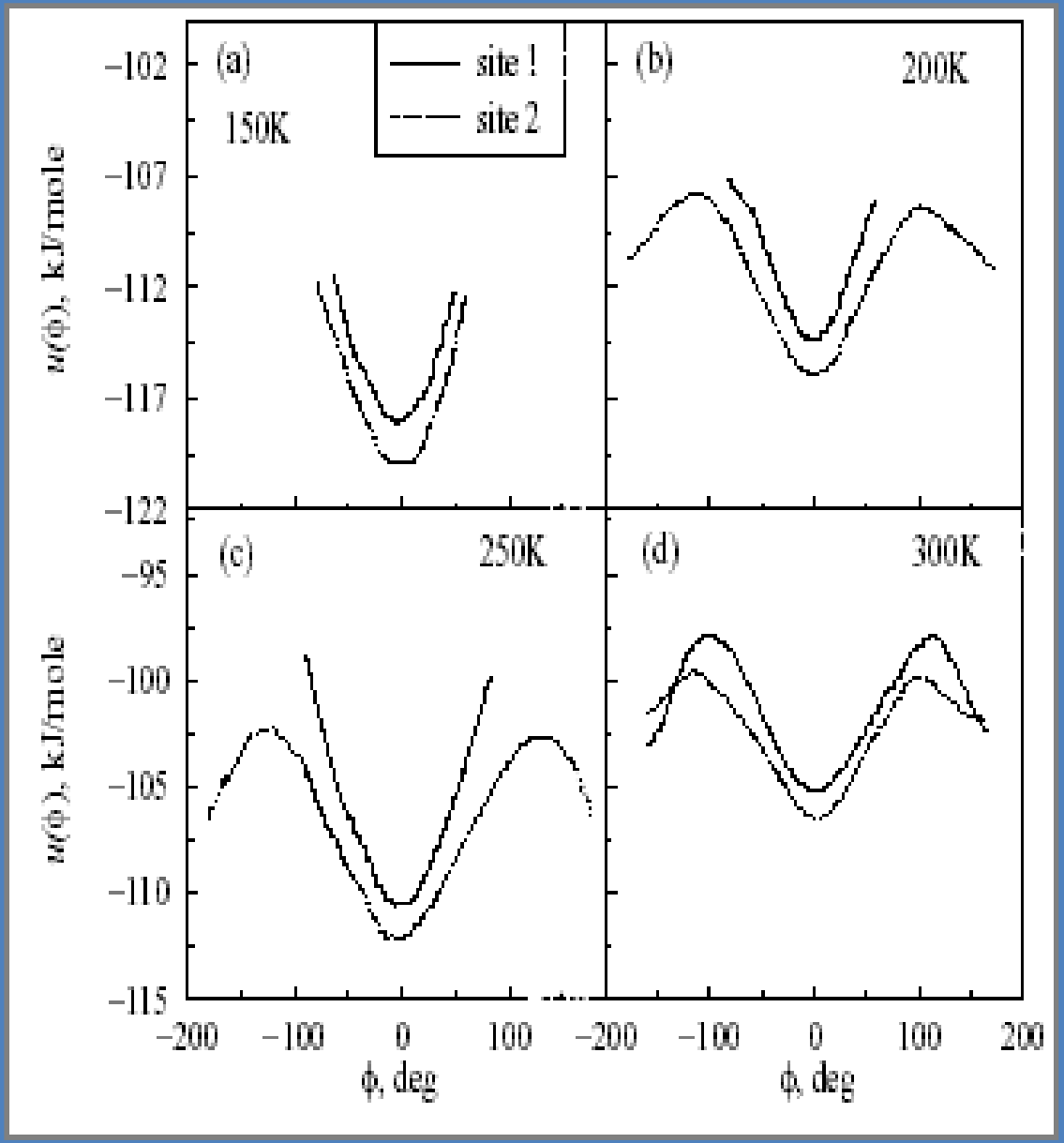

Explaining the two transitions in the range 113K-375K

Raman spectrocopic studies* report **two transitions** in the temperature range **113K-375K** which is comparable to this observation.

The first transition can be attributed to the **disorder** occurring at **site 2.**

The second transition can be attributed to the **disorder** at **site 1**.

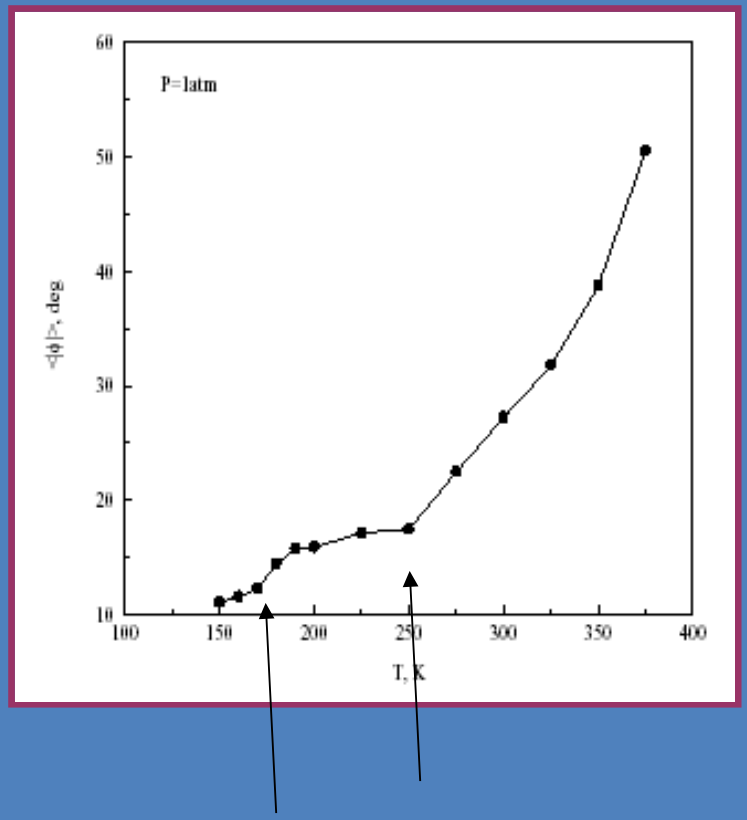

*Chakrabarti, S.; Misra, T.N.; *Bull. Chem. Soc. Jpn.*, **64**, 2454(1991).

Thermodynamically more stable and at the same time Kinetically less stable

Molecules at site 2 are strongly interacting than the molecules at site 1. (***by 2 kJ/mol***)

! So we expect less disorder at site 2

But as the barrier associated with site 2 for the interconversion is lesser by **0.5 kJ/mol** than the barrier for site 1.

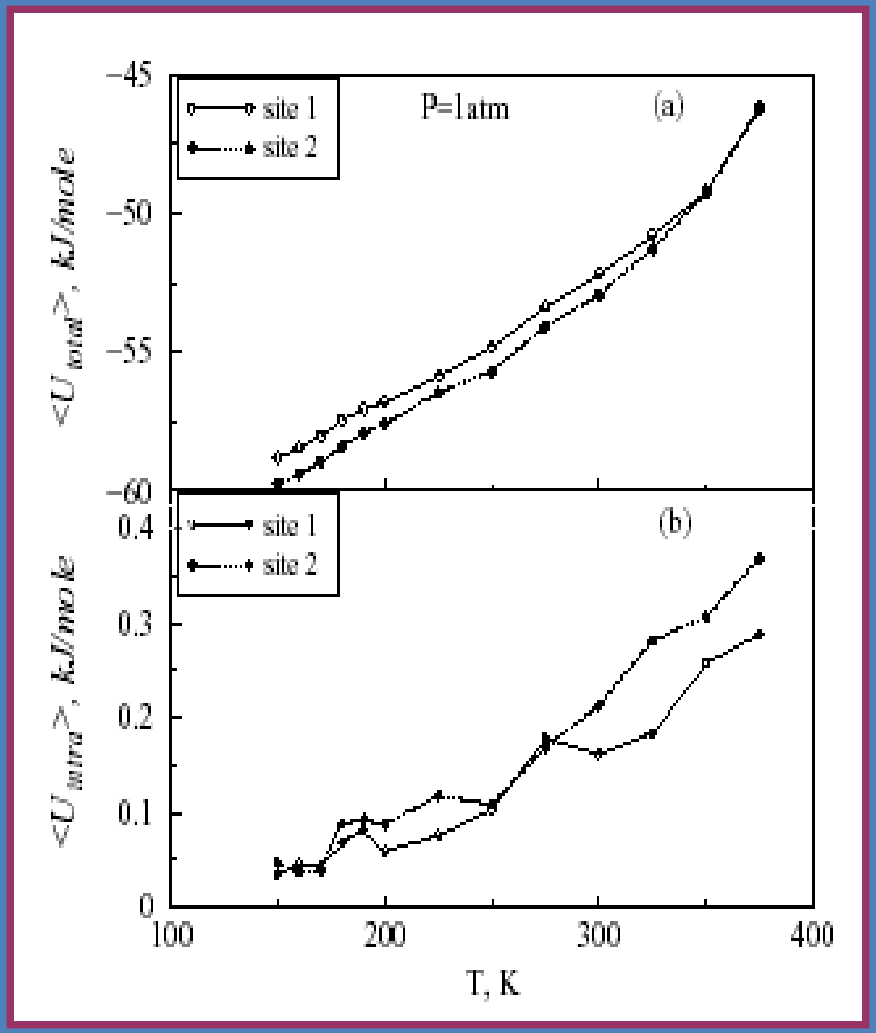

Molecules at Site 2

Strongly interacting but still prone to have more disorder.

From slope of the van't Hoff plot

$\Delta H_{\text{disordered-ordered}}$ = 15.59 kJ/mole

Higher than experimental results*

From slope of the Arrhenius plot

E_a= 12.46 kJ/mol

Better than E_a= 63.4 kJ/mol by Galli et al

Harada, J.; Ogawa, K.; *J. Am .Chem. Soc.,* **126,** 3539(2004**).**
Galli et al., J. *Am. Chem. Soc.,* **121,** 3767 (1999**).**

Snapshots at 150K and 300K and at 1atm pressure

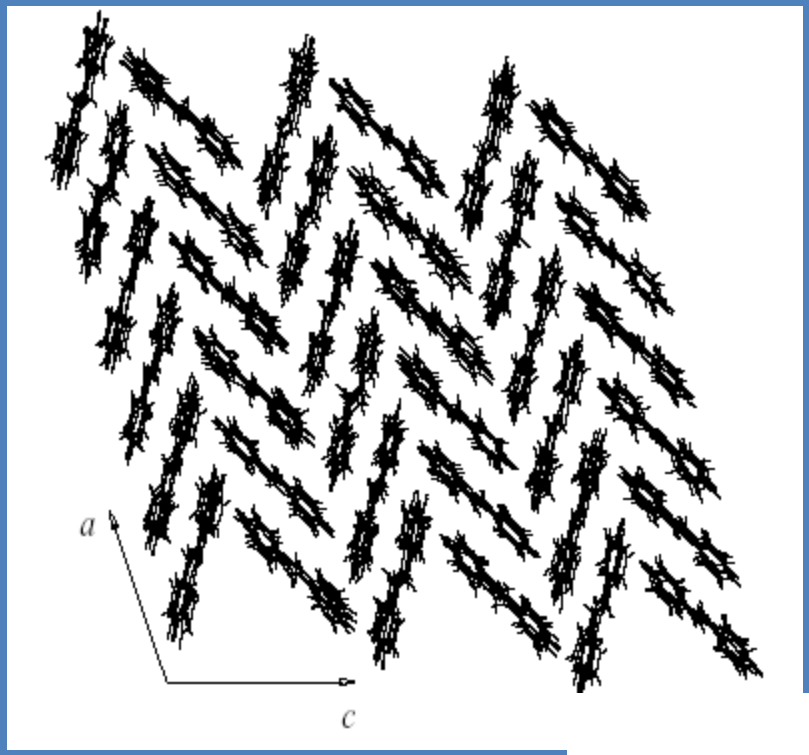

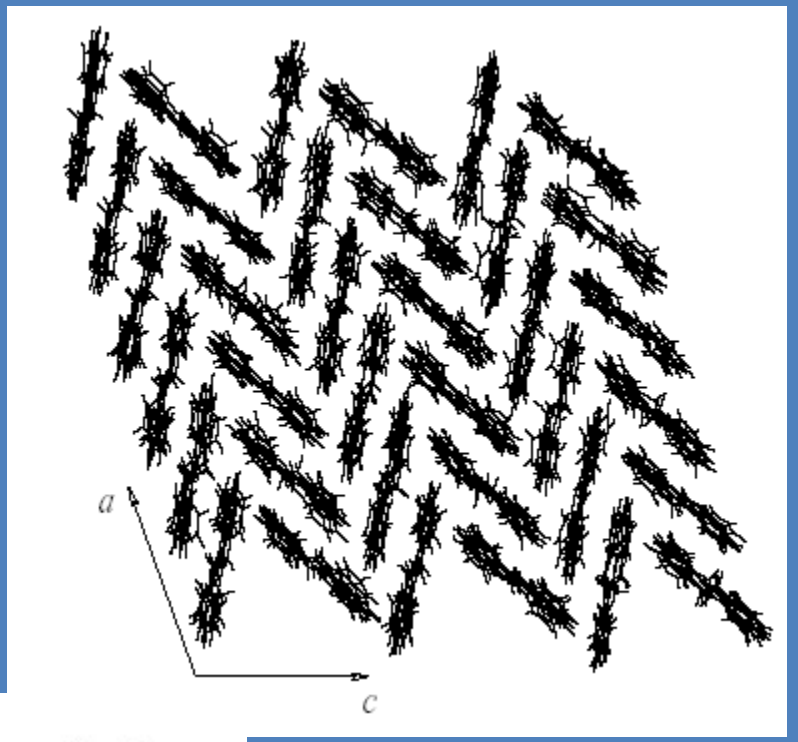

No disorder

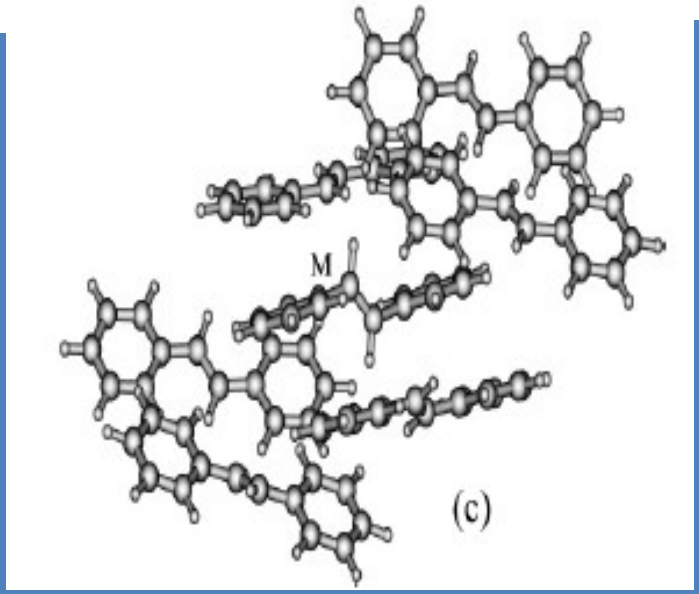

Disorder is 8-10%

Bond lengths variation as a function of temperature

Bond length variation as
function of dihedral angle.
Ab initio calculation at
FT/6-31G(d) – **constrained**
ptimization)

Dihedral angle distributions
s a function of temperature.

Average bond length as a
nction of temperature.

Shows **two** discontinuities

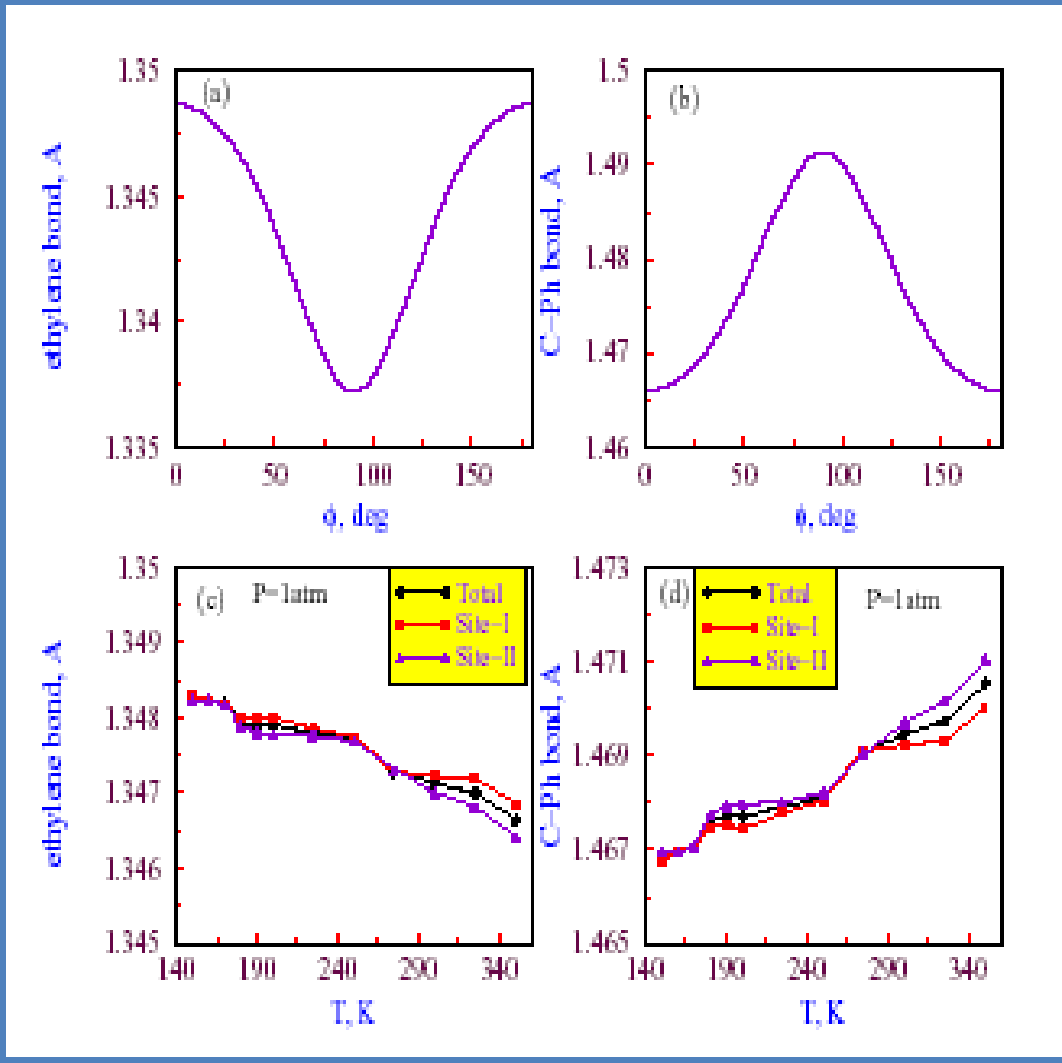

(a) Disorder at site 2 (b) Disorder at site 1

Nature of transition:

Thermal expansion coefficient

At 170K corresponding to the onset of disorder at site 2

At 250K corresponding to the onset of disorder at site 1

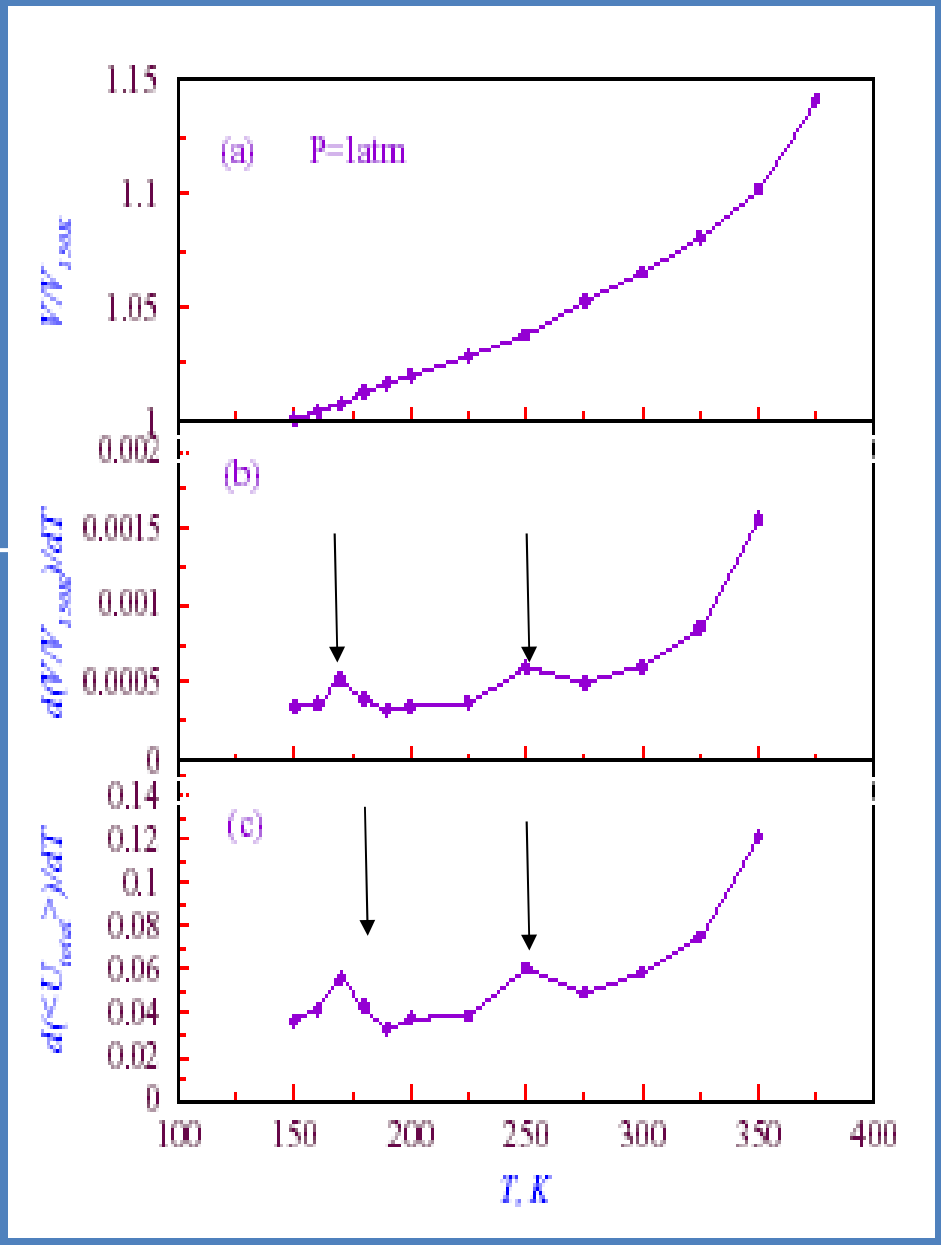

Conclusions

1. Simulation results could show the **dynamical orientational disorder** in stilbene as a function of temperature.

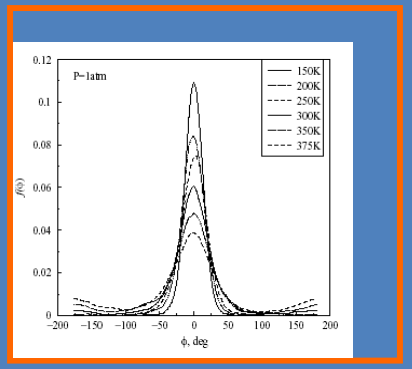

2. Disorder treats molecules in different sites in different way
(a) In site 2 disorder occurs at lower temperature (at 180K) as the activation energy is less compared to that for site 1.
(b) In site 1 disorder occurs at slightly higher T (at 250 K).

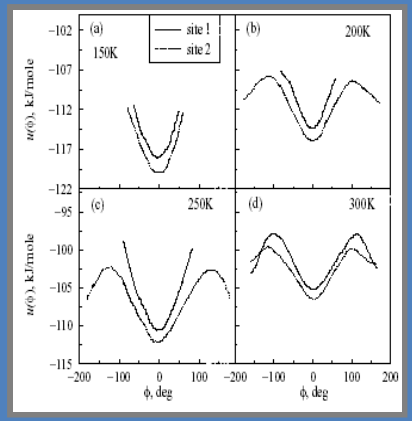

3. Simulation results combined with *ab initio* calculations could show the bond length variation as a function of temperature.

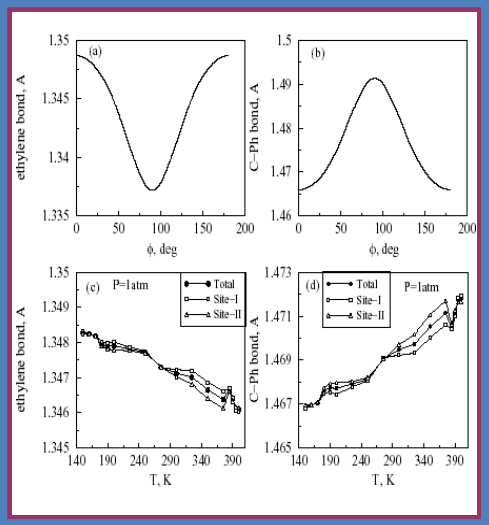

Chapter 5

Site dependent pressure effect on conformational disorder and pedal-like motion in stilbene

What is the effect of pressure on conformational disorder and pedal-like motion in stilbene?

Does the disorder disappear completely as a function of pressure?

Does the pressure affect disorder in different sites in different way?

Average absolute dihedral angle as a function of P

Molecules become Planar at high P.

Better packing Results in stronger Interaction.

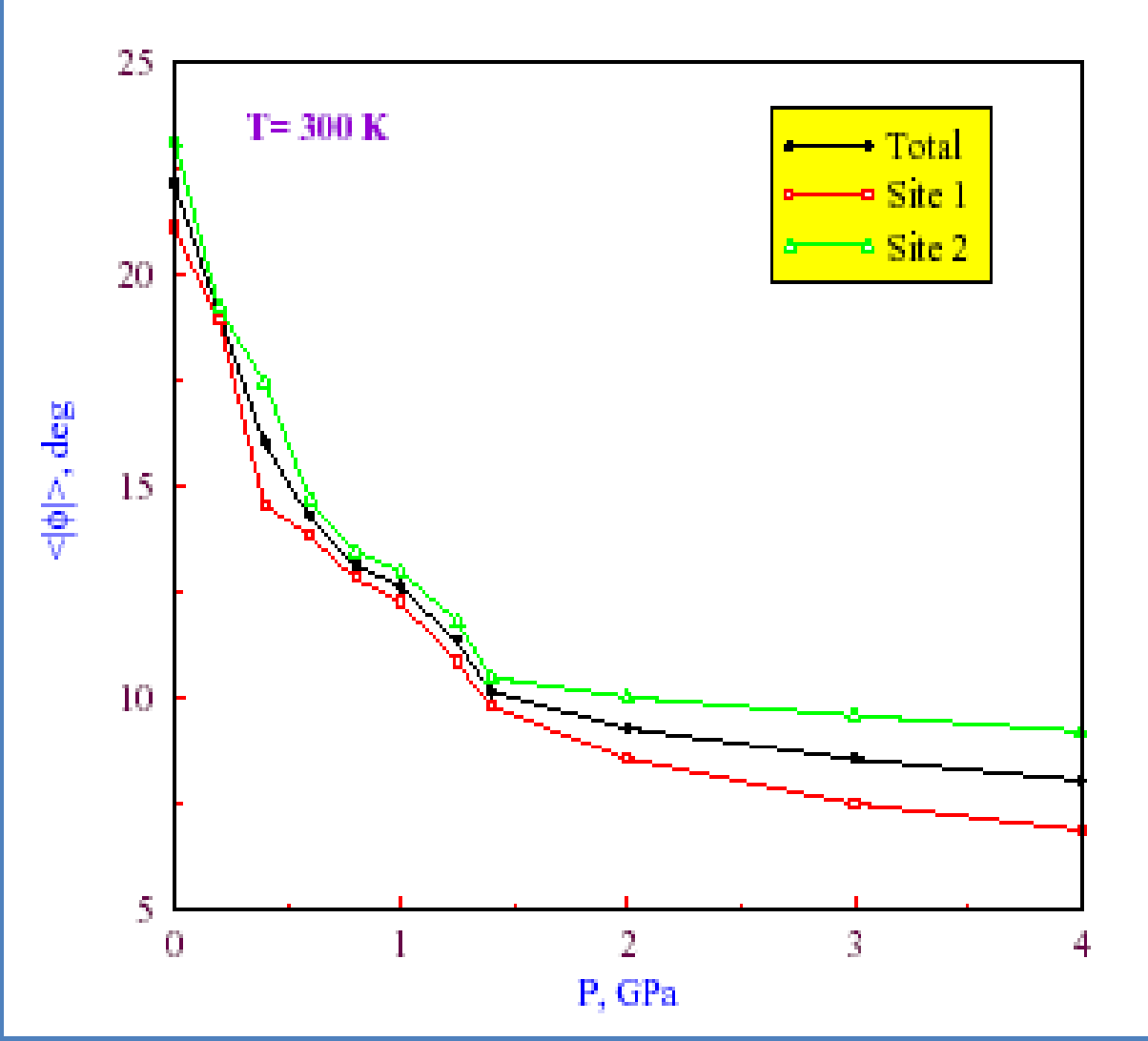

Effect of pressure on pedal-like motion

Pedal-like motion Disappears at Site 1 at 0.8 GPa

Pedal-like motion Disappears at Site 2 at 1.4 GPa

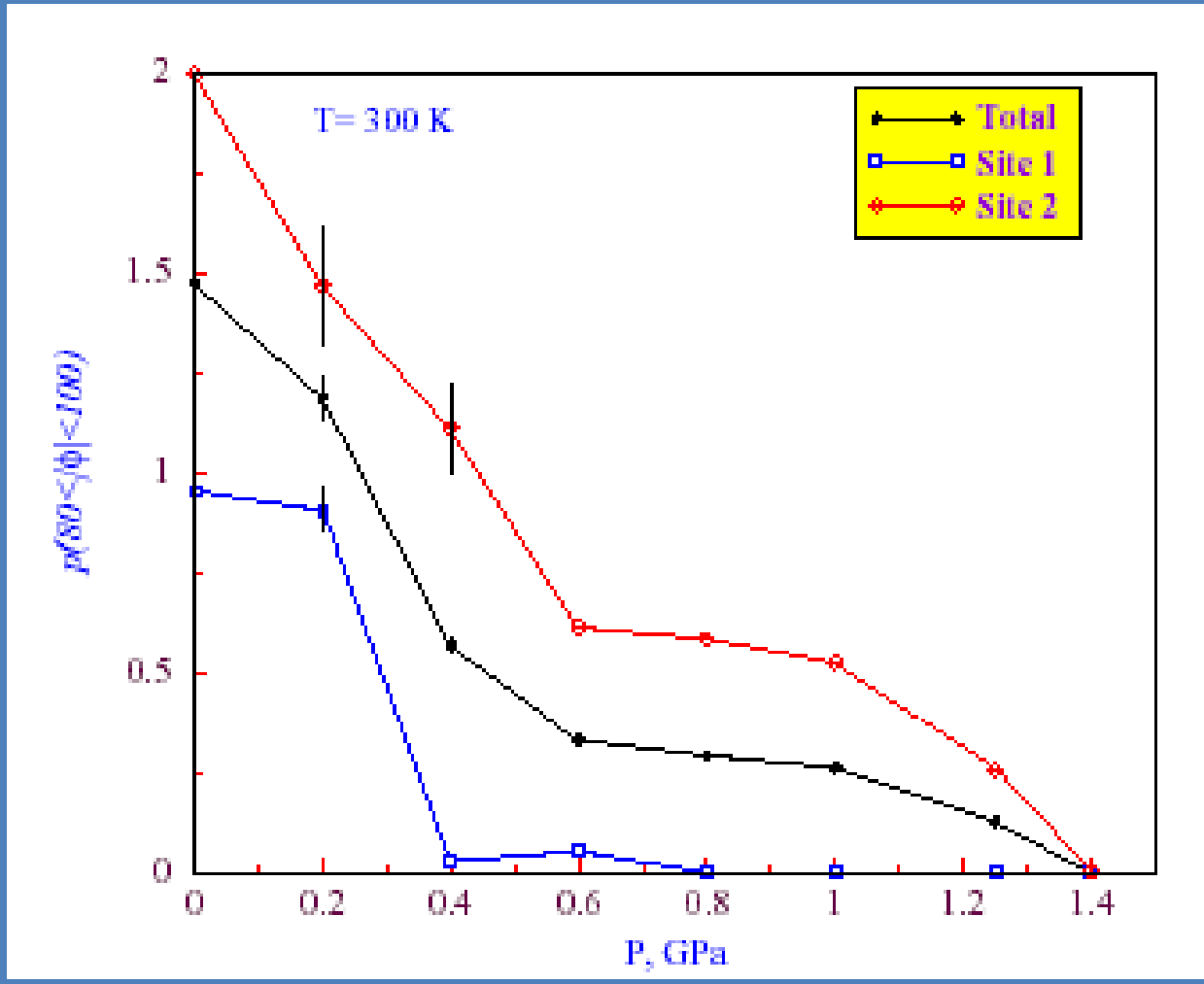

Dihedral angle distribution

At site 1, disorder Doesn't disappear

At site 2, disorder Disappears at 1.25 GPa

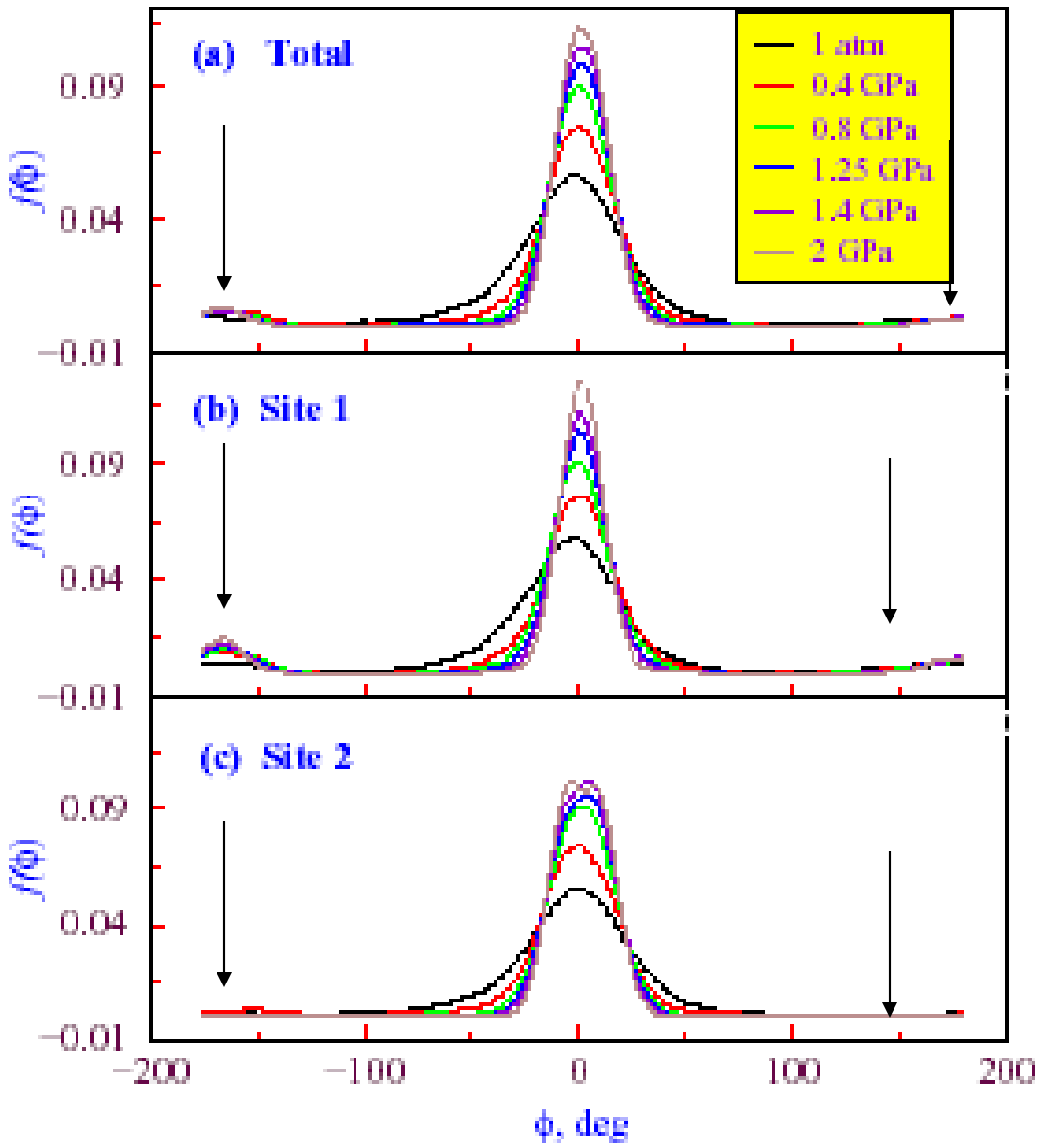

Potential energy landscape

In site 1, the u(Φ) is always double well potential

In site 2, the u(Φ) is always double well potential at low P and single-well at high P.

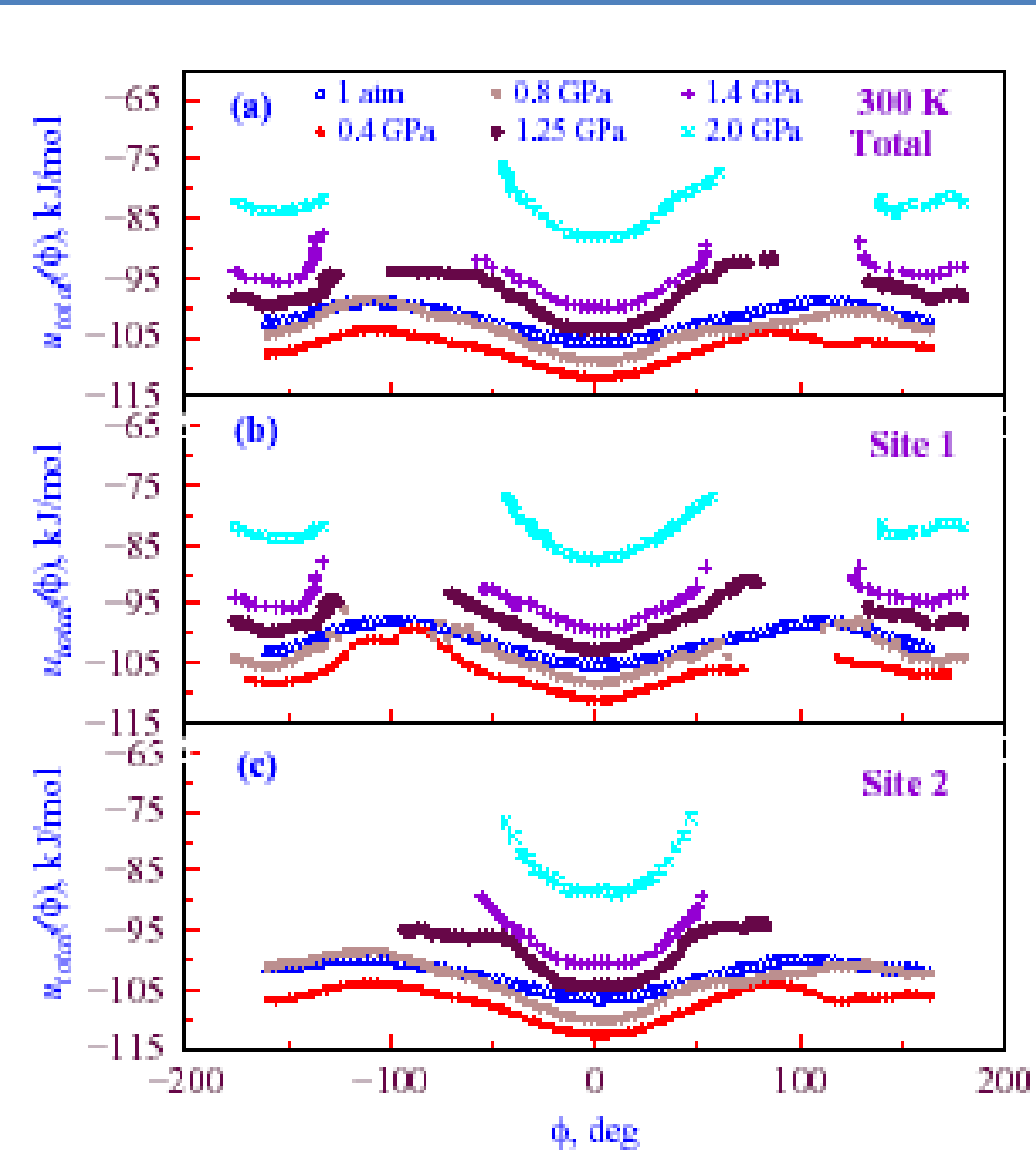

Nature of transition (may not be a first order)

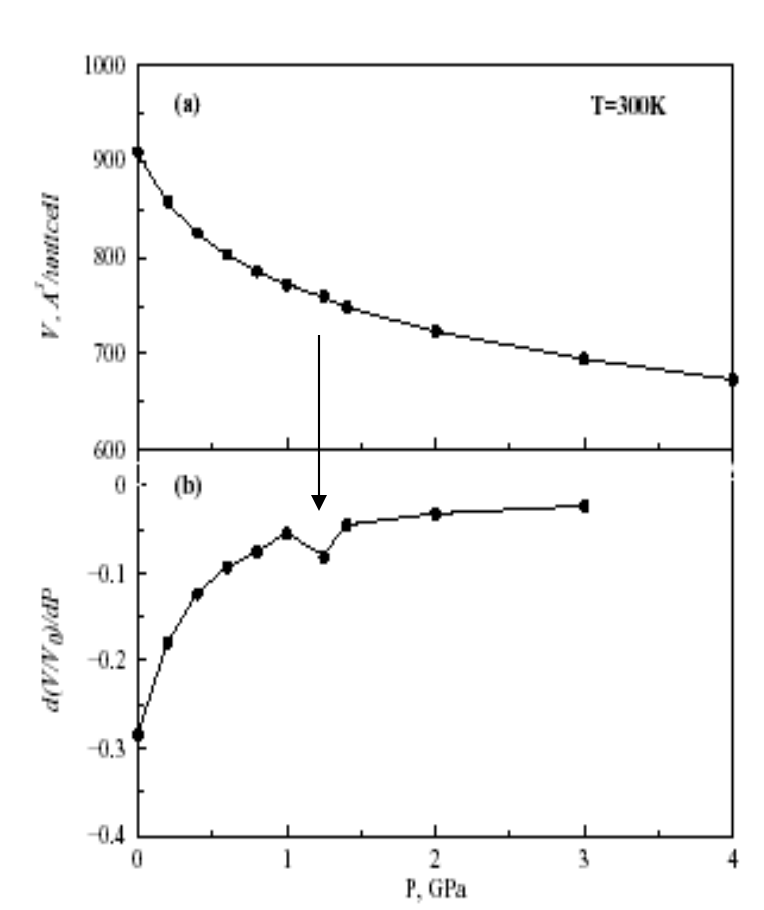

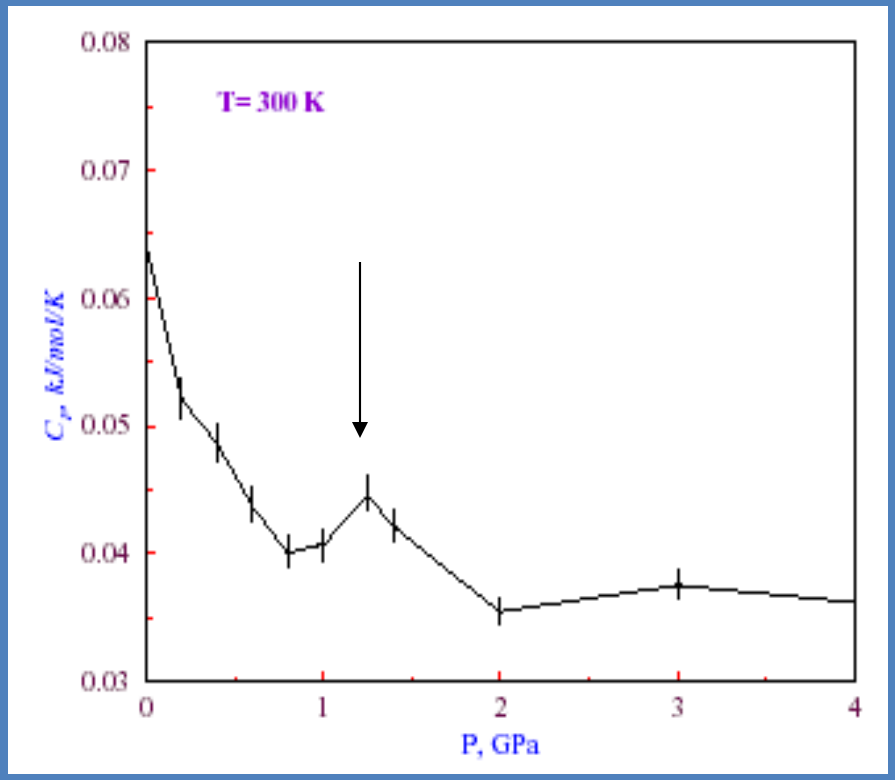

Conclusions

1. Dynamic disorder at site 1 disappears and static disorder remains.

2. Static and dynamic disorder at site 2 disappear at 1.25 GPa.

This is consistent with the earlier observation E_a for pedal-like motion is more for site 1 molecules and less for site 2 molecules.

Chapter 6

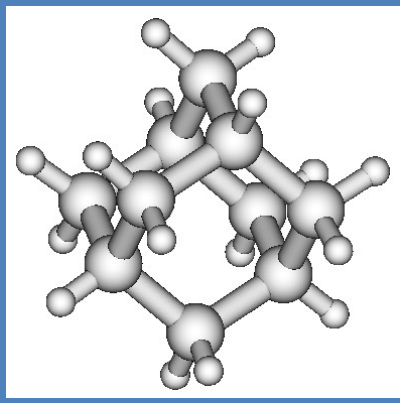

Temperature induced orientational disorder

Crystalline phase (Tetragonal $P\bar{4}2_1/c$) —**Temperature**→ Plastic crystal (Cubic Fm3m)

Pressure induced orientational ordering transition

Plastic crystal (Fm3m) —**Pressure**→ Crystalline phase ($P\bar{4}2_1/c$)

Variation of cell parameters as a function of temperature

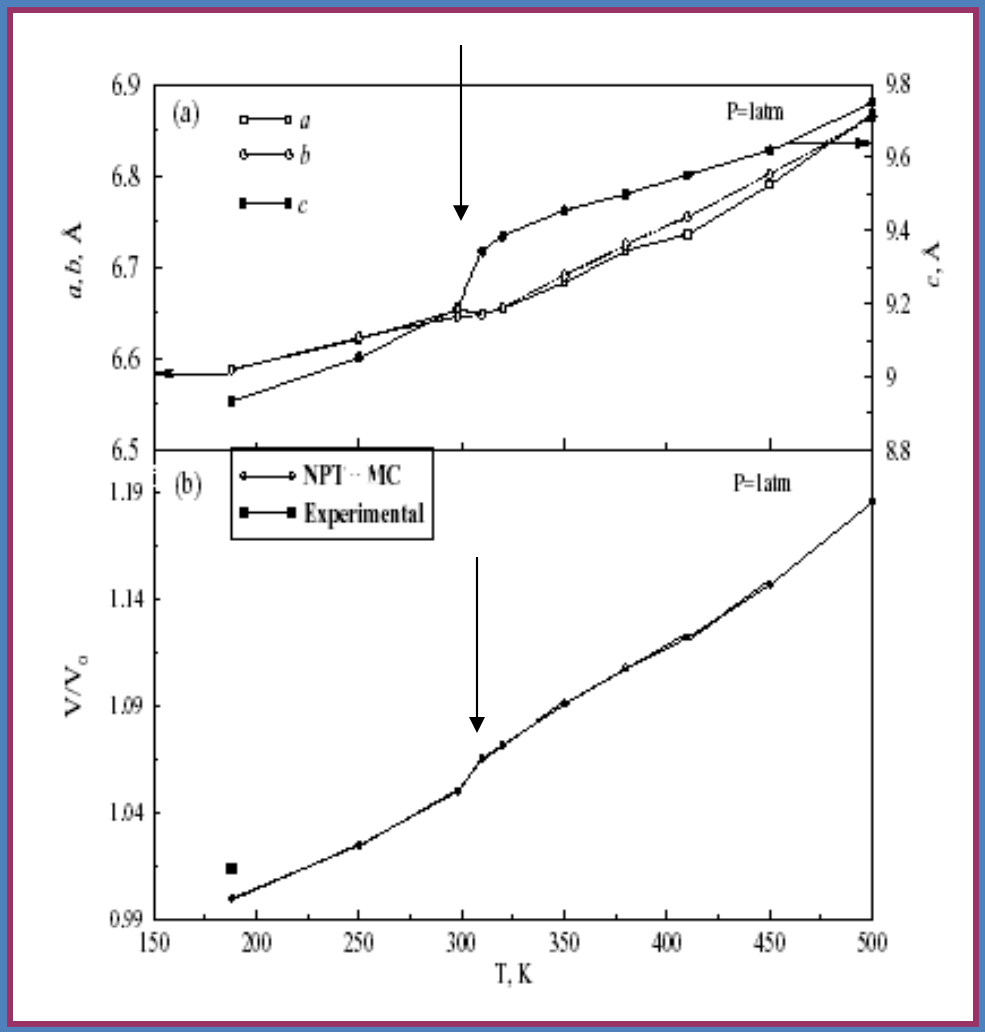

Abrupt change in cell parameters and volume between 300K - 310K suggests first order phase transition

RDF as a function of temperature

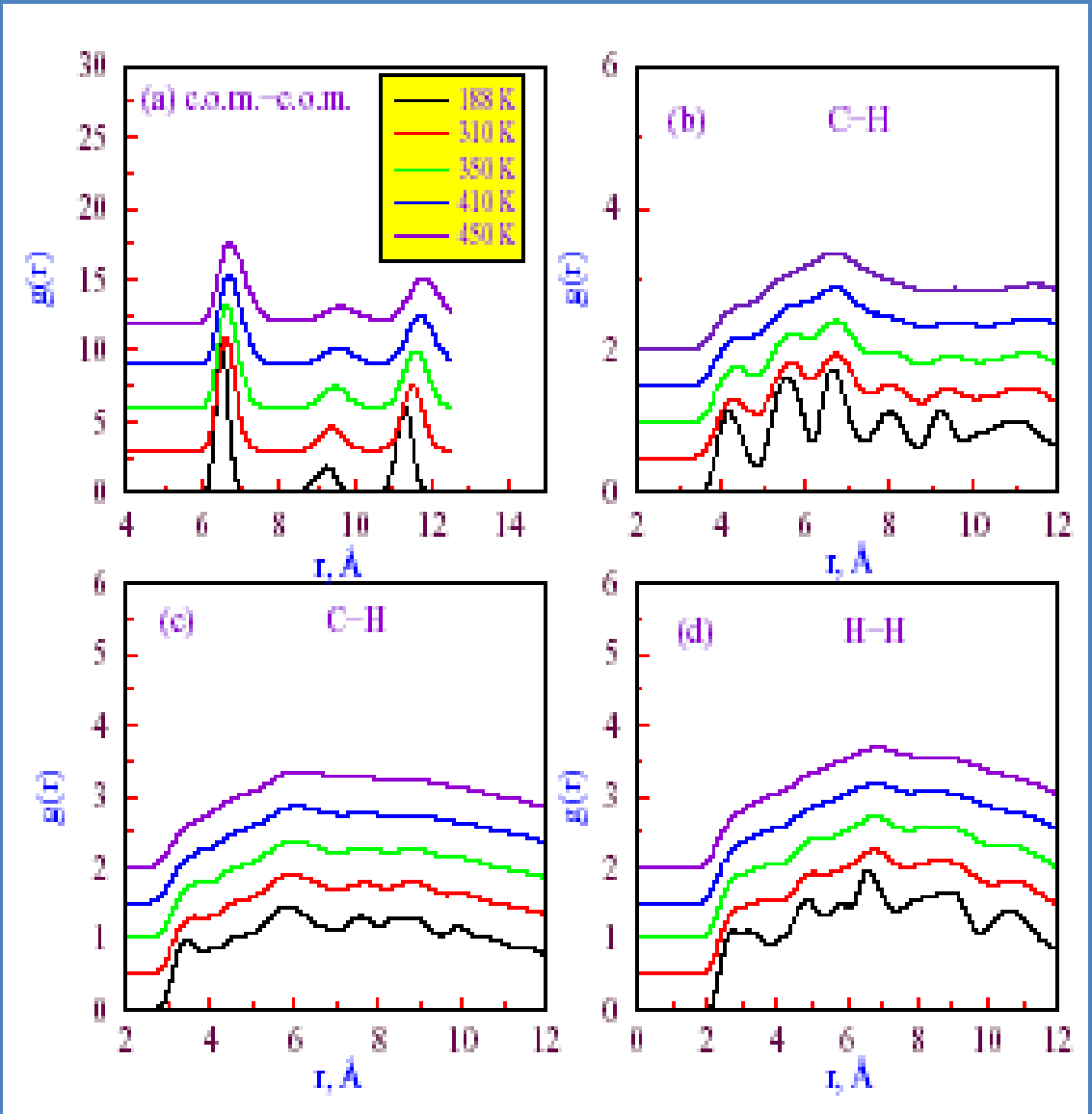

Orientational correlation function

$$O_i = \sum_{j=1}^{12} s_i s_j \qquad s_i, s_j = \pm 1$$

<o$_i$>=non-zero for Crystals orientationally ordered

<o$_i$>=zero for orientationally disordered crystals

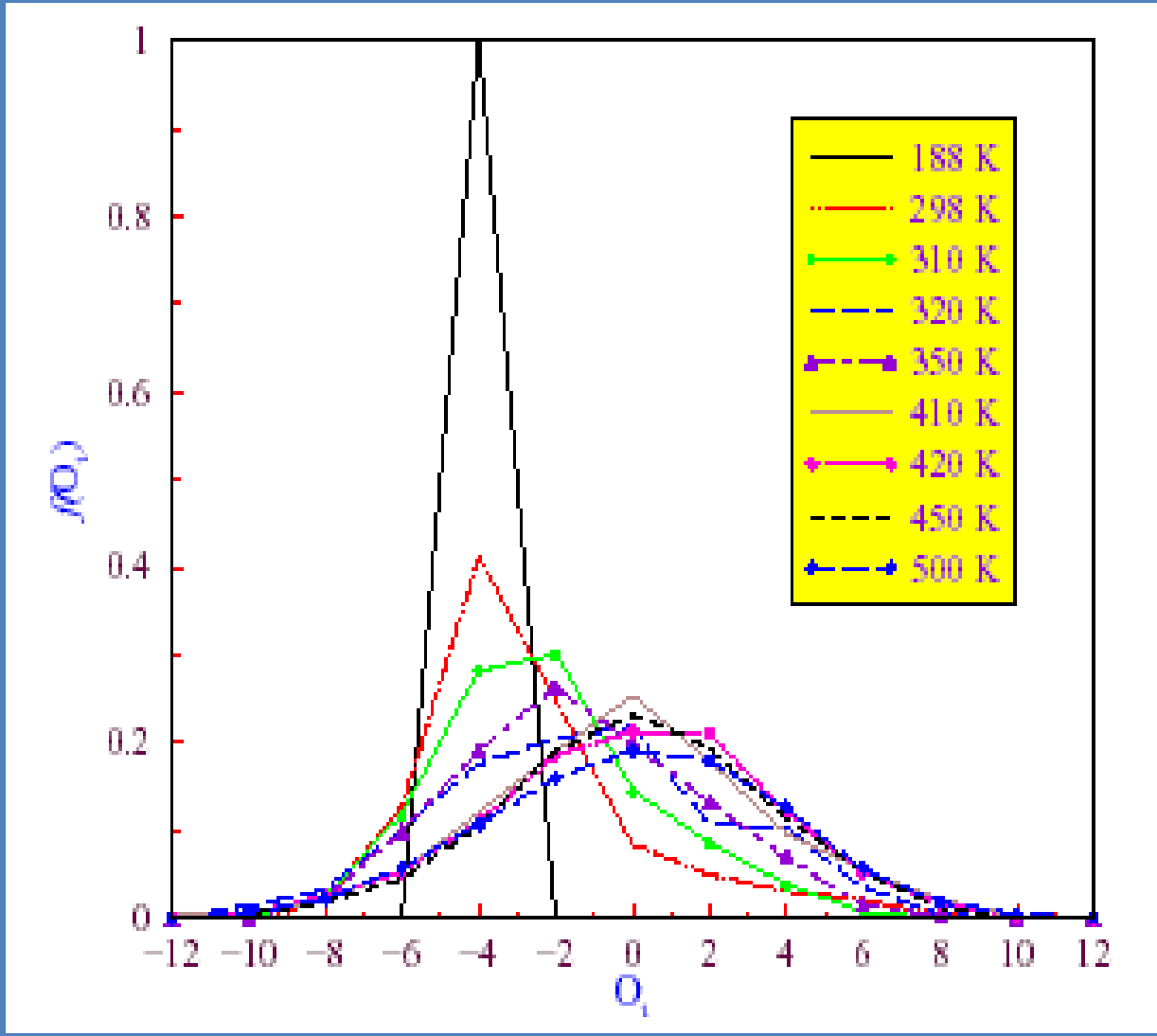

Cell parameter variation as a function of pressure.

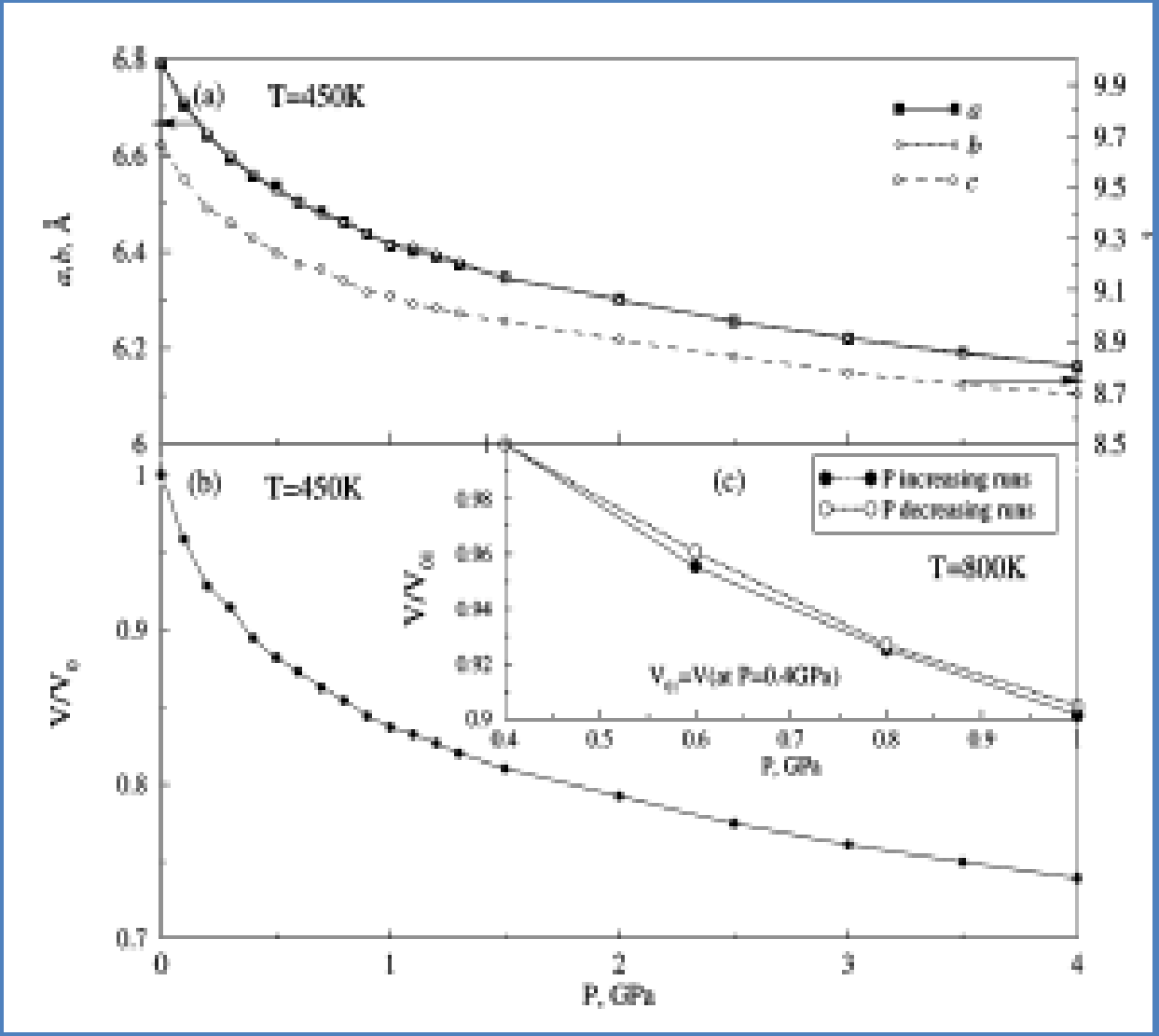

RDF as a function of pressure

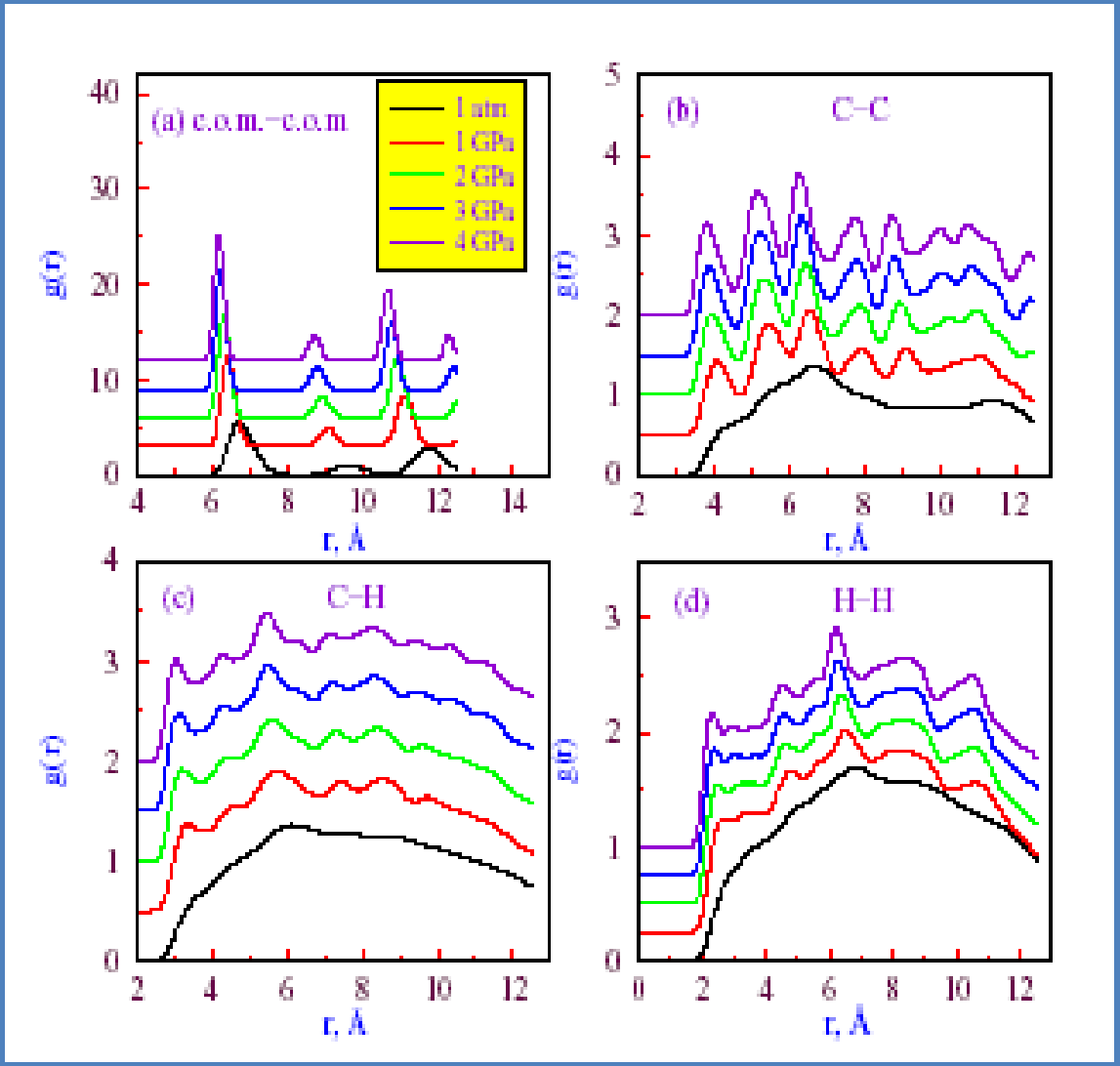

Variation intermolecular energy as a function of pressure

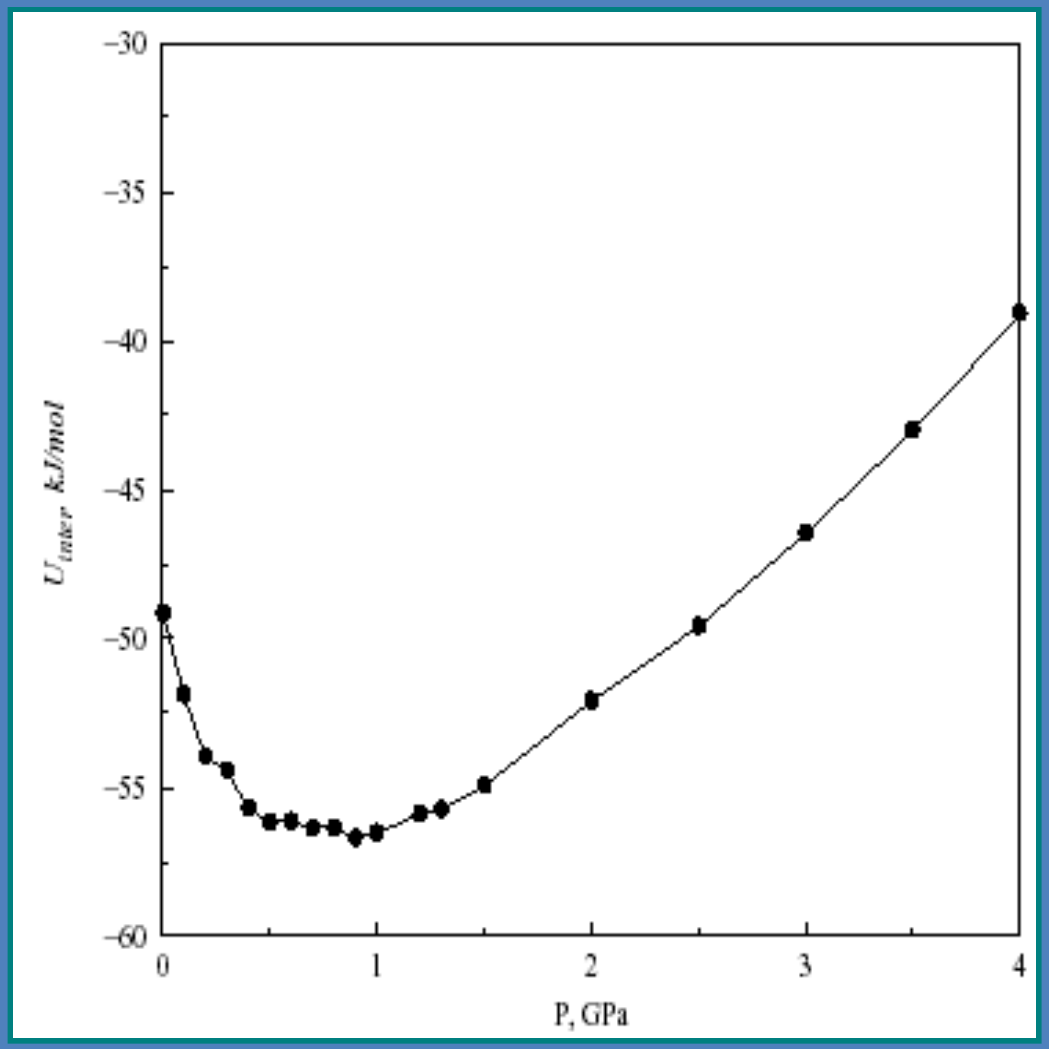

U_{inter} shows a minimum at the pressure where the orientational ordering occurs

Low T tetragonal phase and high pressure phase are isostructural

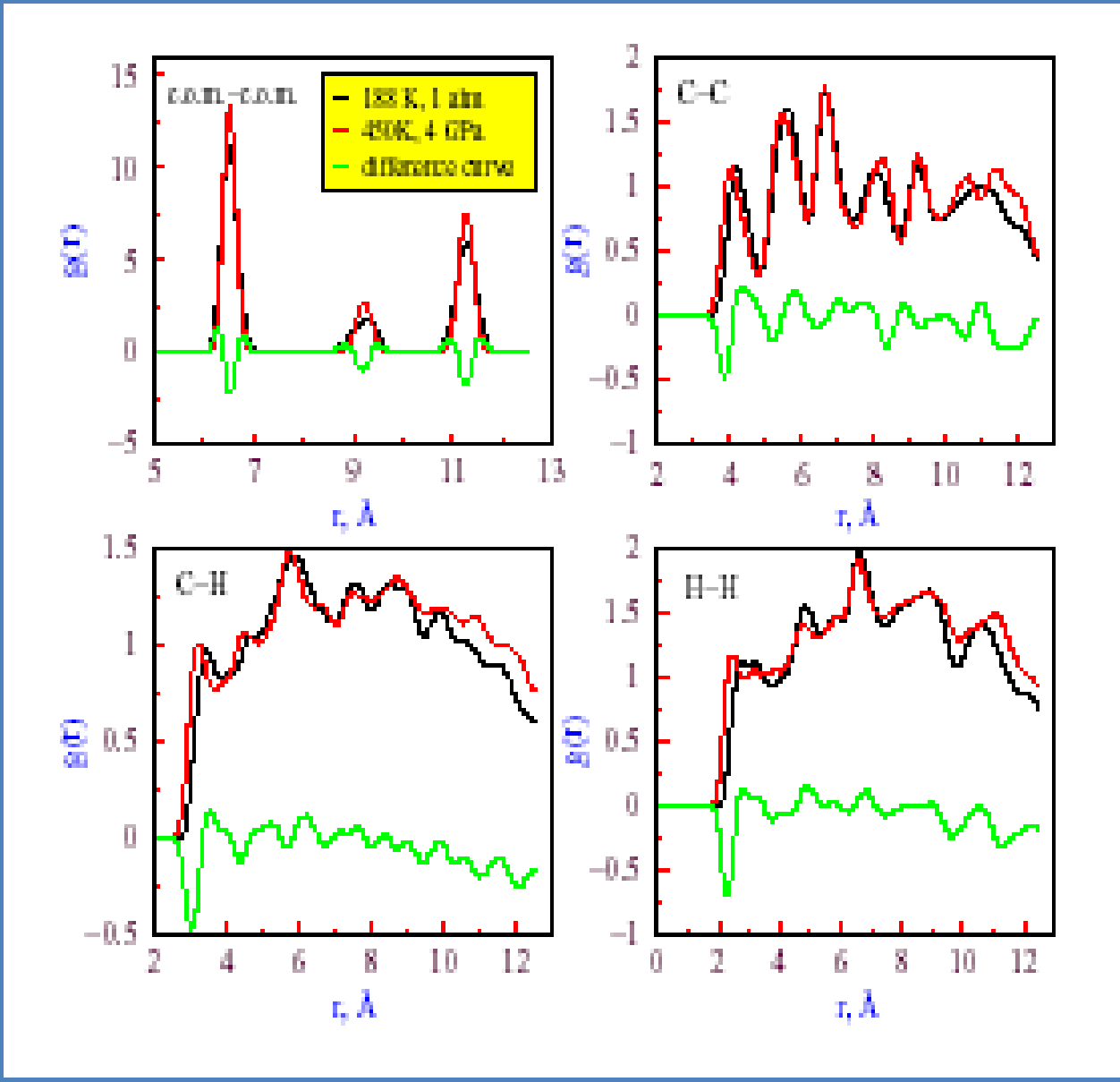

Snapshots of simulations

Crystalline
(Orientationally and translationally ordered)
(T = 188K P = 1atm)

Temperature

Plastic crystalline
(Orientationally disordered and translationally ordered)
(T = 450K P= 1atm)

Pressure

Crystalline
(Orientationally and translationally ordered)
(T = 450K P= 4 GPa)

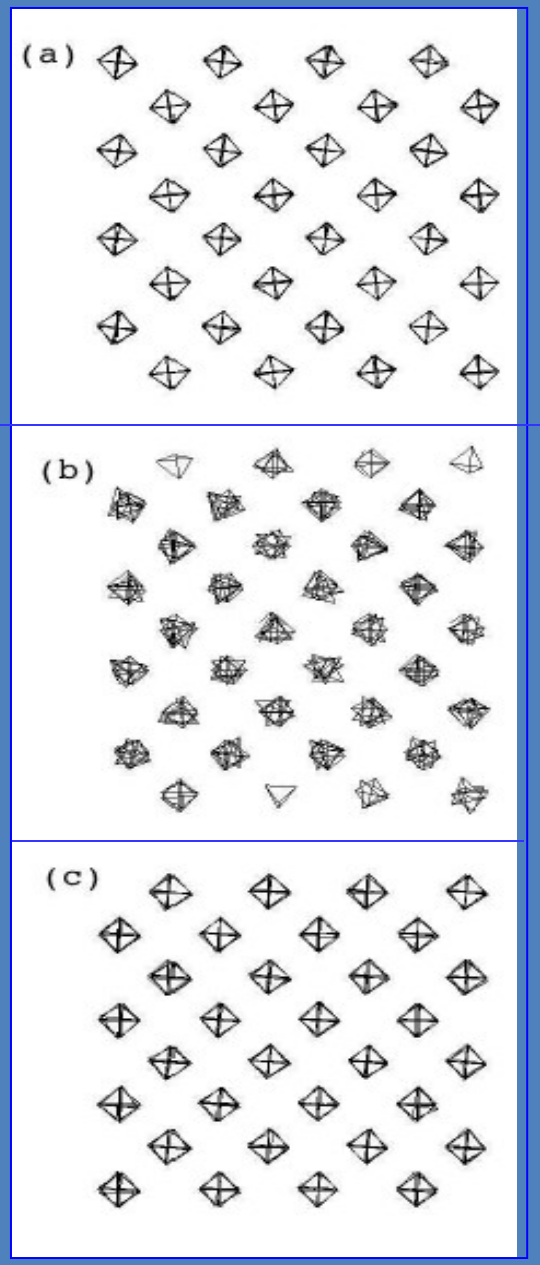

Phase diagram (200-2000 K and 1atm – 4 GPa)

T variation and P variation runs result in same coexistence curve

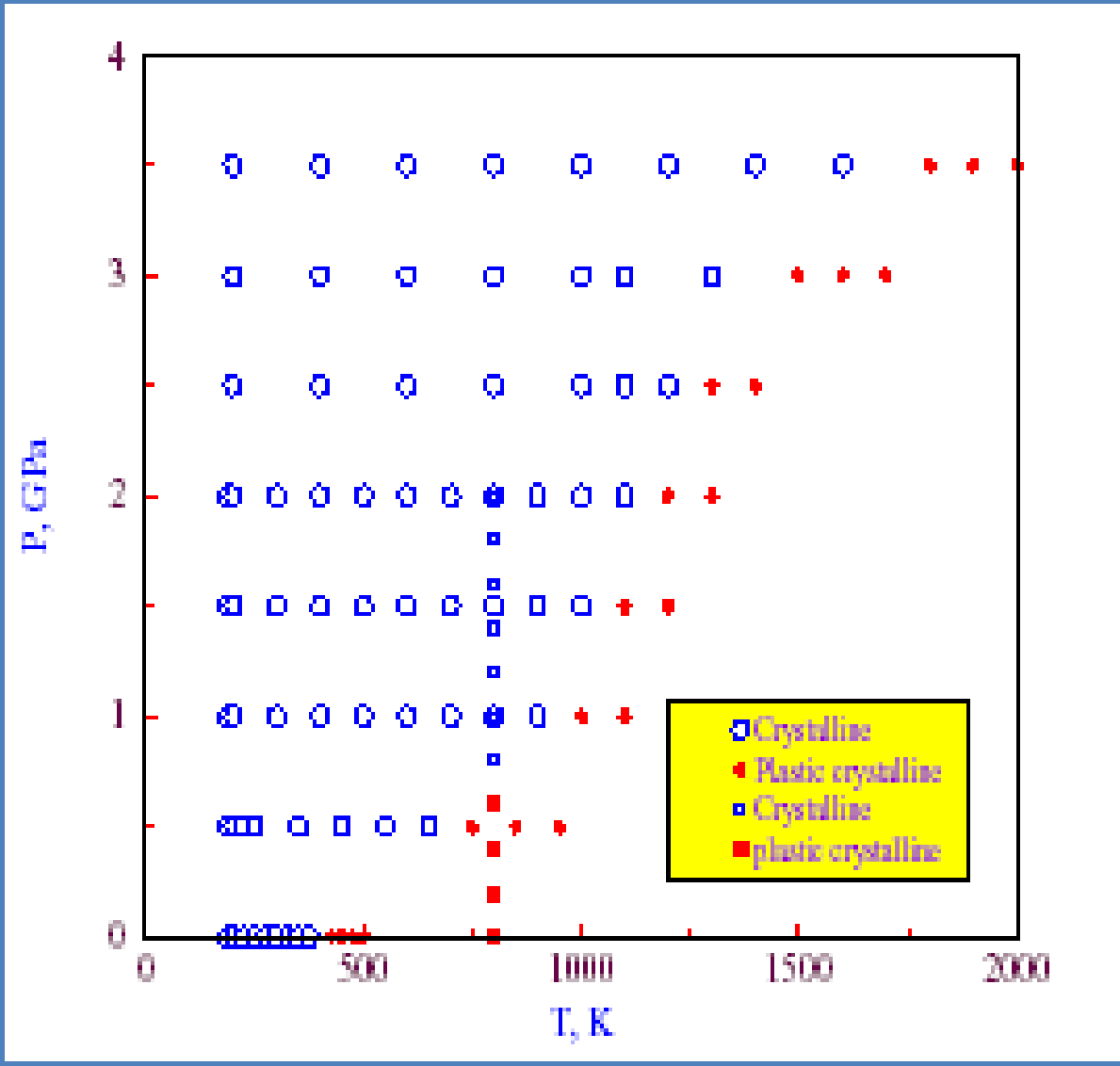

Chapter 7

High pressure phases of adamantane

Structural investigations (X-ray)* and Raman spectroscopic# studies at pressures up to 26 GPa (T=300K) report **five different transitions**

1. First transition is associated with the **disorder-order** transition occurring at **0.5 GPa**

2. Pressure dependence of internal mode frequencies suggest four phase transitions in the pressures **2.8 GPa, 8.5 GPa, 16 GPa (tetragonal) and at 24 GPa (monoclinic)**
(These results are also supported by structural investigations.)

* Vijayakumar, V. *et al. J. Phys.: Condens. Matter*. **13**, 1961(2001)
# Rekha Rao *et al. J. Chem. Phys.* **112**, 6739(2000)

Objectives of our calculations

To compute equation of state c/a variation and compare with experimental results

To look at the structural changes (at unit cell level) as a function of pressure

To look at nature of molecular geometry distortion as a function of pressure.

Computed equation of state compared with the experimentally calculated.

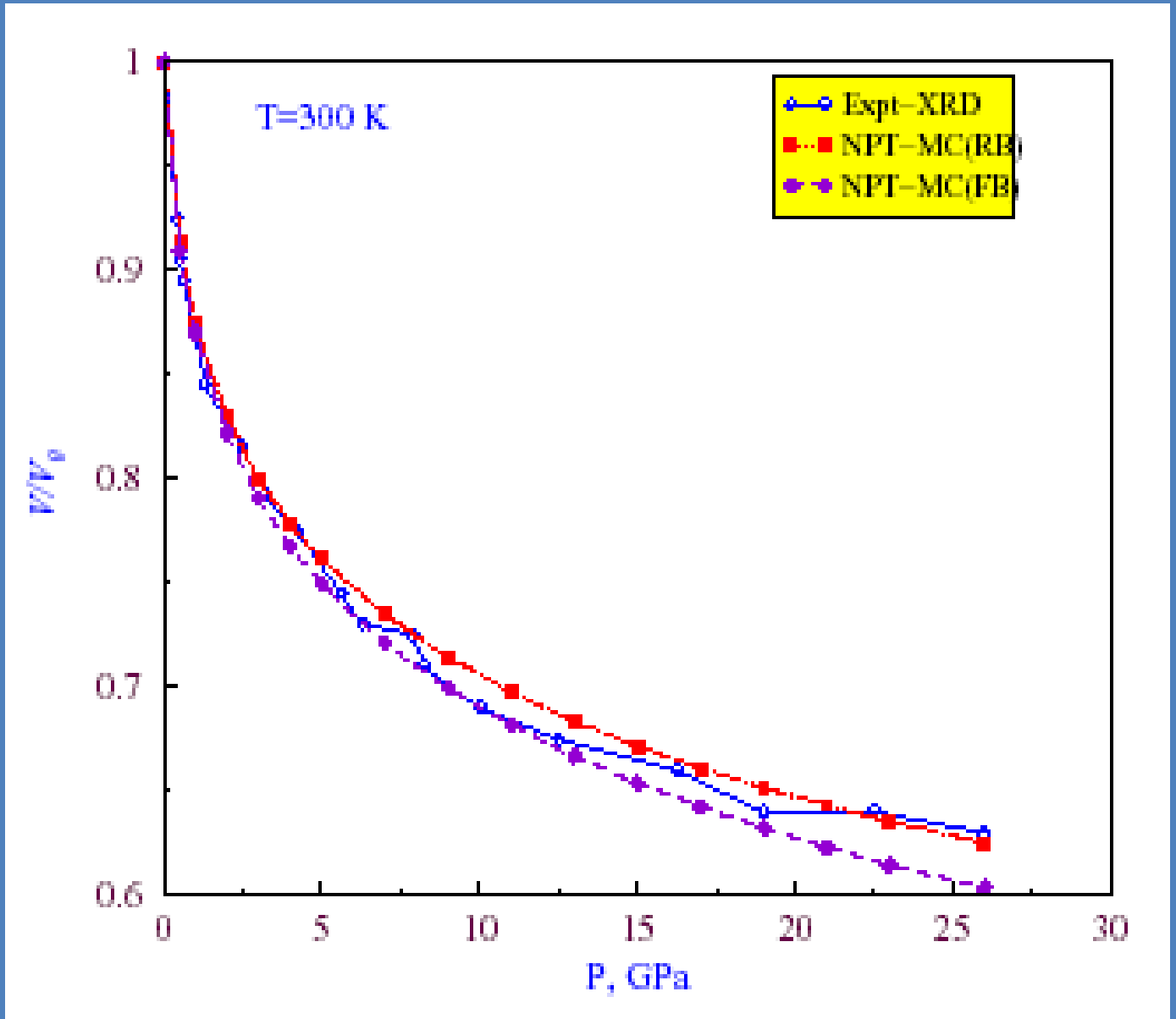

c/a variation as a function of pressure

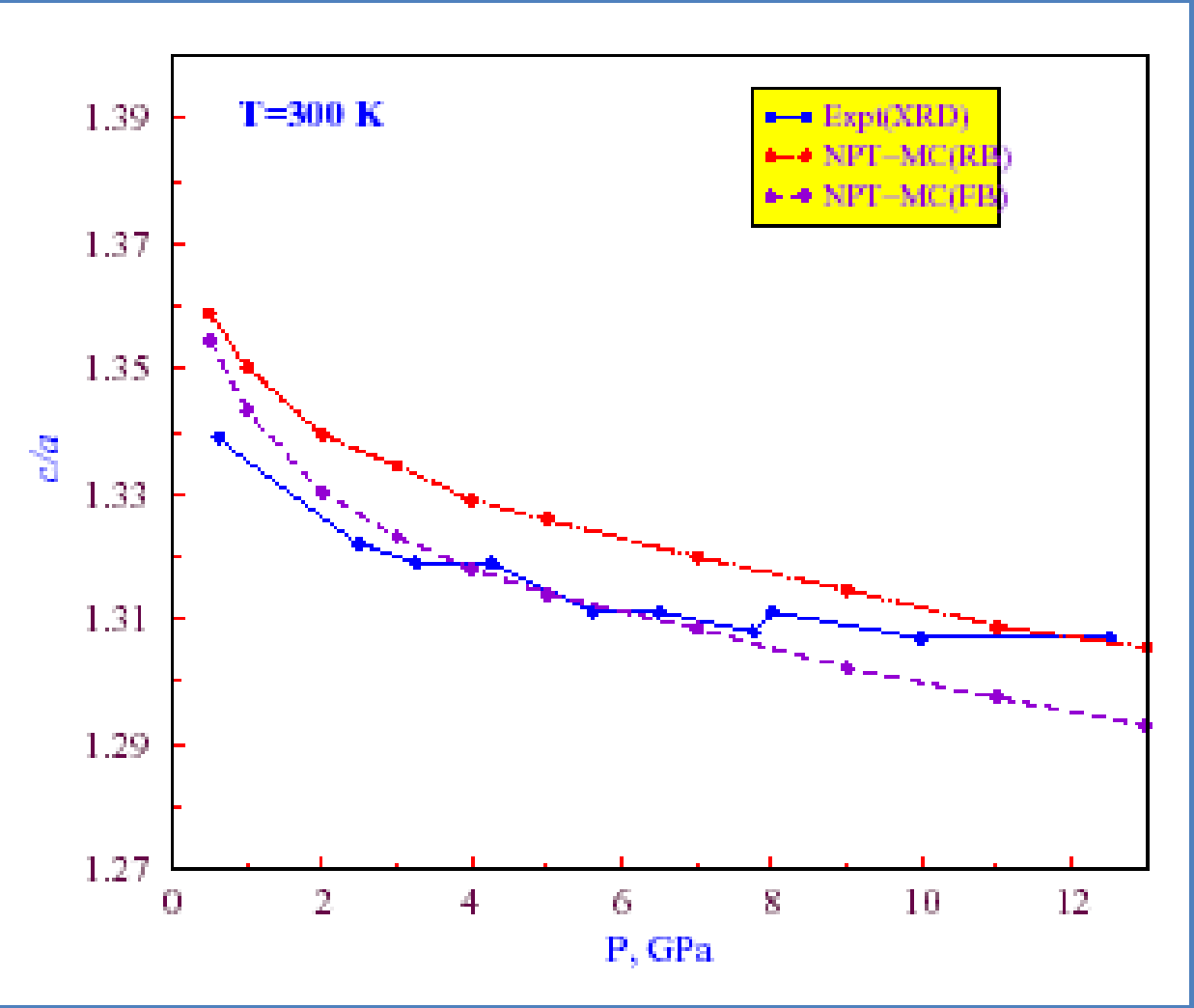

Appearance of new peaks! (signature of structural phase transitions)

0.5 – 1 GPa
(2nd peak)

2.0 – 3.0 GPa
(3rd peak)

6.0 -7.0 GPa
(1st peak)

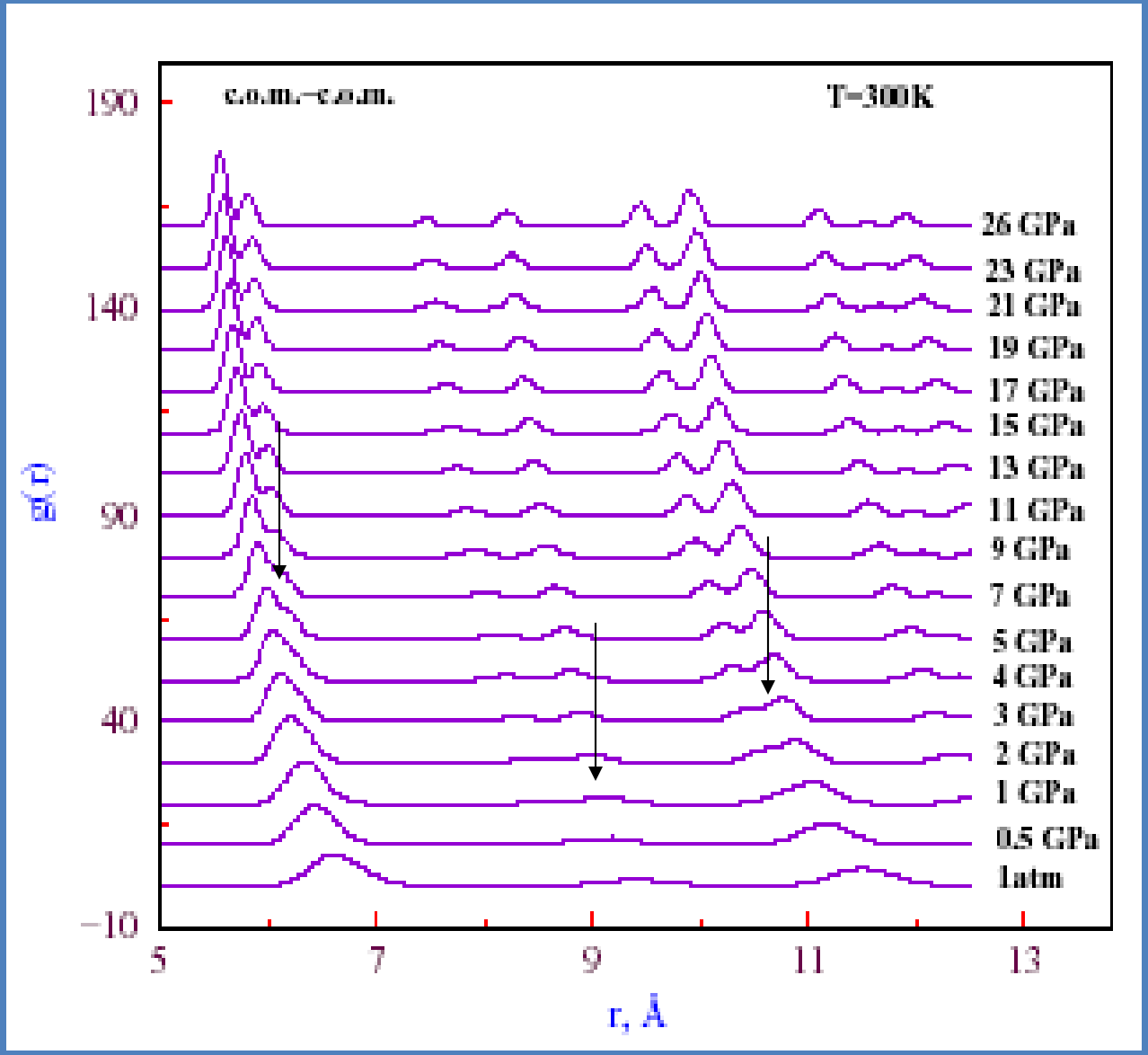

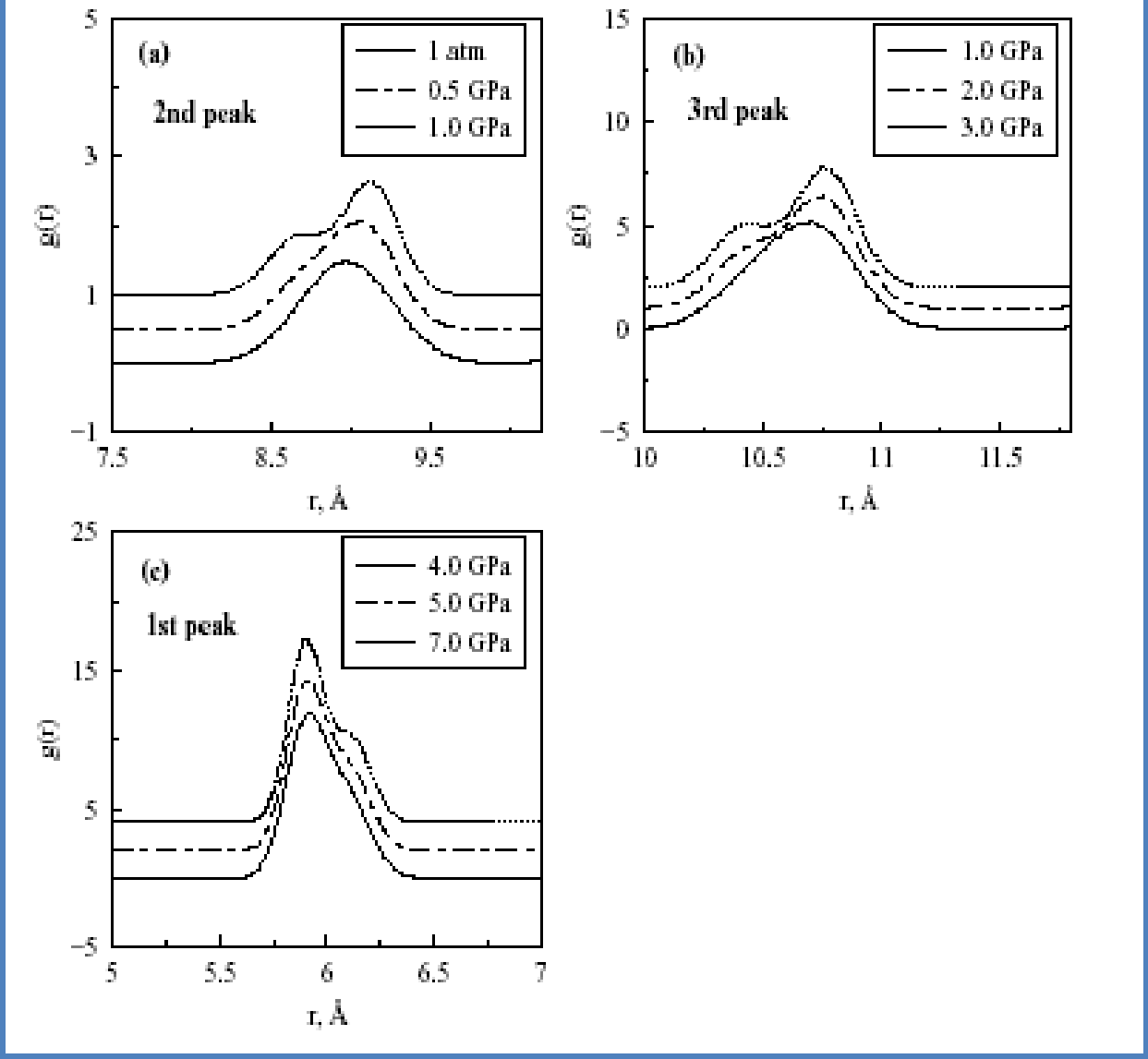

Simulations could predict 3 structural phase transitions In the pressure range 1atm -16 GPa.

Nature of molecular distortion in site 1 molecules

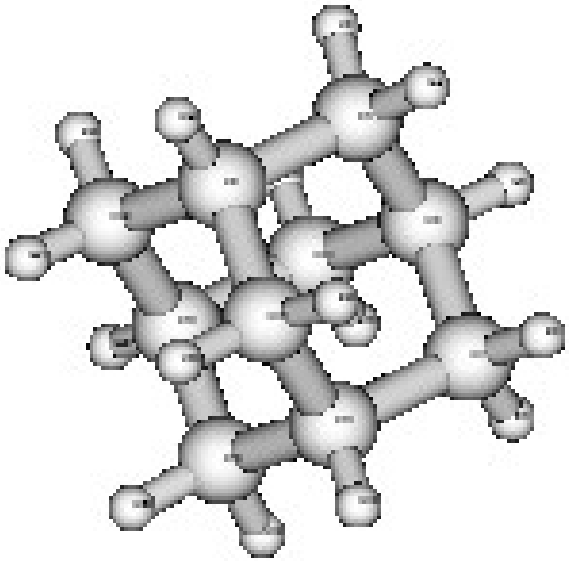

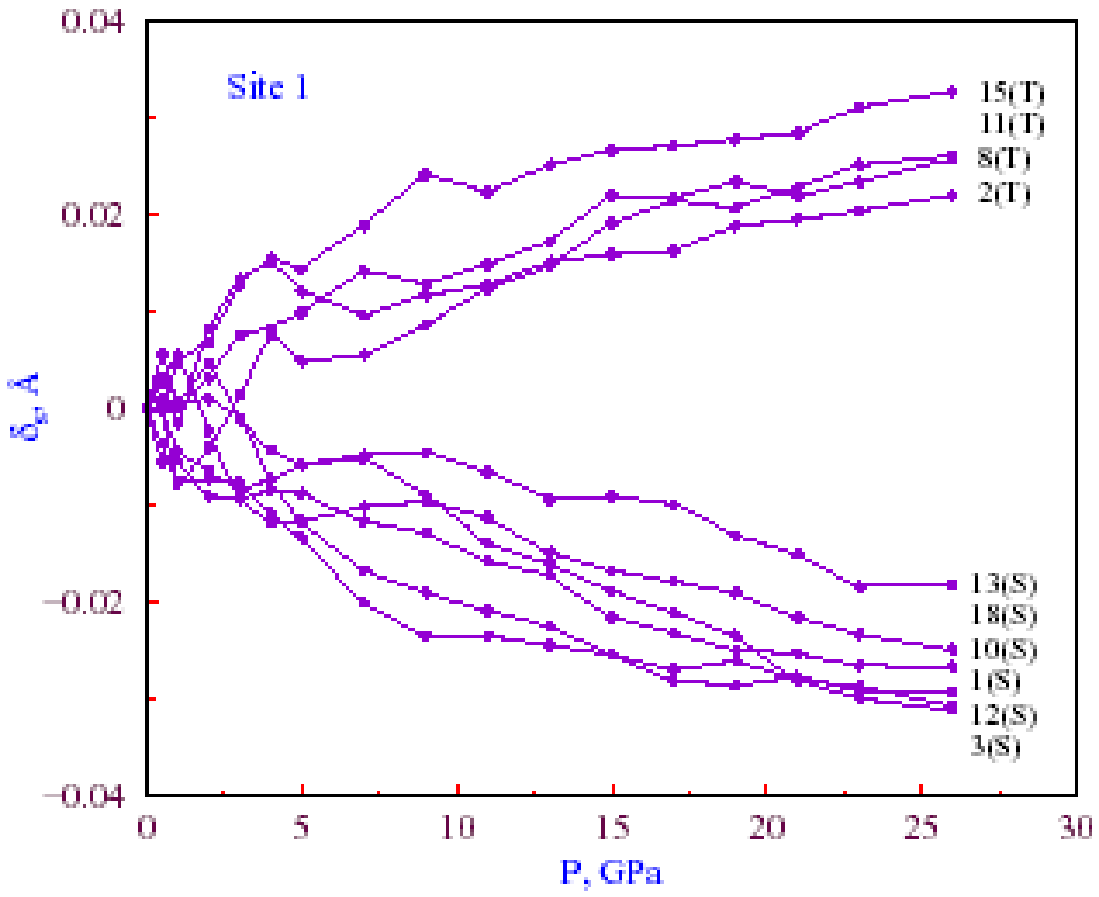

$$\Delta\bar{r}_{i\text{-}c}(P) = \bar{r}_i(P) - \bar{r}_{centr.}(P)$$

$$\delta_d(P) = \Delta\bar{r}_{i\text{-}c}(P) - \Delta\bar{r}_{i\text{-}c}(1\,atm)$$

Tetrahedra expand
Octahedra contract

Nature of distortion of molecules in site 2 molecules

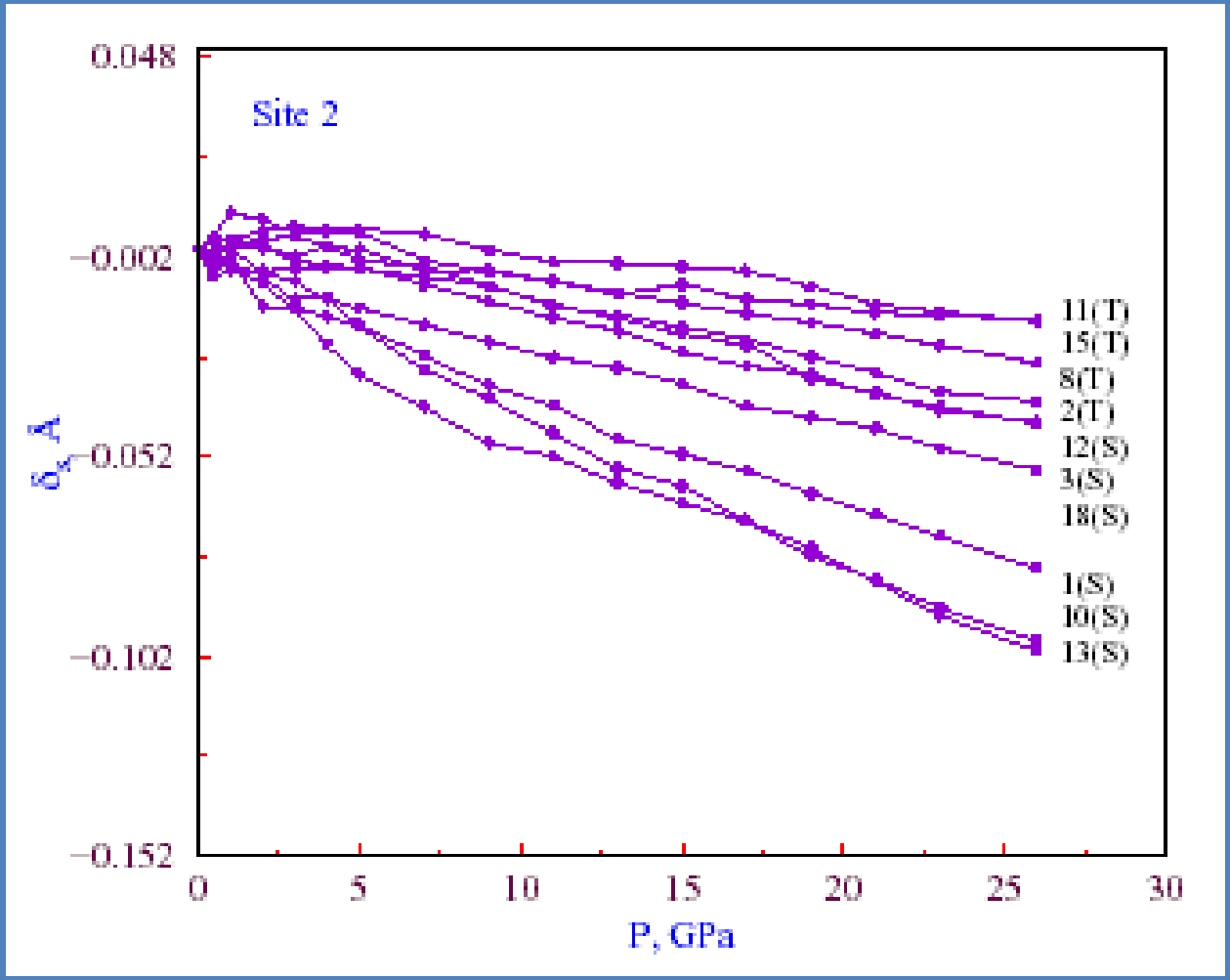

Tetrahedra contract

Octahedra contract

Molecules in different sites have different molecular Environment.

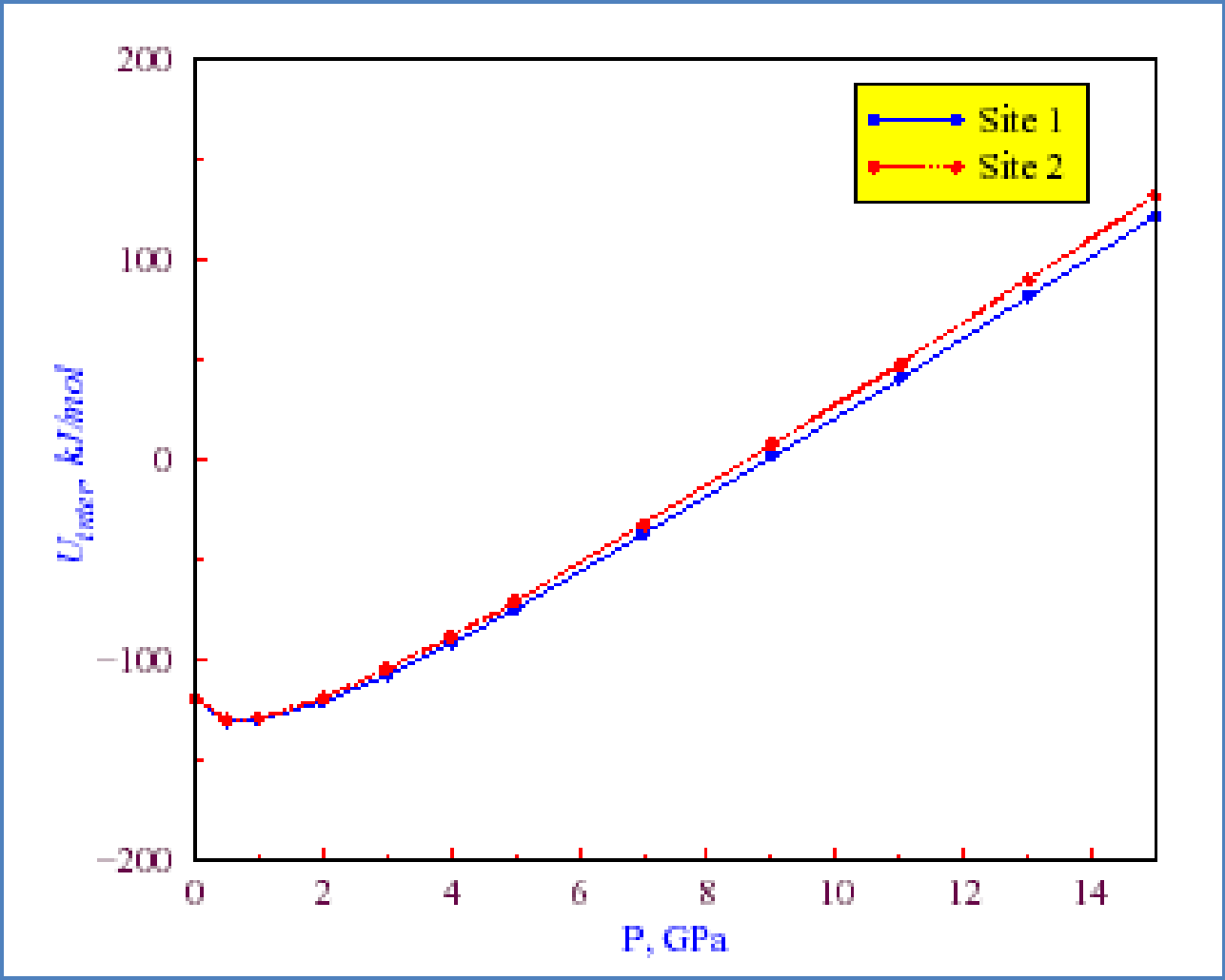

Various Examples

Crystal to plastic crystal transition in CCl_4 (MC simulation)

- ✓ Solid carbon tetrachloride exists in five phases Ia, Ib, II, III and IV.
- ✓ Ia and Ib are plastic-crystalline.
- ✓ Ia exists only at low pressures and is metastable with respect to Ib.
- ✓ Phase II exists at intermediate pressures and has complicated ordered structure.
- ✓ Phase III exists only at high pressures with the simplest ordered structure.
- ✓ Phase III is crystalline.
- ✓ Extended Monte Carlo method in the isothermal isobaric ensemble is employed to investigate the crystal(phase III) to plastic-crystal transition in CCL_4.

The transition in CCl_4

Initially the experimental structure of phase III of CCl_4 is taken

The lattice parameters are a = 9.079, b = 5.764, c= 9.201Å and β = 104.29^0

Initially the simulation was carried out at 280 K and 1.0GPa.

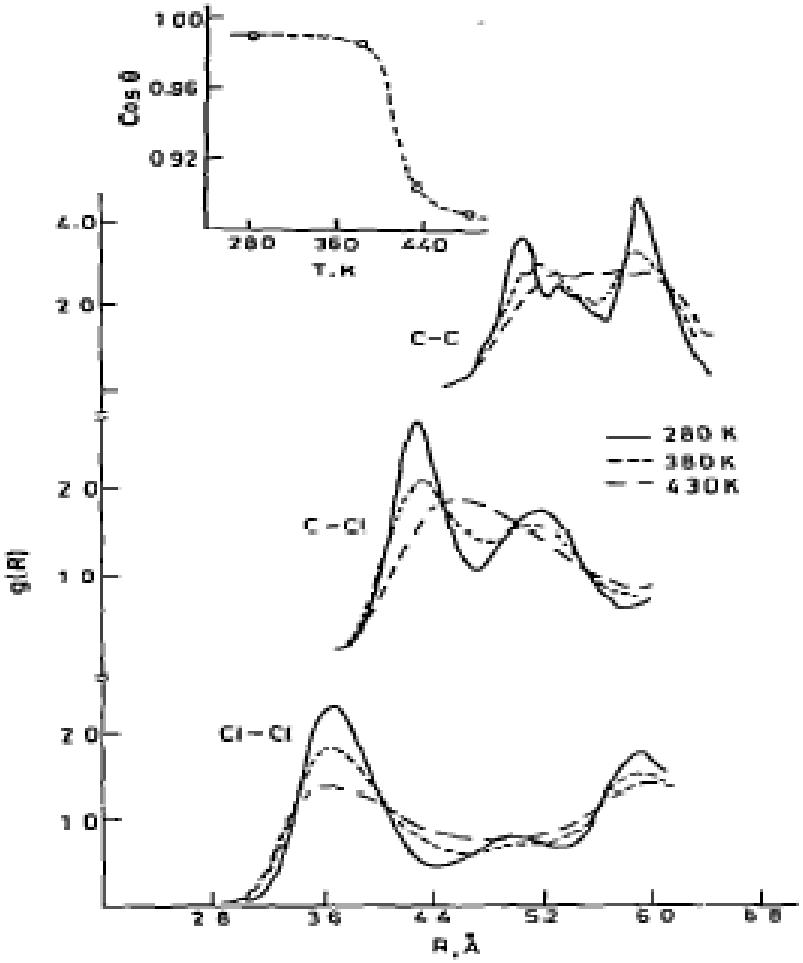

✓ When the temperature is increased to 380 K, the peaks of the rdf broaden and also volume and configurational energy increases. The broader peaks of the rdf suggest increased molecular motion and presence of orientational ordering.

✓ Further increase in temperature to 430 K results in considerable changes. The rdfs also shows significant changes. The broad nature of the rdf peaks suggests that the molecules are orientationally disordered. Thus CCl_4 has undergone a transition from ordered phase III to a disordered plastic crystal phase on going from 380 to 430 K

Structural transitions in superionic conductors

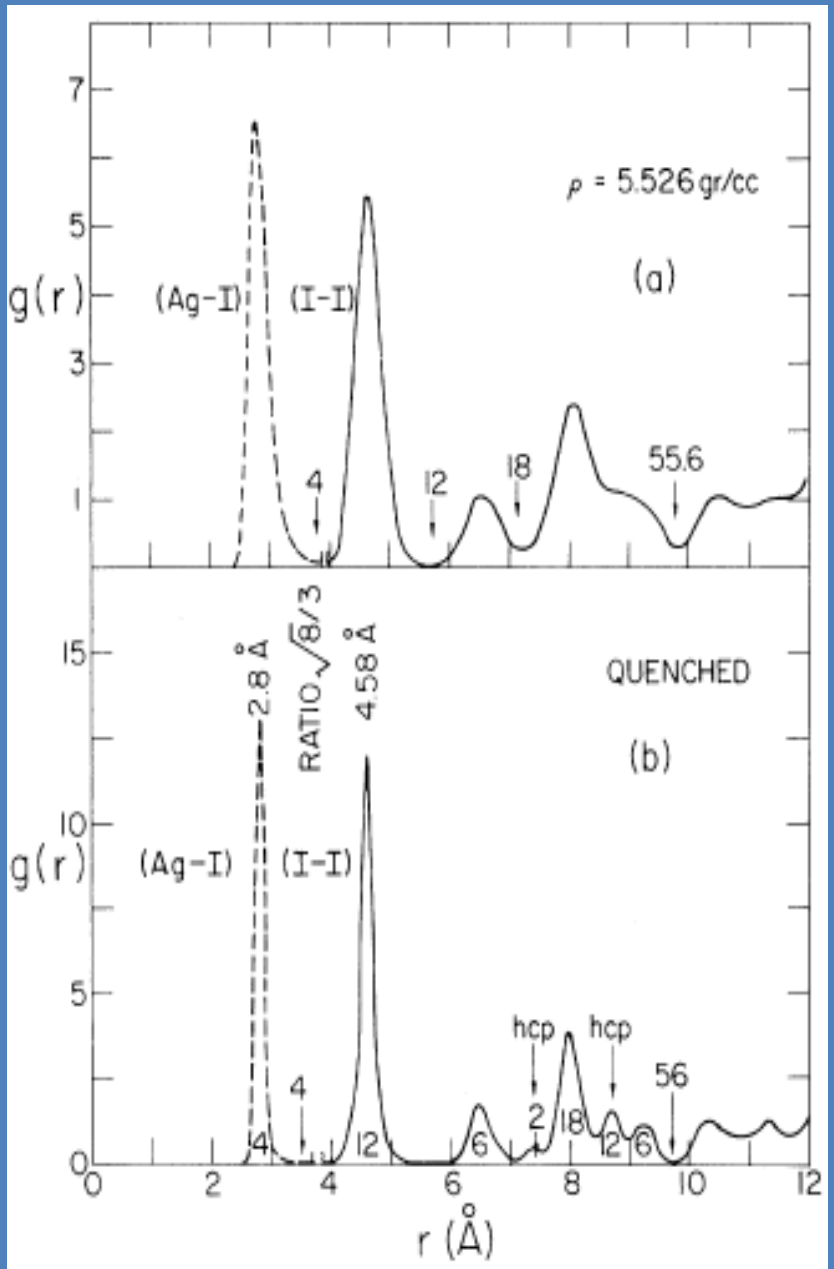

Variable shape molecular dynamics technique was used to study the α ↔ β phase transition in AgI.

Upon heating of β-AgI, the iodine ions undergo a hcp → bcc transformation and silver Ions become mobile.

The reverse transformation is observed on cooling of α-AgI.

(a) Pair correlation function after cooling from α phase at 700 K.

(b) Pair correlation function at 343.8 K on quenching to a very low temperature. The two peaks marked hcp contains two and twelve particles. This shows that the pair correlations are for β-AgI with a wurtzite structure.

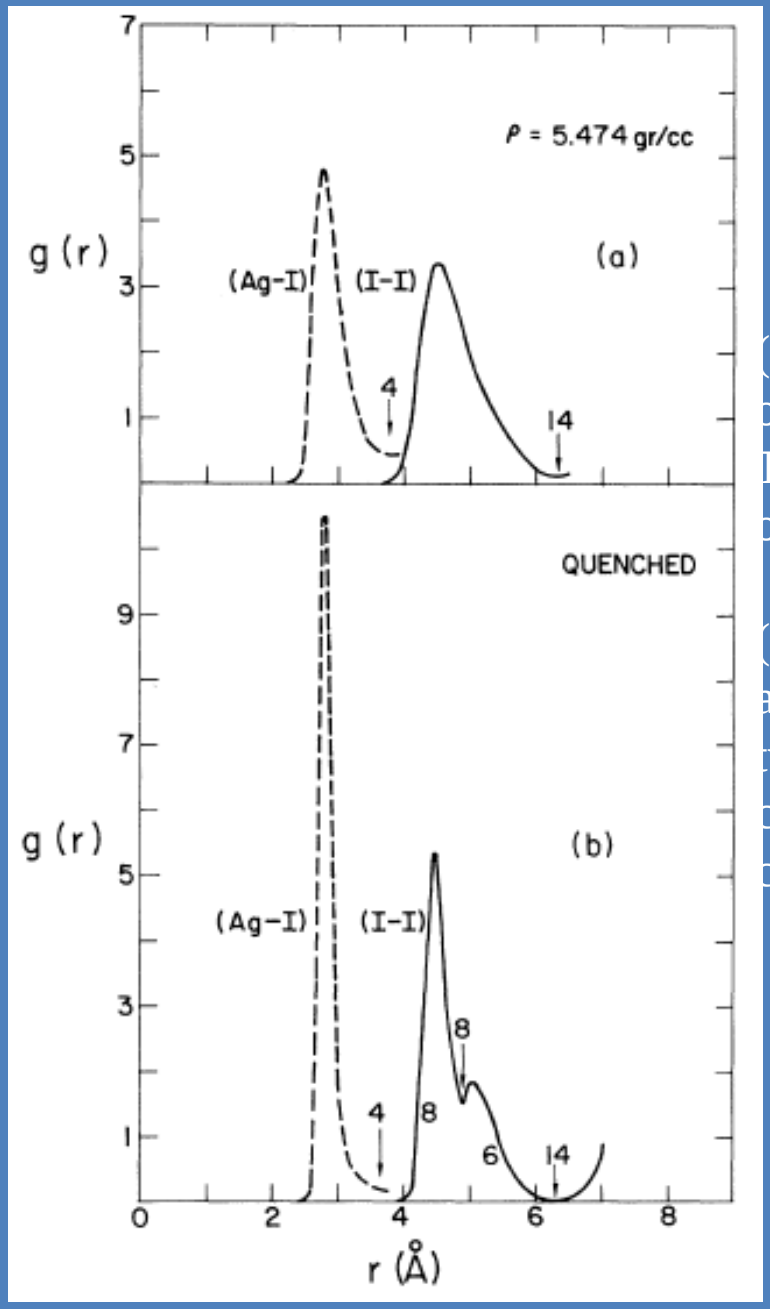

(a) Pair correlation functions at 494.7 K obtained by heating from β-AgI at 343.8 K. The peaks for Ag-I and I-I show coordinations of 4 and 14 respectively.

(b) Pair correlation functions at 494.7 K after quenching. The I – I correlation shows two peaks containing 8 and 6 iodines. This confirms that the figure described the pair correlation functions of α-AgI.

Transition in adamantane

At low temperatures (say 110 K) adamantane exists as an ordered tetragonal solid.

As the temperature is increased (say to 298 K), adamantane undergoes a structural transition from tetragonal ordered solid to an orientationally disordered cubic phase.

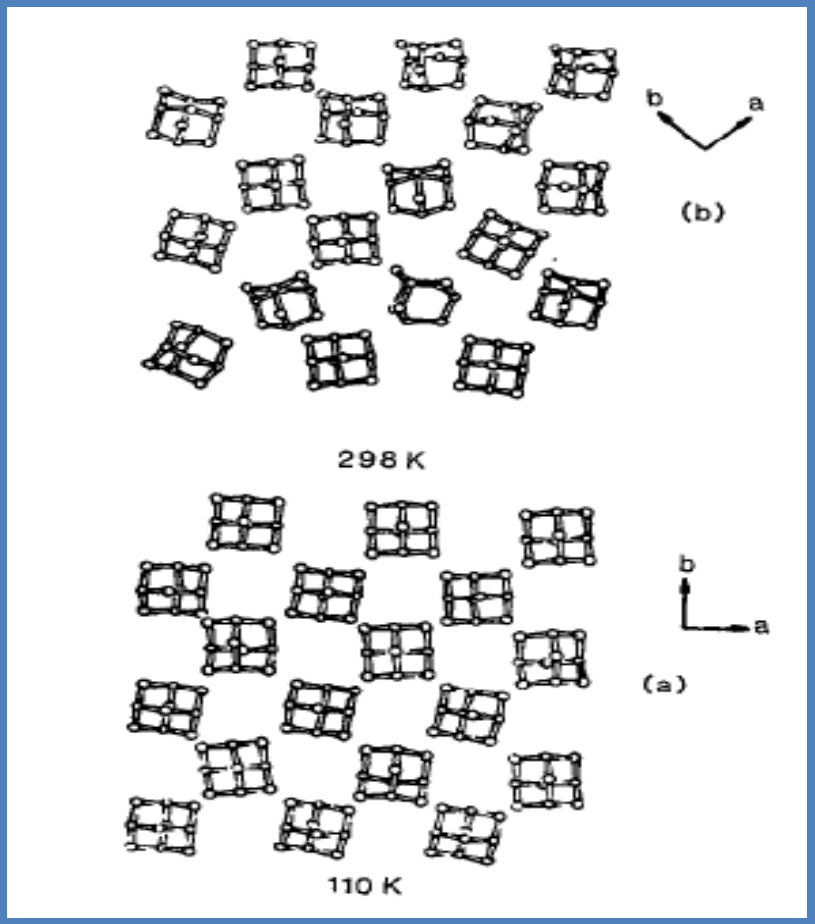

(a) Ordered tetragonal solid at low temperature.

(b) Orientationally disordered cubic phase at higher temperature.

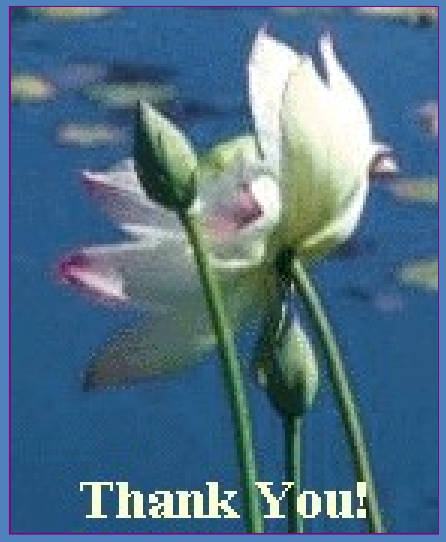
Thank You!